Carla Sandra Mota Castro

DEVELOPMENT OF METHODS BASED ON BIOMIMETIC SYSTEMS FOR EVALUATION OF ANTIOXIDANT PROPERTIES

Tese do 3º Ciclo de Estudos Conducentes ao Grau de Doutoramento em Ciências Farmacêuticas na Especialidade de Química Analítica

Trabalho realizado sob a orientação de

Prof. Doutora Marcela Alves Segundo (Orientadora)

Prof. Doutor José Luís Fontes da Costa Lima (Co-Orientador)

Doutora Marlene Susana Dionísio Lúcio (Co-Orientador)

Outubro 2012

Carla Sandra Mota Castro


FCT
Fundação para a Ciência e a Tecnologia
MINISTÉRIO DA CIÊNCIA, TECNOLOGIA E ENSINO SUPERIOR


POPH
PROGRAMA OPERACIONAL POTENCIAL HUMANO


QREN
QUADRO
DE REFERÊNCIA
ESTRATÉGICO
NACIONAL
PORTUGAL 2007.2013


UNIÃO EUROPEIA
Fundo Social Europeu

Acknowledgements

Though the following dissertation is an individual research work, I could never have reached the heights or explored the depths without the help, support, guidance and efforts of a lot of people. Therefore, here is a small tribute to all those people.

To Faculdade de Farmácia da Universidade do Porto (FFUP) for receiving me as a PhD student.

To Fundação para a Ciência e Tecnologia (FCT), for the PhD grant SFRH/BD/41627/2008.

To Prof. Dr. José Luís Costa Lima for the challenge of the PhD in this department and for providing me all the necessary conditions to do my work.

To my supervisor Dr. Marcela Segundo, for her excellent guidance and for inspiring me the qualities of being a "good scientist". Special thanks also for her friendship, enthusiasm, availability and effort made for the realization of this work.

To Dr. Marlene Lúcio for the co-supervision and guidance of my work.

To Prof. Dr. Salette Reis, my special thanks for accompanying the progress of my work and for being always available when I needed.

To all my colleagues and friends in the FFUP, for the help and friendship.

To Prof. Dr. Luis Camacho and Dr. Juan Casares for receiving me in the department of Física Química y Termodinámica, Universidad de Cordoba. The time spent there had an enormous contribution in my knowledge about how to do research. Thanks also for their friendship

To Luís Magalhães my special thanks for accompanying the progress of my work and for his friendship.

To my friend Mariana Arêde for the help in laboratory work and her friendship. Thank you.

To all my friends who were always present and available.

To all my family for the support and the encouragement.

To my lovely parents and my sisters, all my thanks. Without their help this work could never be done. They were always supporting and encouraging me along these years to pursue my interests.

To Jorge and my children, Rui e Mariana, for the love, and to whom I dedicate this thesis.

Abstract

Biological systems exhibit an enormous complexity upon their structure, components, function and controlling systems towards homeostasis.

This high degree of complexity derives from the diversity of biological processes, namely the reactions involved in cellular respiration, which depend on the presence of oxygen, fostering an expectable increase in reactive species of oxygen, among others.

During the past few years, studies towards the causes and consequences about the production of free radicals in organisms were performed, along with studies aiming to unveil biological targets prone to attack and the possible consequences from these events. Actually, nowadays it is clearly known that the biological membranes are the main targets of free radical attacks, resulting in peroxidation conditions. In organisms, there are natural antioxidants, such as glutathione, uric acid and ascorbic acid, which are able to neutralize the action of these reactive species, avoiding the damage caused by them.

Aiming at studying how the generation of free radicals affect biological stability, several experiments were carried out along this thesis, focusing on understanding the role, the efficacy and possible interactions between biological membranes and free radicals. Moreover, some aspects related to the location of these antioxidants within the membrane (hydrophilic/hydrophobic media) and how the products of such reaction can interfere with membrane structure were focused. For this, different biomimetic models were assessed, namely micelles, liposomes and Langmuir monolayers, using lipid mixtures similar to those found in biological membranes. During these work, standards, reference compounds for evaluation of peroxidation were applied, including Trolox and vitamin E.

Moreover, methodologies relying on application of fluorimetric probes were developed, aiming to achieve a simple method with optimized experimental conditions in order to evaluate peroxidation in different locations of membrane models (aqueous phase, interface and lipophilic media). Other biomimetic models were also assessed, with different features concerning their size, lamellar structure and lipidic composition, in order to enlighten how these variation and complex aspects interfere with the evaluation of oxidative or antioxidant capacity of different compounds.

Keywords: biomimetic model, peroxidation, antioxidant

Resumo

Os sistemas biológicos exibem uma elevada complexidade no que concerne a estrutura, constituição, função e sistemas de controlo da sua homeostase.
A sua elevada complexidade deve-se à diversidade de processos biológicos a eles inerente, nomeadamente as reações envolvidas na respiração celular, cuja dependência de oxigénio em muitos deles, acarreta um natural incremento de espécies reativas de oxigénio, entre outras.
Ao longo do tempo foi-se estudando e conhecendo algumas das causas e consequências da produção de radicais livres no organismo, assim como o estudo dos seus alvos de ataque e possíveis alterações daí resultantes, estando hoje bastante bem relatadas que as membranas biológicas pela sua constituição essencialmente lipídica, são um dos maiores alvos de ataque de radicais livres com consequente peroxidação. Existem no organismo antioxidantes naturais como a glutationa, o ácido úrico e o ácido ascórbico capazes de eliminar estas espécies reativas, evitando os danos potencialmente causados por estas.
No sentido de estudar a forma como a geração destes radicais afetam a estabilidade biológica, foram realizados ao longo deste trabalho alguns ensaios com o intuito de perceber melhor o papel, a eficácia e as eventuais interações com as membranas biológicas dos radicais produzidos, a forma como estes antioxidantes biológicos protegem as membranas dependendo da sua localização (meio hidrofílico/meio hidrofóbico), assim como os produtos da reação radical/antioxidante poderão interferir com as características membranares. Para tal recorreu-se ao uso de diferentes modelos biológicos, nomeadamente com a preparação de micelas, lipossomas e monocamadas de Langmuir, utilizando misturas lipídicas de composição semelhante à das membranas biológicas. Ao longo de todo o trabalho realizado foram utilizados calibradores, compostos de referência para estudo de peroxidação lipídica, Trolox e vitamina E.
Foram ainda utilizadas metodologias envolvendo a utilização de sondas fluorescentes por forma a otimizar algumas condições experimentais baseada em metodologia simples, a serem utilizadas em estudos de avaliação da peroxidação lipídica, em diferentes localizações da membrana (meio aquoso, interface e meio lipofílico).
Foram estudados modelos biomiméticos distintos em tamanho, número de lamelas e composição como forma de incrementar o conhecimento sobre a forma como estas variações e complexidade interferem dificultando a avaliação da ação oxidante ou antioxidante de diferentes compostos.

Palavras-chave: modelo biomimético, peroxidação, antioxidante

Tables of Contents

Chapter 1

Chapter 3

Chapter 4

Chapter 5

Chapter 6

List of figures

Chapter 1

General introduction

Chapter 2

Material & methods

Chapter 3

Insights about α-tocopherol and Trolox interaction with phosphatidylcholine monolayers under peroxidation conditions through Brewster Angle Microscopy

Chapter 4

Interaction of soluble biological antioxidants with phosphadylcholine monolayers

Figure 6.1. Fluorescence intensity upon reaction time for different concentrations of lipophilic probe C11-BODIPY$^{581/591}$ obtained in the presence of 10 mM of AAPH. The concentration ratio between large unilamellar vesicles of egg L-α-phosphatidylcholine (EPC) and fluorogenic probe was fixed at 300:1, respectively.

Figure 6.2. Fluorescence intensity obtained for fluorescent hydrophilic probe (fluorescein), fluorescent interface probe (5-dodecanoylaminofluorescein, DDAF) and for fluorogenic lipophilic probe C11-BODIPY$^{581/591}$ in the presence of different concentrations (μM) of large unilamellar vesicles of egg L-α-phosphatidylcholine (EPC). Fluorescein was added to LUV suspension immediately before the measurements, while the DDAF and C11-BODIPY$^{581/591}$ were incorporated during vesicles preparation. For experiments using C11-BODIPY$^{581/591}$, the concentration of peroxyl radical generator (AAPH) was fixed at 10 mM. The circles show the EPC concentration selected for further studies.

Figure 6.3. Relative fluorescence intensity (%) of fluorescein (6 nM), DDAF (50 nM) and C11-BODIPY$^{581/591}$ (50 nM) in the presence of large unilamellar vesicles of egg L-α-phosphatidylcholine (EPC) (800 μM) and different concentrations (μM) of peroxyl radical generator AAPH: A) (1) 0, (2) 25, (3) 50, (4) 75, (5) 100, (6) 150, (7) 200; B) (1) 0, (2) 25, (3) 50, (4) 75, (5) 100, (6) 150; C) (1) 5; (2) 10, (3) 25, (4) 50, (5) 75. The arrows indicate the concentration of AAPH (50 mM) that was selected.

Figure 6.4. Relative fluorescence intensity (%) of fluorescein (A and B) and antioxidant capacity (C and D) obtained in the presence of different concentrations of indomethacin (0, 5, 10, 15, 20 μM) and tolmetin (0, 5, 10, 15, 20, 30, 40 μM) in large unilamellar vesicles of EPC (800 μM) and with the AAPH concentration (50 mM). Antioxidant capacity was determined using the following equation, $[(AUC_{Trolox/NSAIDs} - AUC_{blank}) / (AUC_{blank})] \times 100$. For both drugs, AUC was calculated after 240 min. LUV:FL, correspond to the fluorescent intensity obtained by liposomes in the presence of aqueous fluorescent probe (fluorescein) in the absence of peroxyl radical species.

Figure 6.5. Relative fluorescence (%) intensity of lipophilic fluorogenic probe C11-BODIPY$^{581/591}$ in the presence of large unilamellar vesicles of EPC (800 μM), AAPH concentration (50 mM) and different concentrations of Trolox (0, 4, 8, 12, 16, 20 μM), etodolac (0, 5, 10, 15, 20, 30 μM) and indomethacin (0, 5, 10, 15, 20, 30 μM). The numbers (1 to 6) correspond to increasing concentrations of Trolox or NSAIDs. Relative fluorescence was determined by dividing the fluorescence intensity at a given time by the maximum of fluorescence intensity obtained for probe's oxidation in the absence of antioxidant species (see section 2.4).

List of tables

Chapter 1

General introduction

Chapter 3

Insights about α-tocopherol and Trolox interaction with phosphatidylcholine monolayers under peroxidation conditions through Brewster Angle Microscopy

Chapter 4

Interaction of soluble biological antioxidants with phosphadylcholine monolayers

Chapter 5

Evaluation of antioxidant capacity using lipidic biomimetic structures

Chapter 6

High-throughput fluorimetric methodologies for assessment of antioxidant capacity of drugs at different locations of phospholipid bilayer

CHAPTER 1

General introduction

1. INTRODUCTION

1.1 Biological membranes and oxidative stress

1.1.1 Structure and functions of biological membranes

The cells are the basic structural and functional unit of organisms and, at the same time, they are highly organized with many functional organelles constituted by one or more lipid membranes (Demel et al., 1967).

Each biological cell is enclosed by its outer plasma membrane which controls the interaction between the cell and its environment. This applies both to the relatively small cells of bacteria or prokaryotes, which have no cell nucleus and without defined compartments, and to the much larger cells of eucaryotes, which have such a nucleus and compartments delimited. The latter class of cells is present in all animals and plants as well as in single-celled microorganisms such as amoeba or yeast (Lipowsky and Sackmann, 1995). Furthermore, all eukaryotic cells contain internal membranes which represent the boundaries of the internal organelles such as the nucleus, mitochondrial, Golgi complex, chloroplasts, among other structures.

The fluid mosaic model introduced the idea that membranes were formed by a fluid bilayer in which proteins and lipids could move freely (Singer, 1993). Nowadays, the extended fluid mosaic model contemplates additional structural and functional restraints on membrane organization (Vereb et al., 2003).

One general construction principle which has emerged from molecular cell biology is the use of membranes of different composition, organization, complexity and diversity, in order to organize space into different compartments (Lipowsky and Sackmann, 1995).

The basic function of biomembranes is to provide different spatial compartments and to act as a highly selective barriers for the exchange of molecules between the different compartments, sustaining the concentration gradients between theses compartments, fostering signal transduction and mechanical support (Escribá et al., 2008).

As indicated all membranes of eukaryotic cells separate functional compartments, but the cell surface membrane - the plasma membrane - is an extreme. It is the frontier, with different physical and functional properties. The plasma membrane is composed by a lipid bilayer (Edidin, 2003), ensuring the above mentioned functions because it is composed of specific mixtures of different lipids (mainly amphiphilic) and proteins.

Biological membranes are centrally involved in the control and execution of a great variety

of cellular process, thus requiring the maintenance of their proper structure and function (Brown and London, 1998; Kinnunen, 1991; Kinnunen et al., 1994), and this is correlated with their composition, essentially lipid bilayer to which proteins and carbohydrates may be associated or covalently linked.

The lipids are a heterogeneous group, with amphiphilic structure, with a hydrophilic head group and usually two lipophilic hydrocarbon chains. The essential characteristic of the lipids is its insolubility or very low solubility in water. Lipids have also been acknowledged as key elements in numerous processes (Escribá et al., 2008). Despite the matrix of lipids, whose structure and composition is far from simple, due to the number of different lipid molecules found in the plasma membrane (that can exceed 1000). The high number of structures formed by lipids *in vitro* indicates that the structural properties of membranes can greatly vary *in vivo*, since the interaction of lipid molecules to form membranes is not determined by covalent bonds, like it is with amino acids in proteins (Escribá et al., 2008). Membrane lipids can be classified into three main groups: i) Glycerol-based lipids, ii) cholesterol and iii) ceramide-based sphingolipids.

Furthermore, glycerophospholipids can be classified according to their headgroup, originating: phosphatidylethanolamine, phosphatidylcholine, phosphatidylserine, phosphatidylglycerol and phosphatidylinositol 4,5-bisphosphate.

In the membranes, the lipids aggregate and form bilayers, which are two-dimensional systems, with thermodynamic phases, e.g, fluid phase at high temperatures and one or several gel or solid-like phases at low temperatures. Membrane lipids participate in dynamic interactions that facilitate changes in their relative position in membranes, and that determine membrane thickness, surface packing, along with lateral and rotational mobility (Escribá et al., 2008). Hence, it is a difficult task to study the membrane structure because it presents polymorphisms, requiring a variable composition to act as mimetic to the biological membranes (Cullis et al., 1996).

One of the most important components of biomembranes is cholesterol that interacts with the phosphate headgroup of phospholipids, whereas the bulky steroid region interacts with phospholipid acyl chains, bearing an important role in regulating membrane fluity, membrane packing, non-lamellar phase propensity and the formation of microdomains.

The proteins present on membrane, also have many functions, correlated with their position. Their role includes allowing the passage of substances into and out of the cell, acting as receptors of the membrane, receiving signals from substances that carry a message to the cell, promoting the adhesion of adjacent cells in a tissue, working as an anchor point for the cytoskeleton (Cullis et al., 1996). Therefore, most of the important

roles in membranes have been attributed to the membrane proteins. Hence, the proteins can inserted into the membrane or partially integrated into it, being designated as intrinsic or extrinsic proteins, respectively.

The transmembrane proteins have many interactions with lipids pertaining to membranes, because these last molecules interact with amino acids from the proteins in the hydrophobic environment of the membrane core while the interactions taking place at the interface are more less defined, and to a certain extent regulated by the features of the proteins (Escribá et al., 2008).

Furthermore, both lipids and proteins interact for determining the barrier function in the cells and they may be both subjected to regulatory processes in response to pathophysiological situations or nutritional/pharmacological interventions, which in turn may alter the activity and functions of the membrane.(Escribá et al., 2008) Lipids and proteins may respond to environmental situations and conditions, which can promote changes in the structure and function, consequently causing changes in cell functions, their homeostasis, communication and responses.

In conclusion, membranes constitute a meeting point for lipids and proteins, both fulfilling prominent roles in almost all cellular processes.

1.1.2 Lipid peroxidation

The lipids are the most studied components of the membrane, including aspects pertaining to its oxidation, because of they susceptibility, as one important target to attack by free radicals (the direct promoters of peroxidation). Hence, the lipid peroxidation products (Figure 1) are frequently used as to assess indices oxidative stress, usually coming from attack by free radicals to polyunsaturated fatty acids.

Lipid peroxidation plays a central role in many physiologic and pathological processes (Mattson, 2004; Poon et al., 2004a; b; Schnitzer et al., 2007b), and may be promoted by different inducers, as depicted in Figure 2.

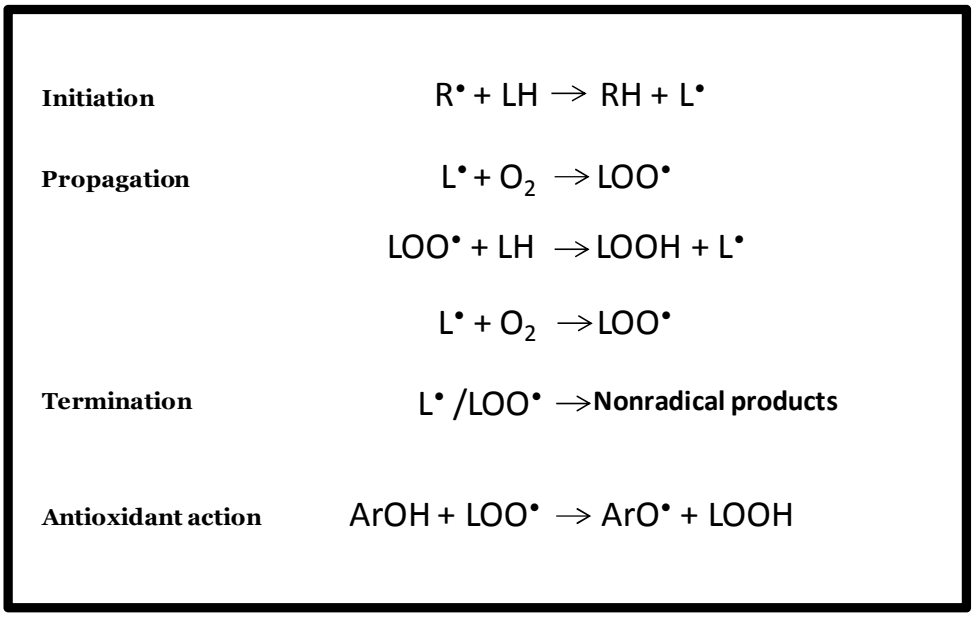

Figure 1.1: Representation of the chain-reaction process and inhibition in the presence of antioxidants. Adapted from (Stojanovic et al., 2001)

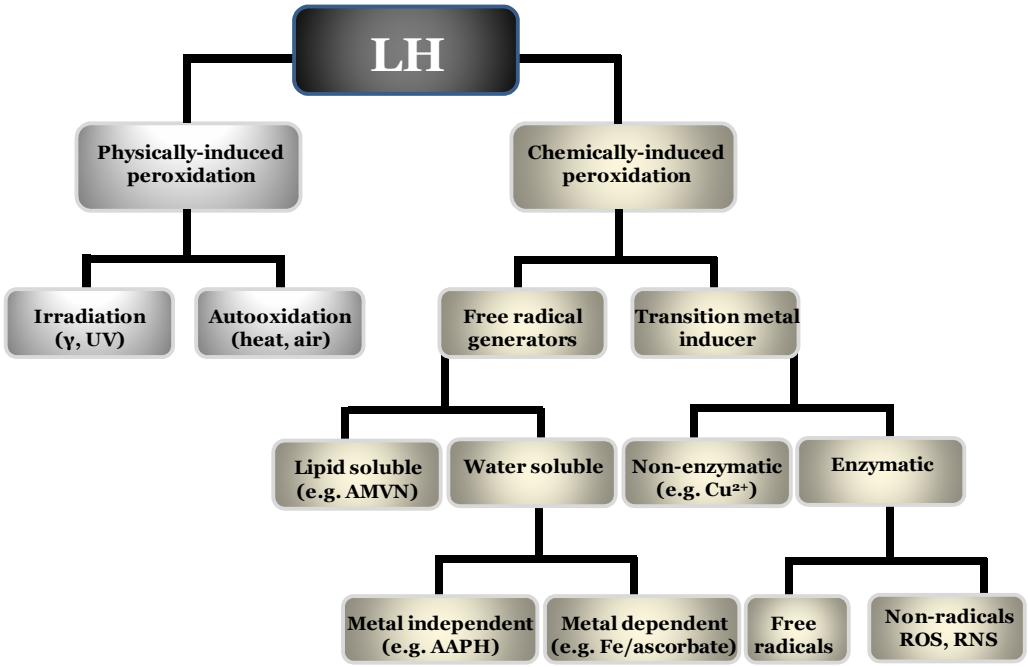

Figure 1.2: Classification of inducers of lipid peroxidation. Adapted from (Schnitzer et al., 2007b)

Therefore, much effort has been devoted to gain understanding about the mechanism responsible for peroxidation, especially in the context of oxidative stress-related diseases.
The lipid compounds representing the end-products of these pathways must bestow significant evolutionary advantages to the cellular or multicellular systems in which they reside, implying particular functional roles for each component (Cullis et al., 1996).
Peroxidation may also be induced by free radicals, that produced within the system (e.g. upon metal-catalyzed decomposition of preformed hydroperoxides). The free radicals, involved in many biochemical and physiological processes, are formed due to the continuous use of oxygen by aerobic cells and their level are kept under control by the different endogenous antioxidants which remove oxidizing species at a similar rate at which they are formed (Gutierrez et al., 2003).

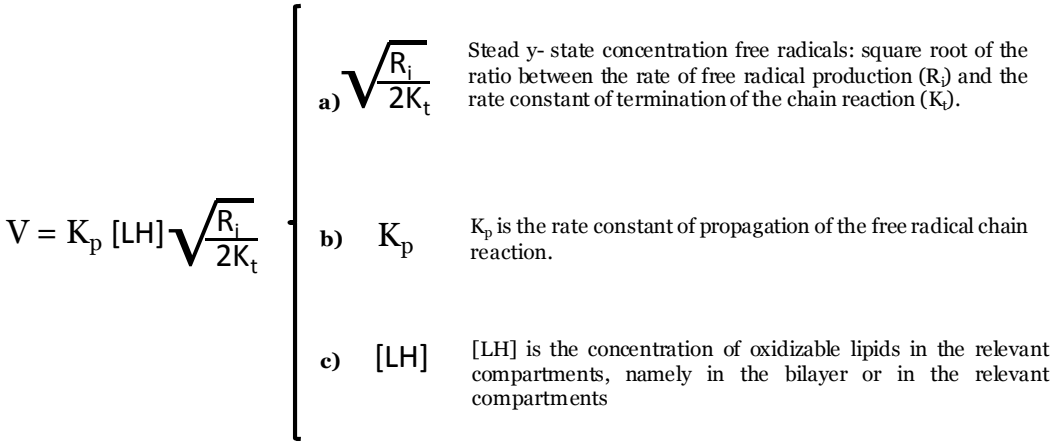

Figure 1.3: Schematic representation of equation and its components applied for calculation of peroxidation rate. Adapted from (Halliwell and Gutteridge, 1999)

The rate of peroxidation (V) is given by Figure3. When the rate of free radical production is constant and the membrane is homogeneous, the dependence of peroxidation on membrane properties is governed by the two rate constants: K_p and K_t. The first is the rate constant of propagation of the free radical chain reaction and second is the rate constant of termination of the chain reaction.
Biomembranes may possess different susceptibility to lipid peroxidation since they contain proteins, antioxidants, cholesterol and different kinds of lipids (Udilova et al., 2003).

1.2 Oxidative stress

All organisms are exposed to stressful conditions such as oxidative stress due to metabolic reactions (Costantini and Verhulst, 2009), but the term "oxidative stress" cannot be defined in universal terms, possibly because there are several types of "oxidative stress" due to the complexity of the biological systems and the mechanism of peroxidation (Dotan et al., 2004). Therefore, the term oxidative stress is defined intuitively and qualitatively, resulting in apparent inconsistencies between the results of different studies where this term is not well defined. The most common definition of oxidative stress is the imbalance between the concentrations of reactive species of oxygen and nitrogen (ROS and RNS, respectively) and the defense mechanisms of the body (Dotan et al., 2004; Pinchuk et al., 2012; Sies, 1986).

Nevertheless, some other definitions are also applicable, namely: 1) The rate at which oxidative damage is generated (Costantini and Verhulst, 2009); 2) Existence or development of oxidative damage attributed to species considered as markers of this type of damage. We proposed that the term oxidative stress of any given type (Dotan et al., 2004) is context-dependent and that oxidative stress evaluation should be based on the use of the most sensitive probe of oxidative damage (Dotan et al., 2004) ; 3) Is possible to quantify the oxidative stress with the ratio between the lag in presence and absence of the studied antioxidant (Pinchuk et al., 2012).

In some definitions for oxidative stress the idea that it is continuous variable and unlikely to ever be exactly zero is implicit since pro-oxidants are continually produced and some oxidative damage is always generated (Costantini and Verhulst, 2009).

The term or concept of the "oxidative stress" appears associated a to lipid peroxidation, because the lipids are labile components of membranes prone to oxidation, and therefore potentially affected causing changes in membrane properties and, consequently, structure and function. In this context, the biomedical literature is full of claims that free radicals and other reactive species (RS) are involved in human diseases (Halliwell and Gutteridge, 2007).

In the Table 1 and 2 presents a list of reactive species (RS) involved in biological oxidative stress.

Table 1.1. Principal reactive species (non radicals) free radicals presents in organism. Adapted from (Halliwell and Gutteridge, 2007).

Free radicals	Nomenclature	Types	Formula
Reactive oxygen species	**ROS**	Superoxide	$O_2^{\bullet -}$
		Hydroxyl	$OH^{\bullet}$
		Hydroperoxyl	$HO_2^{\bullet}$
		Carbonate	$CO_3^{\bullet -}$
		Peroxyl	$RO_2^{\bullet}$
		Alkoxyl	$RO^{\bullet}$
		Carbon dioxide	$CO_2^{\bullet -}$
		Singlet	$O_2{}^1\sum g^+$
Reactive chlorine species	**RCS**	Atomic chloride	$Cl^{\bullet}$
Reactive Bromine species	**RBS**	Atomic bromine	$Br^{\bullet}$
Reactive nitrogen species	**RNS**	Nitric oxide	$NO^{\bullet}$
		Nitrogen dioxide	$NO_2^{\bullet}$
		Nitrate	$NO_3^{\bullet}$

Table 1.2. Principal reactive species (non radicals) presents in organism. Adapted from (Halliwell and Gutteridge, 2007)

Non radicals	Nomenclature	Types	Formula
Reactive oxygen species	**ROS**	Ozone	O_3
		Singlet oxygen	$^1O_2$
		Hydrogen peroxide	H_2O_2
		Hypochlorous acid	HOCl
		Peroxynitrite anion	$ONOO^-$
		Peroxynitrite anion	$ONOO^-$
		Peroxynitrous acid	ONOOH
		Alkyl peroxynitrite	ROONO
		Nitroxyl anion	NO^-
		Nitrosyl cation	NO^+
		Nitronium anion	NO_2^+
		Nitrous acid	HNO_2
		Dinitrogen trioxide	N_2O_3
		Dinitrogen tetraoxide	N_2O_4
		Nitryl chloride	NO_2Cl

1.3 Consequences to membrane and organisms exposed to oxidative stress

Peroxidation of lipids, particularly polyunsaturated fatty acid residues (PUFA) of phospholipids and cholesterol esters, and consequently, oxidative stress in cells and organism, is a process of marked implications (Pinchuk et al., 2012), therefore it is generally accepted that such an imbalance plays a pivotal role in many pathologies (Dotan et al., 2004).

The consequences of oxidative stress can include any, or any combination of, the following, to an extent that depends on the cell type and the severity of the oxidative stress, including increased proliferation, adaptation of the cell or organism by upregulation of defence systems (completely protecting against damage or protecting against damage to some extent but not completely or over protect), cell injury, senescence, and ultimately cell death (Halliwell and Gutteridge, 2007).

For an organism exposed to oxidative stress, it is important to evaluate its "oxidative status" from the composition of its body fluids and tissues with respect to oxidation products, promoters and/or inhibitors of peroxidation.

Regarding membrane biophysics, it is possible to establish a causal relationship between chemical and biophysical consequences of lipid peroxidation (Schnitzer et al., 2007b). Essentially, the peroxidation of polyunsaturated fatty acid residues of membrane phospholipids result in changes of the membrane composition, which also alter the physical properties of the membrane (Schnitzer et al., 2007b).The peroxidation of lipids is usually accompanied by oxidation of membrane proteins (Mattson, 2004), thus, all oxidation processes affect the composition, packing, fluidity, structure and function of the biological membranes. Hence, the but the evaluation of the consequences to membrane is indeed difficult, because of the various and complexes process and consequently, in many cases, the results of different studies are apparently contradictory, namely concerning conclusions regarding "fluidization" or "rigidization" of the biological membranes as consequence of the peroxidation. (De Guidi et al., 2005; Marathe and Mishra, 2002)

Upon these changes in biological membranes, the organisms are affected. In fact, there are various studies in the literature about the effect of oxidative stress and lipid peroxidation

in cytotoxicity, cellular damage, pathogenesis of cancer, genetic alterations, diabetes mellitus, cardiovascular pathologies (atherosclerosis), different malignant diseases (rheumatoid arthritis, cystic fibrosis, intestinal ischaemia), virus infections (including AIDS), and neurodegenerative diseases (Halliwell and Gutteridge, 2007; Schnitzer et al., 2007b; Udilova et al., 2003) (including over 150 disorders)(Costantini and Verhulst, 2009).

However, in most diseases, oxidative stress is a consequence and not a cause of the disease (Figure 1.4), for example, many of the biological consequences of excess radiation exposure are due to oxidative damage and dietary deficiencies (Halliwell and Gutteridge, 2007).

Although it has not been yet conclusively understood if reactive species are a cause or consequence, the answer probably differs for each pathological condition and may even differ from patient to patient depending on his/her antioxidant oxidative defence status.

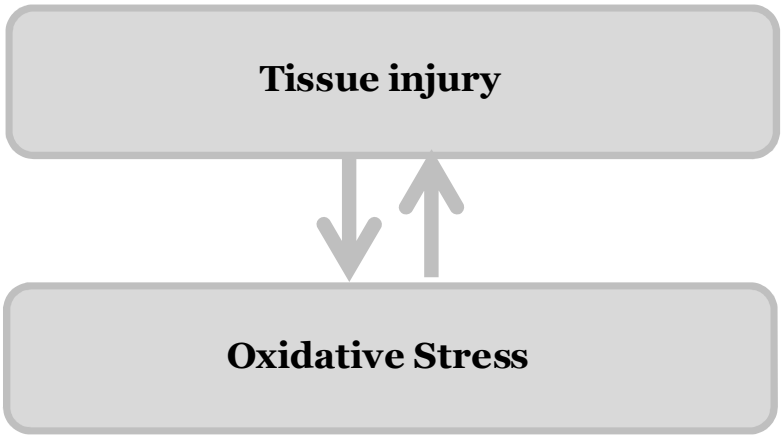

Figure 1.4: Schematic relationship oxidative stress and tissue injury.

All these observations suggest that oxidative stress plays a role in human diseases taking to the proposal that health might be improved by increased dietary intake of antioxidants (Ames et al., 1993), because there exist a health balance between oxidants (such as free radicals) and antioxidants (such as vitamins E and C and protective enzymes) in vivo (Baublis et al., 2000). Beyond these, drugs (including both prescription only and over the counter medicines) with antioxidant indications may also have a functional relationship between health status and disease state (Aruoma, 1996; Pryor, 1982). This role that food and drugs might play in the management of health is shown schematically in Figure 1.5.

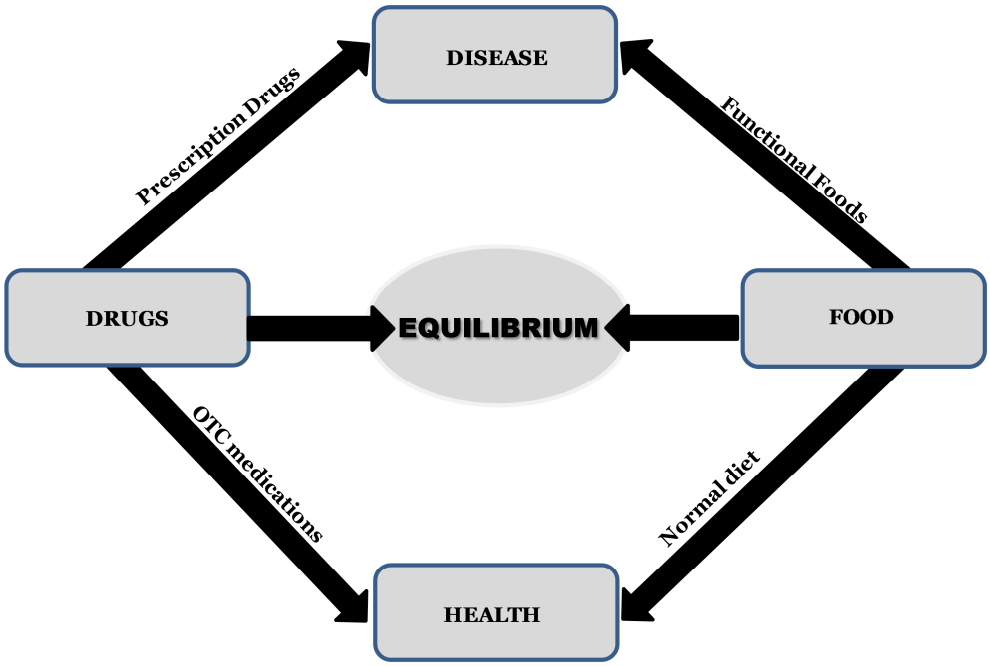

Figure 1.5: Representation of the relationship between Food and/or drugs with Equilibrium, health or disease. Adapted from (Aruoma et al., 1998)

1.4 Biomimetic sytems

Over time, the need to study the structure and dynamic changes in biomembranes (and consequently in the organisms) couple to addressing the problem of applying methodologies that are not comparable to biological systems, biomimetic systems, such as liposomes, have been employed (Lúcio et al., 2007) in order to try to make conditions more closer to those found in vivo.

Several types of model structures have been employed so far, including here liposomes. Liposomes are in fact an important system in their own right in medical, cosmetic and industrial applications (Samuni et al., 2000), however, in many cases their instability upon storage is one of the major obstacles to their more spread use.

For investigating the basic characteristic of lipid membranes, simpler models, such as micelles, are also applicable. They are usually formed by a surfactant, for example miltefosine (hexadecylphosphocholine, HePC). HePC is an current used as alternative

drug to reduce and postpone the emergence of resistance of the protozoan parasite *Leishmania donovani* (usually fatal if untreated) upon conventional therapy for Visceral Leishmaniasis with pentavalent antimonials (Menez et al., 2007; Rangel-Yagui et al., 2005). Furthermore, HePC is a structural analogue of phospholipids, therefore a good and simple biomimetic system that, form a micellar system, which have been used to increase the aqueous solubility of hydrophobic compounds. However, in order to have formation of micelles, it is necessary to use concentrations higher than critical micellar concentration (CMC), which can pose problems for expensive lipids or can cause spectral interferences upon measurements.

Liposomes constitute a system used in investigation for commercial application (cosmetic area, among others), medical and pharmaceutical industry (as previously mentioned) with special attention to its physical properties, protocol for preparation, formation and fusion mechanism, pH gradients, membrane transport, capabilities, and interaction with biological structures (Santos, 2002). Indeed, liposomes are colloidal vesicles where a membrane is formed by one or more phospholipids (having a hydrophobic tail and a hydrophilic head to assemble the vesicular structures) bilayers. Liposomes have been classically applied as a drug carriers, as many kinds of molecules can be encapsulated in this inner phase while hydrophobic molecules can be trapped in the bilayer of the lipid membrane. In addition, liposomes can be modified with different molecules anchored at the surface, applied as biomimetic systems (Kojima et al., 2008), with special interest to areas, mostly due to their well characterized membrane properties.

The liposomes most frequently used are the large unilamellar vesicles (LUVs), with diameters larger than 100 nm and the small unilamellar vesicles (SUVs), with diameters between 20 to 50 nm. There structure is well bearing simple interpretation for interaction phenomena, comparatively to multilamellar vesicles. There are also oligolamellar vesicles (OVs), namely SOV, LOV and GOV, corresponding to small, large and giant variants, respectively (Figure 1.6).

Beyond the size and lamellar number, the chemical nature of the phospholipids that constitute of utmost importance because they determine other parameters of the vesicles structures, namely the charge, the stability, the membrane phase, the curvature of bilayer(s) and the formation of domains.

Other model frequently applied as a membrane surrogate is composed by monolayers, which have been known considerably longer before than micelles or liposomes. The amphiphilic nature of the substances dictates the orientation of the molecules at the interface (air/water). Lipid monolayers are very well defined, stable, homogeneous bidimensional systems with planar geometry. Although monolayers do not reflect the

complexity of membrane structure, they are considered useful models to learn about interactions at interfaces (Deleu et al., 2005) a 2D system.
Therefore, the various available models of biomembranes: micelles, liposomes and monolayers, can be select for the studies pertaining to interactions with biological membranes. In Figure 5 the structure of these models, concerning its size and lamellarity, are represented.
As mentioned previously, it is possible to study many properties/characteristics of the biological membranes with the use of liposomes, including their applications to studies of peroxidation of liposomal lipids.

1.5 Methods for assessments of antioxidants

In biological systems, the oxidation of membrane and lipoprotein lipids plays a central role in many pathology processes (Mattson, 2004; Poon et al., 2004a), especially in the context of oxidative stress-related pathologies referred to above. The aerobic organisms survive only in presence of oxygen, necessarily producing free radicals. Therefore, the antioxidant defences are extremely important in this mechanism as inhibitors of lipid peroxidation. The antioxidants can be synthetized *in vivo* or taken in from the diet. Similarly to the therms "oxidative damage" and "oxidative stress", is the term "antioxidant" widely used but surprisingly difficult to define clearly (Halliwell and Gutteridge, 2007). In this context, there is also is an increasing interest in the efficacy of antioxidant activity of the inumerous naturally occurring molecules in food and biological systems, with potential to minimize oxidative damage *in vivo* and/or to retard the oxidation of easily oxidizable materials food (Lúcio et al., 2007).
Several methods have been applied to measure antioxidant capacity of tissues, biological fluids or single classes of antioxidants, usually with the aim to quantify oxidative stress (Halliwell and Gutteridge, 2007) or protection conferred by foreign compounds.

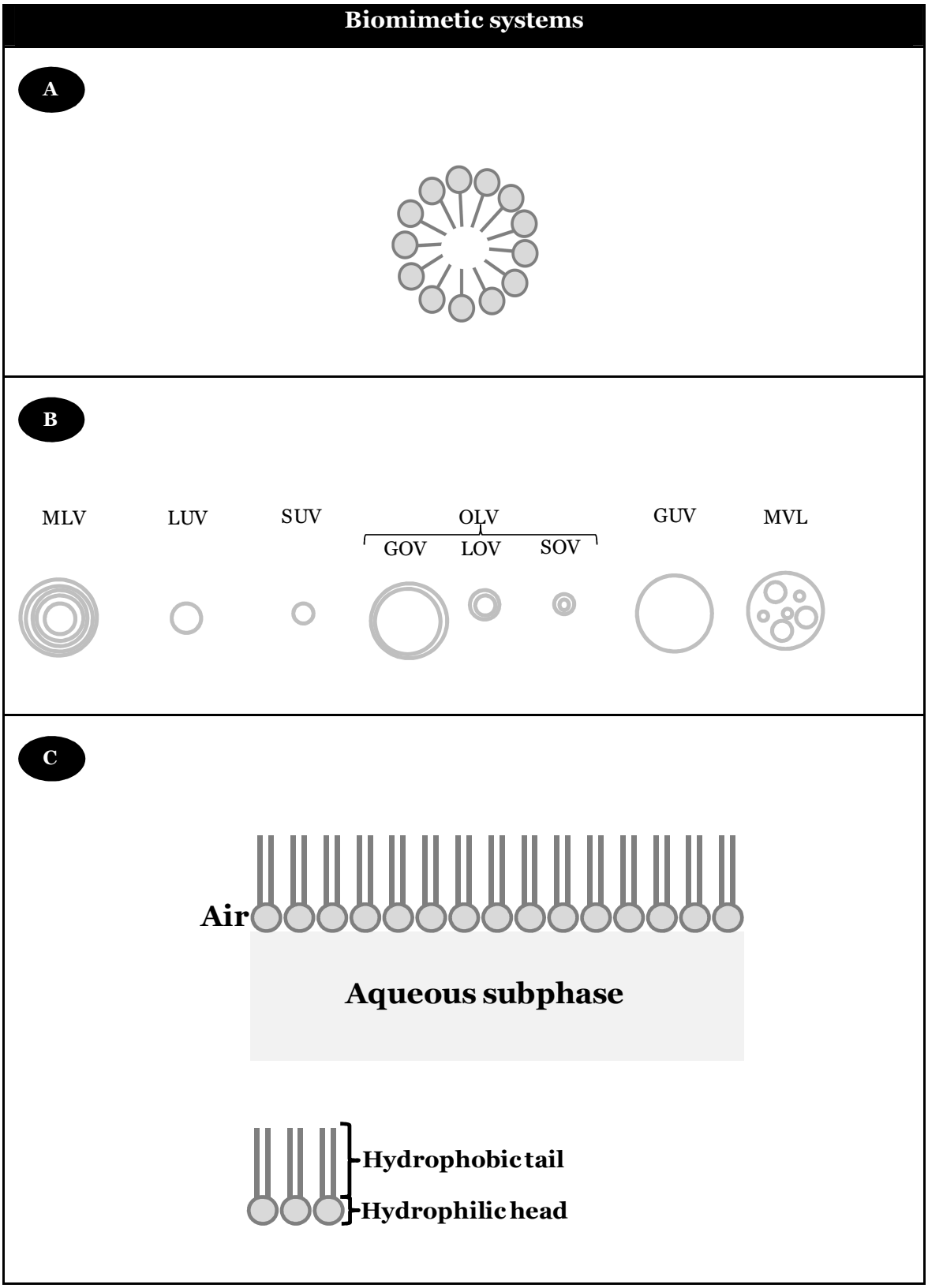

Figure 1.6: Schematic illustration of : **(A)** structure of the micelles; **(B)** liposomes structure (size and lamellarity); **(C)** Monolayer representation.

The evaluation of antioxidant capacity in matrixes such as plasma, beverages, vegetables, and fruits as well as that of pure compounds (i.e., phenols, peptides) has become a rather disputable issue during the past decade. Methods and data are questioned for providing meaningful information to interested parties (Nenadis et al., 2007). Regardless, current methods are still frequently applied, providing an enormous amount of information in the past few years.

Among the several available methods, they can be classified into two groups, depending on the reaction mechanism: methods based on hydrogen atom transfer (HAT) and methods based on electron transfer (ET) (Huang et al., 2005).

The majority of HAT-based assays apply a competitive scheme (depicted schematically in Figure 7), in which antioxidant compound and target (representing a biomolecule which may be attacked *in vivo*) compete for the reactive species (in this work, represented by thermally generated peroxyl radicals through the decomposition of azo-compounds). Hence, the assessment of antioxidant capacity can also be divided concerning their simple (non-competitive) or more complex (competitive) reaction schemes, as depicted schematically in Figure 1.7:

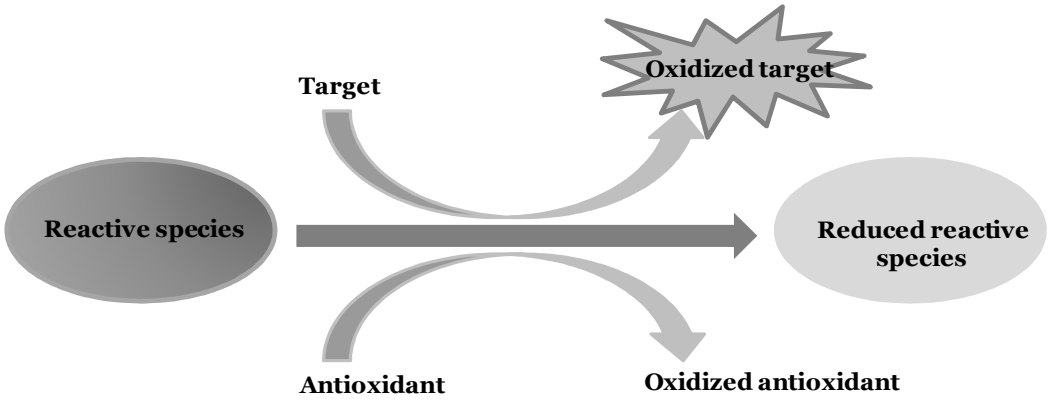

Competitive Shceme

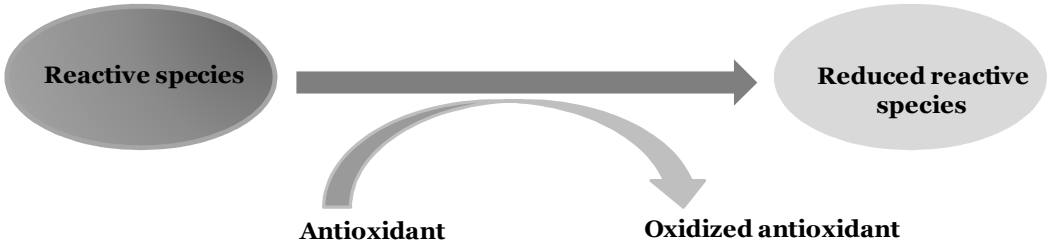

Non-competitive scheme

Figure 1.7: Schematic representation of competitive and non-competitive approaches, for in vitro determination of antioxidant capacity. Adapted from (Magalhães et al., 2008)

In the competitive Scheme, the determination of antioxidant capacity relies on the quantification of an extra compound (probe) that facilitates the analytical measurement. In most of the competitive assay, the probe is the target species or its oxidized form. Moreover, the probe can also be a compound added after the above cited reaction that allows the quantification of the remaining reactive species or target molecules. Using the first type of strategy, the antioxidant capacity of a given compound is dependent on: (i) the concentration ratio of the target, probe, antioxidant and reactive species produced, (ii) the rate of the reaction between antioxidant compound and probe or target molecules, (iii) if the rate of oxidized probe is due only reactive species attack, (iv) rate of target and probe.
On the other hand, in the non-competitive scheme, putative antioxidant compound reacts with the reactive species in the absence of any other competing agent. In this case, only two components are involved in the initial reaction mixture: the antioxidant compound and the reactive species. Therefore, this strategy deploys a reaction simpler than that applied in competitive schemes, suitable for screening assays (Magalhães et al., 2008).

1.6. Scavenging capacity assays against specific ROS/RNS

1.6.1 Peroxyl radical ($ROO^{\cdot}$) scavenging capacity assays

Several methods have been proposed to address these determinations, from which the oxygen radical absorbance capacity (ORAC) and total radical trapping antioxidant parameter (TRAP) are included. Indeed, the ORAC assay is one of the most common

methods for assessing scavenging capacity against ROO· as a HAT method (Frankel and Meyer, 2000), developed initially by Cao, Alessio, and Cutler (1993).

The principle of this assay is based on the intensity of fluorescence decrease of the target/probe along time under reproducible and constant flux of peroxyl radicals, generated from the thermal decomposition of AAPH in aqueous buffer (Magalhães et al., 2008). In the presence of a sample that contains chain-breaking antioxidants, the decay of fluorescence is inhibited. The method measures the ability of the antioxidant in the sample to protect. In ORAC assay, the reaction is monitored for extended periods (≥ 30 min) and the quantifications is based in the area under curve (AUC) that represents the oxidation of the probe along time. The protective effect of antioxidants is evaluated from the net integrated area under the fluorescence decay curves ($AUC_{sample} - AUC_{blank}$) - Figure 1.8, and results are expressed as μM of Trolox equivalents. The advantage of the AUC approach is that it can be applied for antioxidants that exhibit distinct lag phases and also to those samples that have no lag phases. The principles of the ORAC assay can be adapted to determine the action against other reactive oxygen species (Ou et al., 2001). The assay is based on the intensity of fluorescence decrease of the target/probe along time under reproducible and constant flux of peroxyl radicals, generated from the thermal decomposition of AAPH in aqueous buffer. In the presence of a sample that contains chain-breaking antioxidants, the decay of fluorescence is inhibited (Glazer, 1990).

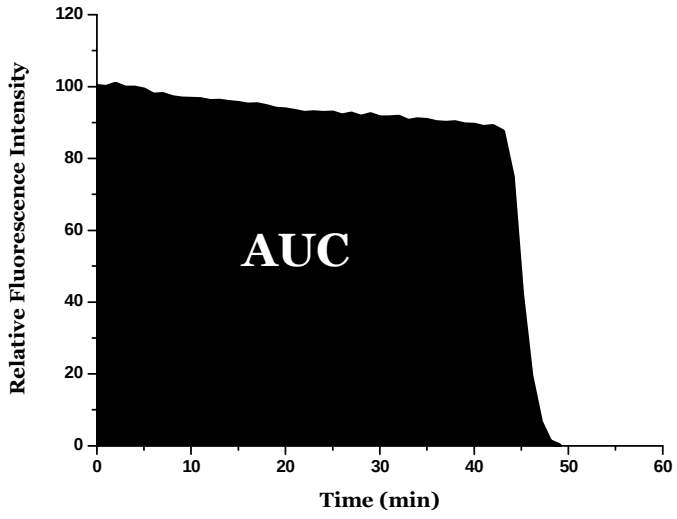

Figure 1.8: Schematic representation from the net integrated area under the fluorescence decay curves.

The TRAP assay was introduced by (Wayner et al., 1985), for the determination of the antioxidant status of human plasma. This method was based on the measurement of the

time period in which oxygen uptake was inhibited by plasma during a controlled ROO· peroxidation reaction induced by the thermal decomposition of an azo-compound. In this assay, the target was the human plasma while the oxygen consumed in the oxidation of plasma material is the probe molecule used to follow the action of antioxidants. The measurement is based on the "lag time" that corresponds to the time period between the beginning of the assay and the beginning of the oxidation of the target molecules. One of the major problems with the original TRAP assay lies in the utilization of the oxygen electrode as detector, since it may not maintain its stability over the period of time required (Magalhães et al., 2008).

1.6.2 Other ROS/RNS scavenging capacity assay

Along with peroxyl radicals, other ROS/RNS subject biological organisms to oxidative stress. A summarized account of current merhods for evaluation of scavenging capacity superoxide radical anion ($O_2^{\cdot-}$), hydroxyl radical (HO·), hypochlorous acid (HOCl), singlet oxygen ($^1O_2$) and nitric oxide radical (NO·) is given in the following paragraphs. A more comprehensive account can be found elsewhere (Magalhães et al., 2008).

Superoxide radical anion ($O_2^{\cdot-}$) is produced as a result of the donation of one electron to oxygen. This radical arises either from several metabolic processes or following oxygen activation by irradiation (Halliwell, 2006). Generally, the analytical methods for determination of $O_2^{\cdot-}$ scavenging capacity make use of the system XOD/hypoxanthine or xanthine at pH 7.4 to generate superoxide anion radical.

Due to the high reactivity of hydroxyl radicals, almost anything in biological systems can be regarded as an HO· scavenger. Hence, this task is not performed by any specific molecule or enzyme. Thus, the evaluation of direct scavenging of HO· may be irrelevant for evaluation of antioxidant action of a compound or matrix, simply because very high concentrations of scavenger are required to compete with adjacent molecules in vivo or in the food matrix for any HO· generated. For these reason, it is more relevant and useful to quantify the capacity of putative antioxidants to scavenge or block the formation of its precursors ($O_2^{\cdot-}$, H_2O_2, HOCl) and/or to sequester free metal ions related to HO· formation. Scavenger compounds that act in in this way would behave as preventive antioxidants.

There are a several in vitro methodologies for determination of HO· scavenging capacity, including: i) absorbance increase due to reaction of thiobarbituric acid with oxidation

products from deoxyribose is inhibited by antioxidants; ii) formation of DMPO-OH adduct is measured by ESR and it is inhibited by antioxidant; iii) DHBA, formed due to oxidation of salicylic acid, measured using HPLC-ED and its formation is inhibited by antioxidants; iv) fluorescence decay along time due to oxidation of fluorescein is delayed/inhibited by antioxidants (ORAC method with different inducer); v) CL emission due to oxidation of luminal is inhibited by antioxidants (Magalhães et al., 2008).

HOCl is generally obtained from the enzymatic system myeloperoxidase/H_2O_2/Cl^- or by acidifying commercial sodium hypochloride to pH 6.2 with sulphuric acid(Aruoma, 1997). The former approach can be applied if the sample species do not interfere with HOCl generation (e.g. inhibition of myeloperoxidase activity or direct reaction with H_2O_2). In the second approach, the determination of the concentration of HOCl solution must be performed daily (Halliwell et al., 1995). For assessment of scavenging capacity against HOCl, direct spectrophotometric determination of this species along time is performed. Alternative methods are based on luminal-derived chemiluminescence.

Singlet oxygen ($^1O_2$) is an excited state of molecular oxygen that has no unpaired electrons and it is known to be a powerful oxidizing agent, reacting directly with a wide range of biomolecules (Davies, 2004). Due to its decay to the lower energy ground state, $^1O_2$ emits characteristic phosphorescence at 1270 nm. Therefore, the $^1O_2$ scavenging ability of several compounds was measured through the decay rates of the light intensity (Tournaire et al., 1993; Wilkinson et al., 1995).

NO has emerged as a fundamental signaling molecule regulating virtually every critical cellular function, as well as a potent mediator of cellular damage in a wide range of conditions. Recent evidence indicates that most of the cytotoxicity attributed to NO is rather due to peroxynitrite -nitric oxide radical ($NO^{\cdot}$), for this reason it has indeed pivotal role in the regulation of diverse physiological and pathophysiological processes (Pacher et al., 2007).

Vriesman et al. developed a relatively simple method for the quantification of $NO^{\cdot}$ scavenging capacity of sulfur-containing compounds in aqueous solution using an amperometric $NO^{\cdot}$ sensor. The assessment of $NO^{\cdot}$ scavenging capacity has also been performed using ESR spectrometry (Asanuma et al., 2001) and fluorimetry.

1.6.3 Scavenging capacity assays against stable, non-biological radicals and evaluation of total reduction capacity

Several methods have been reported for evaluation of total antioxidant capacity, namely those relying on colored radicals, 2,2'-azinobis-(3-ethylbenzothiazoline-6-sulphonate) radical cation ($ABTS^{\bullet+}$) and 2,2′-Azinobis-(3-ethylbenzothiazoline-6-sulphonate) radical cation. Other methods, relying to electron transfer, have also been successfully employed, including here Ferric reducing antioxidant power (FRAP assay), Folin-Ciocalteu reducing capacity (FC assay) and Total reducing capacity estimated by electrochemical methods.

The TEAC assay, mediated by $ABTS^{\bullet+}$ species, involves the generation of the long-lived radical cation chromophore $ABTS^{\bullet+}$ which has absorption maxima at 414, 645, 734, and 815 nm. The original TEAC assay, developed by Miller et al., was based on the activation of metmyoglobin, acting as peroxidase, with H_2O_2 to generate ferrylmyoglobin radical, which then reacted with ABTS to form the $ABTS^{\bullet+}$ radical cation (Miller et al., 1993).

In this strategy, the sample to be tested is added previously to the formation of the $ABTS^{\bullet+}$ radicals formed and the lag phase, which corresponds to the delay time in radical formation, is measured (competitive scheme-Figure 7). This method has been executed using commercial available Kits for standardized total antioxidant status measurement in an individual's serum or plasma. The disadvantage is the price and the reagent cost per sample estimated in the Kit-TEAC assay is approximately nine times that in the ORAC assay (Cao and Prior, 1998).

In DPPH assay, the purple chromogen radical 2,2-diphenyl-1-picrylhydrazyl radical ($DPPH^{\bullet}$) is reduced by antioxidant/reducing compounds to the corresponding pale yellow hydrazine (Magalhães et al., 2008). The scavenging capacity is generally evaluated in organic media by monitoring the absorbance decrease at 515-528 nm until the absorbance remains constant (Magalhães et al., 2008) or by electron spin resonance (Calliste et al., 2001).

The FRAP assay measures the ability of antioxidants to reduce the ferric 2,4,6-tripyridyl-s-triazine complex $[Fe(III)\text{-}(TPTZ)_2]^{3+}$ to the intensely blue coloured ferrous complex $[Fe(II)\text{-}(TPTZ)_2]^{2+}$ in acidic medium (Benzie and Strain, 1996; 1999). This method has also been adapted to 96-well microplate reader, giving better reproducibility and higher sample throughput (Tsao et al., 2003).

The exact chemical nature of the Folin-Ciocalteu reagent is not known, but it is accepted that is contains phosphomolybdic/phosphotungstic acid complexes (Singleton and Rossi, 1965). The chemistry behind the FC assay relies on the transfer of electrons in alkaline medium from phenolic compounds and other reducing species to molybdenum, forming

blue complexes that can be detected spectrophotometrically at 750-765 nm (Singleton et al., 1999).

Finally, the electrochemical properties of pure compounds, foods, and biological samples may be used for the evaluation to their reducing/antioxidant capacity, since the electric oxidation potential has conceptually relation with the expected antioxidant capacity. This determination has been frequently automated using flow injection analysis schemes (Magalhães et al., 2009).

1.7 Methods for antioxidants assessment with biomimetic structures

A schematic representation of all factors, including physical and chemical features, are depicted in Figure 1.8. It is important to highlight that a major concern in these studies should be the effect of antioxidants depends on both the composition, physical properties and structure (LUV, MLV, SUV, etc) of the liposomal system chosen and the inducer.

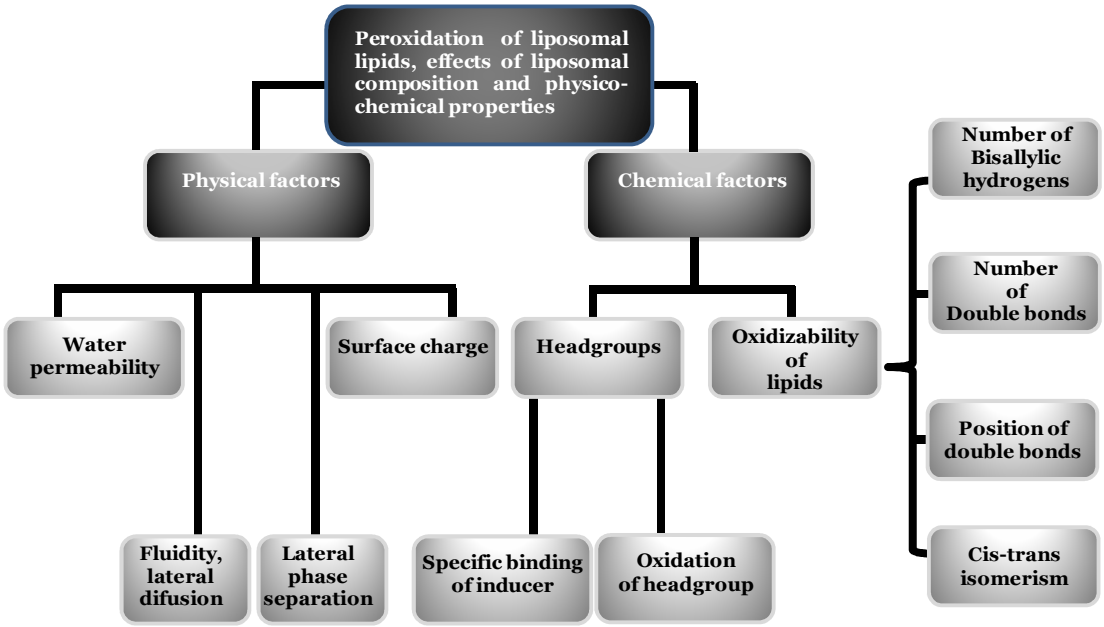

Figure 1.9: Physical and chemical factors that affect the peroxidation of liposomal lipids. Adapted from (Schnitzer et al., 2007b)

In order to illustrate the different conditions used for oxidation/antioxidant evaluation with biomimetic structures, Tables 1.3 to 1.6 are presented, where a summary lipid, preparation method, oxidation initiator, principle of measurement of detection system, calibrator, data treatment, applications, references for each method given. Selected aspects of these methodologies are discussed in the following sections.

1.7.1 Type of biomimetic systems

In studies of lipid peroxidation the biomimetic structures of the biological systems, used were essencially micelles, MLVs, LUVs and SUVs, comprising structures with different lipid composition, size, lamellarity, stability and preparation protocol, whose nomenclature was defined in the 1980s.

As discussed before, liposomes are classified by their lamellarity and size range (Figure 5). Both these aspects are relevant towards lipid peroxidation for at least two reasons: i) they constitute a simple and convenient system where the oxidation process can be reproduced with different levels of complexity and ii) liposomes are currently being used for diagnostic and therapeutic purposes and lipid oxidation may impair their stability.

Concerning their complexity features, all structures being about advantages and disadvantages. For instance, the MLVs have a more simpler preparation comparatively for LUVs and SUVs, but the interpretation of results may not be so easy because the structure is not well defined, with several lipidic layers.

Therefore, when using MLVs in the presence of inducers of oxidation the outer monolayer is more to oxidative attack, but the layer inside are not accessible.

Hence, unilamellar liposomes seem to be a more suitable model for studding the free radical oxidation that take place *in vivo*, because biomembranes, in general, consist of unilamellar structures. The LUVs have a more resemblance with the biological membrane structure but studies as those performed by Barclay et al (1987) demonstrated that the oxidizability of PC in unilammelar liposomes was higher than that in multilamellar liposomes, because of the different packing of the lipid chain in LUV compared to that in MLV. Furthermore, despite the more complex LUV preparation its size is well defined.

Table 3 Methods for assessment of antioxidant capacity using LUVs.

Lipid	Preparation method	Oxidation Initiator	Principle of Measurement or Detection System	Calibrator	Data treatment	Applications	Reference
DPPC +LA	Lipid dissolution organic solvent, evaporation of solvent, hydration with Tris buffer pH 7.4, vortex agitation, extrusion	AAPH	Absorbance measurement at 233 nm due to formation of conjugate dienes	α-tocopherol	% inhibition of oxidation	n.a	(Castelli et al., 1997)
Egg or Soybean PC	Lipid dissolution organic solvent, evaporation of solvent, hydration with Tris-HCl buffer pH 7.4, vortex agitation, sonication, extrusion	AAPH or AMVN (was mixed with PC before preparing liposomes)	HPLC quantification of formation of PC hydroperoxides	n.a	Rate of initiation and rate of peroxidation	n.a	(Koga et al., 1997)
PC	Lipid dissolution organic solvent, evaporation of solvent, hydration with Tris-HCl buffer pH 7.4, vortex agitation, sonication, extrusion	AAPH	HPLC quantification of formation of PC hydroperoxides	BHT	Evaluation of hydroperoxides concentration vs time profile	Extracts of cereal grains	(Zielinski and Kozlowska 2000)
PC or DMPC	Lipid dissolution organic solvent, evaporation of solvent, hydration with Hepes buffer pH 7.4, extrusion	Cu(II)	Measurement of TBARS (absorbance at 530 nm) and peroxides (SCN^- method)	n.a	Evaluation of malondialdehyde (MDA) equivalents vs time profile	Xanthophylls	(Rengel et al., 2000)
Egg PC	Lipid dissolution organic solvent, evaporation of solvent, hydration with Hepes buffer pH 7.4, extrusion	n.a	Measurement of changes on acyl chain composition (GC)	n.a	Evaluation of residual fraction of acyl chains along time	Estimation of liposome oxidation upon storage in presence of tempol and α-tocopherol	(Samuni et al., 2000)
Soybean PC	n.g	AAPH	HPLC quantification of conjugated dienes	n.a	Evaluation of PC-OOH formation along time; rate of oxidation	Newly synthesized compounds (4GBE43 and 2BBE43) and α-tocopherol	(Ezure et al., 2001)

Table 3 Methods for assessment of antioxidant capacity using LUVs (continuation).

Lipid	Preparation method	Oxidation Initiator	Principle of Measurement or Detection System	Calibrator	Data treatment	Applications	Reference
β-arachidonoyl-δ-palmitoyl-L-α-phosphatidylcholine	Lipid dissolution organic solvent, evaporation of solvent, hydration with Tris buffer, pH 7.4, ultrafiltration	Fe(II) or AAPH	Measurement of absorbance at 234 nm due to formation of conjugated dienes and measurement of TBARS (absorbance at 532 nm)	HETE (for CD measurement)	% inhibition of oxidation	Carotenoids	(Chen and Djuric 2001)
DHA-PC	Lipid dissolution in organic solvents, solvent evaporation, hydration with distilled water, vortex agitation, sonication, filtered 0.45 μm pore	Fe(II)	Measurement of TBARS (absorbance at 532 nm)	n.a	MDA equivalents	Tea Catechins	(Tang et al., 2002)
PC	Lipid hydration with TRIS -HCl buffer pH =7.4, vortex agitation ultrasonication, extrusion	AAPH	HPLC quantification of formation of PC hydroperoxides	n.a	Evaluation of time related changes in peroxides content	Pea seed coat extract	(Troszynska et al., 2002)
Ethanolamine plasmalogen or egg yolk phosphatidylethanolamine	Lipid dissolution in organic solvents, evaporation of solvent, hydration, vortex agitation, extrusion	AAPH	CL-HPLC quantification of formation of PC hydroperoxides	n.a	Evaluation of time related changes in peroxides content (PCOOH and CHOOH)	Ethanolamine plasmalogens	(Maeba et al., 2002)
PC	Lipid dissolution in organic solvents, evaporation of solvent, hydration with phosphate buffer pH 7.4, vortex agitation, extrusion	ABAP	Monitoring of the fluorescence increase for oxidation of the probe Bodipy at λ_{exc}= 540 nm; λ_{m}=600 nm	n.a	Evaluation of the % lipid peroxide formation	Nitrates and nitrites	(Nicolescu et al., 2002)
PC	Lipid dissolution in organic solvents, evaporation of solvent, hydration with Tris-HCL buffer pH 7.4 containing DTPA, vortex agitation, extrusion	AAPH	HPLC quantification of formation of PC hydroperoxides	n.a	Evaluation of the % inhibition due to calibration curve	Ferrulic acid and its compounds	(Kikuzaki et al., 2002)

Table 3 Methods for assessment of antioxidant capacity using LUVs (continuation).

Lipid	Preparation method	Oxidation Initiator	Principle of Measurement or Detection System	Calibrator	Data treatment	Applications	Reference
1-stearoyl-2-linoleoyl-sn-glycerol-3-phosphocholine (SLPC) and fluorescence probe	Lipid dissolution in organic solvents, solvent evaporation, hydration with buffer (NaCl; EDTA; MOPS) and extrusion	Fe(II)·$4H_2O$	Measurement of the fluorescence decrease pf DPH-PA (λ not given)	n.a	Relative fluorescence	Seed coat methanol extracts, tannin fractions, and pure flavonoids	(Beninger and Hosfield 2003)
DPPC	Lipid dissolution in organic solvents, solvent evaporation, hydration with a solution of rose bengal in D_2O and extrusion	Laser excitation	Laser excitation of rose bengal at 532 nm	n.a	Decay of singlet oxygen/concentration of antioxidant tested	Carotenoids	(Cantrell et al., 2003)
Egg PC	Lipid dissolution in organic solvents, solvent evaporation, hydration with Tris-HCl buffer, vortex agitation, ultrasonication, extrusion	AAPH	Absorbance measurement (λ not given) due to hydroperoxides formation	α-tocopherol and L-ascorbic acid	Rate of peroxidation	Isolated compounds (ethyl acetate soluble fraction, n-hexane extract, water soluble fraction,dichloro methane extract)	(Hisamoto et al., 2003)
Not specified	Lipid dissolution in organic solvents, solvent evaporation, hydration, vortex agitation, extrusion	Fe(III)ADP or Fe(II)/H_2O_2 or AAPH	Absorbance at 532 nm due for formation of TBARS products and fluorescence from DPH-PA (λ_{Exc}=360nm; λ_{Em}=430 nm)	n.a	% inhibition or relative fluorescence values	Phenolic compounds and α-tocopherols	(Gutierrez et al., 2003)
Soybean PC	Lipid dissolution in organic solvents, hydration with sodium phosphate buffer solution pH 7.4, vortex agitation, sonication, extrusion	AAPH	Measurement of absorbance at 234 nm due to formation of conjugated dienes	n.a	Lag phase	Fruits and vegetables	(Roberts and Gordon 2003)

Table 3 Methods for assessment of antioxidant capacity using LUVs (continuation).

Lipid	Preparation method	Oxidation Initiator	Principle of Measurement or Detection System	Calibrator	Data treatment	Applications	Reference
PC	Lipid dissolution in organic solvents, solvent evaporation, hydration with phosphate buffer pH 7.4, vortex agitation, extrusion	Nitroxides	Measurement of absorbance at 234 nm due to formation of conjugated dienes	n.a	Measurement of the % of nitroxides in liposomes at different time points	Aromatic nitroxides	(Gabbianelli et al., 2004)
Soybean PC	Lipid dissolution in organic solvents, solvent evaporation, hydration with phosphate buffer pH 7.4, extrusion	-	Absorbance at 532 nm due for formation of TBARS products	n.a	Measurement % inhibition	α-Carotene, β-carotene, lutein and lycopene	(Shi et al., 2004)
liposomal PE-DHA/phosphatidylcholine, PE-AA/phosphatidylcholine, PLE/phosphatidylcholine, and PC-DHA/phosphatidylcholine	Solvent evaporation, hydatrion with Hepes buffer pH 7.6, frozenin liquid nitrogen, sonication, extrusion	AAPH	Absorbance at 420 nm due to trinitrophenyl products	n.a	Unoxidized liposomes at various times	Different types of liposomes	(Kubo et al., 2005)
DOPC and DPPH	Lipid dissolution in organic solvents, solvent evaporation , hydration with distilled water, vortex agitation, extrusion	n.a	Magnetic field Gauss Electron spin resonance spectra	n.a	DPPH scavenging efficiency of gallic acid derivatives	Polyphenols (gallic acid and its derivatives)	(Lu et al., 2006)
Egg PC	Lipid dissolution in organic solvents, solvents evaporation, hydration with Tris-HCl buffer+DTPA pH 7.4, vortex agitation, extrusion	AAPH	Absorbance at 235 nm due to hydroperoxides	Trolox	Inhibition hydroperoxides formation	Lupinus albus L. var. Multolupa	(Frias et al., 2005)
Soybean PC	Sonication	Cu(II) acetate	Absorbance measurement at 234 nm due to conjugate dienes	n.a	% inhibition of conjugated diene hydroperoxides and hexanal production after 72 h of incubation	Isolated phenolic compounds of olive pulp and olive oil	(Morello et al., 2005)

Table 3 Methods for assessment of antioxidant capacity using LUVs (continuation).

Lipid	Preparation method	Oxidation Initiator	Principle of Measurement or Detection System	Calibrator	Data treatment	Applications	Reference
L-α-phosphatidylcholine	Lipid dissolution in organic solvents, solvents evaporation, hydration with Hepes buffer, extrusor	AAPH or DPPH antiradical	HPLC quantification of formation of hydroperoxides	Trolox	Monitoring oxygen consumption (lag phase) and by measuring the formation of conjugated dienes	Blueberry (Vaccinium myrtillus) extract and two respective anthocyanin-derived extracts	JAFC2005Faria(Faria et al., 2005)
Soybean PC and antioxidants solution	Lipid dissolution in the organic solvents, solvent evaporation, hydration with phosphate buffer pH (not given), vortex agitation, sonication, extrusion	AAPH	Absorbance at 234 nm due to conjugated dienes	n.a	Indution period (IP) for the formation CD	α-tocopherol and the homologues tocotrienols and carotenoids	(Schroeder et al., 2006)
1 stearoyl-2-linoleolyl-sn-glycerol-3-phosphocholine	Lipid dissolution in DMF with DPH-PS, evaporation, re-hydration in MBSE buffer at pH=7, extrusion	Fe(II).4H_2O	Fluorescence measurement of DPH-PA at 384 nm	BHA	Relative fluorescence	Extracts of Hibiscus sabdariffa	(Christian et al., 2006)
PE, cholesterol, dicetylphosphate and quercetin	Dry lipid film dissolution in sodium phosphate buffer, sonication, extrusion and covalently coupled with p-aminophenyl-a-D-mannoside	n.s	Absorbance at 234 nm (formation of conjugated dienes)	n.a	% inhibition	Flavonoids	(Sarkar and Das 2006)
Soybean PC	Lipid dissolution in organic solvents, solvents evaporation, hydration with phosphate buffer, vortex agitation, sonication, extrusion	AMVN or AAPH	Absorbance measurement at 245 and 268 nm due to conjugated diene hydroperoxides	n.a	Lag phase	Puerarin and β-carotene	(Han et al., 2007)

Table 3 Methods for assessment of antioxidant capacity using LUVs (continuation).

Lipid	Preparation method	Oxidation Initiator	Principle of Measurement or Detection System	Calibrator	Data treatment	Applications	Reference
Egg PC prepared with or without lutein or spin labelled lutein	Lipid dissolution in organic solvents, solvents evaporation, hydration with phosphate buffer, vortex agitation, sonication, extrusion	AMVN or (Fe(HQ)3)/ascorbate - modified Fenton reaction using ferric-8-hydroxyquinoline (Fe(HQ)3)	Absorbance at 532 nm due for formation of TBARS products	n.a	Lutein and a nitroxide spin label 3-carbamoyl-2,2,5,5-tetramethylpyrrolidin-1-yloxy (3-CP)	Spin-labelled lutein	(Broniowska et al., 2007)
Soybean PC	Lipid dissolution in organic solvents, solvents evaporation, hydration with phosphate buffer, vortex agitation, sonication, extrusion	(Becker et al., 2007)	Absorbance measurement at 245 and 268 nm due to conjugated diene hydroperoxides	Quercetin	Induction period (IP in min)	Neat sunflower oil, methyl linoleate o/W emulsion	(Becker et al., 2007)
Egg PC	Lipid dissolution in CHCl3/CH3OH, solvents evaporation, hydration with potassium phosphate buffer pH, vortex agitation, extrusion	AAPH	Fluorescence measurement from fluorescein or DPH-PA at λ_{exc}=485 nm; λ_{em}=528 nm	n.a	Fluorescence decay	Phenolic compounds	(Esteves et al., 2008)
Phospholipid	Lipid dissolution in organic solvents, solvents evaporation, hydration with Hepes buffer pH 7.4, vortex agitation, extrusion	ABAP	Measurement of oxygen consumption XXX	n.a	Slope of oxygen consumption	Resveratrol	(Fabris et al., 2008)
Soybean PC	Lipid dissolution in organic solvents, solvents evaporation, hydration, vortex agitation, extrusion	AMVN or AAPH	Absorbance measurement at 234 nm due to formation of conjugated dienes	n.a	Lag phase	Diadzein	JAFC2008Liang(Liang et al., 2008)
Soybean PC	Lipid dissolution in organic solvents, solvents evaporation, hydration, vortex agitation, extrusion	AAPH	Absorbance measurement at 234 nm due to formation of conjugated dienes	n.a	Lag phase	Antioxidants bioconjugate library	(Hunneche et al., 2008)

Table 3 Methods for assessment of antioxidant capacity using LUVs (continuation).

Lipid	Preparation method	Oxidation Initiator	Principle of Measurement or Detection System	Calibrator	Data treatment	Applications	Reference
EPC or DMPC	Lipid dissolution in organic solvents, solvents evaporation, hydration, vortex agitation, extrusion	n.s	Fluorescence at 330-450 nm	n.a	Fluorescence intensity	Ubiquinol-10	(Fiorini et al., 2008)
EPG	Lipid dissolution in organic solvents, solvents evaporation, hydration with TES and EDTA pH 7.4, extrusion	n.s	Absorbance (λ not given)	α-tocopherol	% membrane fusion, % CF leakage	Steady-state anisotropy of membrane lipids	(Hincha 2008)
PC	Lipid dissolution in organic solvents, solvents evaporation, hydration with phosphate buffer pH 5.5-8.5 or citric buffer pH 3.0, vortex agitation, extrusion	AAPH	Fluorescence measurement of C11-BODIPY581/591 at λ_{exc}=505 nm; λ_{em}=520 nm	n.a	Increase in fluorescence intensity of C11-BODIPY581/591	Daidzein	(Dwiecki et al., 2009)
Soybean PC and AMVN	Lipid dissolution in organic solvents, solvents evaporation, hydration with phosphate buffer pH 7.4, sonication, extrusion	AMVN	Absorbance measurement at 234 nm due to conjugated dienes	n.a	Absorbance changes, lag phase	Flavonoids and isoflavonoids	(Han et al., 2009)
Phospholipid	Lipid dissolution in organic solvents, solvents evaporation, hydration with Hepes buffer pH 7.4, vortexed, extruded	-	Absorbance (λ not given)	n.a	% inhibition	Flavonoids and caffeic acid derivatives	(Gregoris and Stevanato)

(n.a – not applicable; n.g – not given)

Table 5 Methods for assessment of antioxidant capacity using SUVs.

Lipid	Preparation method	Oxidation Initiator	Principle of Measurement or Detection System	Calibrator	Data treatment	Applications	Reference
Soybean PC	Lipid dissolution organic solvent, evaporation of solvent, hydration with potassium phosphate buffer pH 7.4, vortex agitation, sonication, centrifugation	Ferric chloride/ADP	Fluorescence increase from reaction of glycine (amine) with aldehydes (derived from lipid oxidation) at $\lambda_{exc=}$360, $\lambda_{em=}$430 nm	n.a	Lag time	Validation of methodology for cell organelles	(Tirmenstein et al., 1999)
DPPC	Lipid dissolution organic solvent, evaporation of solvent, hydration with phosphate buffer pH 7.4, sonication	n.a	Quenching of ketyl radical, formed from UV radiation of pyridoxal-5´-phosphate, measured by absorbance decay at 440 nm	n.a	Quenching rate constants	Pure compounds	(Ledbetter and Schaertel, 1998)
PC	Lipid dissolution organic solvent, evaporation of solvent, hydration with phosphate buffer pH 7.4, sonication	AAPH	Measurement of conjugate dienes (absorbance at 235 nm), PUFA (GC) and peroxides(SCN^- method)	n.a	Evaluation of hydroperoxides concentration vs time profile	Polar carotenoids from marine bacterium	(Matsushita et al., 2000)
PC	Lipid dissolution organic solvent, evaporation of solvent, hydration with Tris buffer pH 7.4, vortex agitation, sonication	AAPH or AMNV or Fe(III)/-ascorbate or UV-C irradiation	Measurement of TBARS (absorbance at 530 nm) and peroxides (SCN^- method) with fluorimetric detection (λ_{exc}=515 nm; λ_{em}=555 nm	n.a	Evaluation of TBARS/mg Lipid vs time profile	Catechin monomers, procyanidins fractions	(Lotito et al., 2000)
Soybean LCT	Lipid dissolution in PBS pH 7.4, sonicated	Cu(II) or AAPH	Measurement of absorbance at 234 nm due to formation of conjugated dienes	n.a	Lag phase duration and rate of propagation	Bamboo leaf extract	(Hu and Kitts, 2000)
LCT	Lipid dissolution in phosphate buffer pH 7.4, sonicated	Fe(III)/ascorbate	Measurement of TBARS (absorbance at 532 nm) and peroxides (SCN^- method)	n.a	% inhibition of oxidation	Water extracts of roasted and unroasted barley	(Duh et al., 2001)

Table 5 Methods for assessment of antioxidant capacity using SUVs (continuation).

Lipid	Preparation method	Oxidation Initiator	Principle of Measurement or Detection System	Calibrator	Data treatment	Applications	Reference
Dry PLPC or to PLPC lyophilized	Lipid dissolution in organic solvents, vortex agitation, sonication	Cu(II)	Measurement of conjugate dienes (234 nm), dienals (268 nm) and turbidity (325 nm)	n.a	Lag time and rate of absorbance change	Pure compounds	(Bittner et al., 2002)
Egg PC	Lipid dissolution in organic solvents, hydration with sodium phosphate buffer solution pH 7.4 or water, sonication	Fe(II)	Absorbance at 532 nm due for formation of TBARS products	α-tocopherol	Evaluation of MDA equivalents (nmol/mg phospholilpid) vs time profile	Lycopene	(Balachandran and Rao, 2003)
PC:PS	Lipid dissolution in organic solvents, solvent evaporation, hydration with Tris-HCl buffer pH 7.4, vortex agitation, sonication	AMVN	Decay in fluorescence (of the DPH or Bodipy) with (λ_{Exc}=540nm; λ_{Em}=600 nm)	n.a	% initial fluorescence	Flavanols (epicatechin, catechin) and their related oligomers, the procyanidins	(Verstraeten et al., 2003)
PC	Lipid dissolution in organic solvents, solvent evaporation, hydration with phosphate dibasic pH 7.0, sonication, centrifugation	Fe(III)/ ascorbate or AAPH	Absorbance at 532 nm due for formation of TBARS products	-	Evaluation of the % inhibition and oxidative activity	Natural antioxidants for foods: ground beef	(Diaz and Decker, 2004)
PC-protein	Lipid hydration, sonication	Cu(II) acetate	Measurement of absorbance at 234 nm due to formation of conjugated dienes, hydroperoxides and formation of hexanal	α-tocopherol	% inhibition	Berry extracts - Anthocyanins, ellagitannins, and proanthocyanidins from raspberry (Rubus idaeus), bilberry (Vaccinium myrtillus), lingonberry (Vaccinium vitis-idaea), and black currant (Ribes nigrum)	(Viljanen et al., 2004)

Table 5 Methods for assessment of antioxidant capacity using SUVs (continuation).

Lipid	Preparation method	Oxidation Initiator	Principle of Measurement or Detection System	Calibrator	Data treatment	Applications	Reference
Soybean lecithin	Lipid dissolution in phosphate buffer pH 7.4, and sonication	Fe(III)/ascorbate	Absorbance at 533 nm due for formation of TBARS products	n.a	% inhibition	Flavonoid-Rich Extract of Hypericum perforatum L. in Vitro (rutin, hyperoside, isoquercitrin, avicularin, quercitrin, and quercetin)	(Zou et al., 2004)
LCT ethanol solution	Solvent evaporation, hydration with Tris-HCl buffer pH pH 7.4, vortex agitation, sonication	γ rays	Fluorescence	n.a	Degradation of DHA-Et	Flavonoids	(Murata et al., 2004)
Egg LC	Lipid hydration with phosphate buffer pH 7.4, sonication	Fe(III)/ ascorbate	Absorbance at 532 nm due for formation of TBARS products	n.a	% inhibition	Methanol extract and punicalagin of pith and CM of pomegranate fruit and synthetic antioxidant BHA	(Kulkarni et al., 2004)
Soybean	Lipid dissolution in organic solvents, solvent evaporation, hydration with phosphate-buffer saline pH 7.6 and treated with ultrasound	-	Absorbance at 532 nm due for formation of TBARS products	n.a	%inhibition, Oxidation index, peroxide index		(Cimato et al., 2004)
LC	Lipid dissolution in deionized water, sonication	Cu(II) acetate	Absorbance at 234 nm due to conjugated dienes and hexanal formation	α-tocopherol and catechin	%inhibition	Rapeseed Meal Phenolics isolated(aqueous methanol, aqueous ethanol, hot water, and enzymatically with ferulic acid esterase)	(Vuorela et al., 2004)

Table 5 Methods for assessment of antioxidant capacity using SUVs (continuation).

Lipid	Preparation method	Oxidation Initiator	Principle of Measurement or Detection System	Calibrator	Data treatment	Applications	Reference
Egg PC	Lipid dissolution in organic solvents, hydration with Tris:HCl buffer pH 7.4, vortex agitation , sonication	UV radiation from a bactericidal lamp 253.7 nm and TOC	Absorbance at 532 nm due for formation of TBARS products	n.a	% of PC liposome oxidation and % inhibition	Prooxidant action of toxic organometallic compounds (TOC)	(Gabrielska et al., 2004)
LC	Lipid hydration with phosphate buffer pH 7.4, sonicated	Fe(III) /ascorbate	Absorbance at 532 nm due for formation of TBARS products and MDA	n.a	% inhibition	Water extracts of pu-erh tea, various tea extracts and tocopherol	(Duh et al., 2004)
Unsaturated lipid mixture (DPPC, cholesterol, EPC) or saturated lipid mixture (DPPC, cholesterol)	Lipid dissolution in organic solvents, solvents evaporation, hydration with buffer , vortex agitation, sonication and centrifugation	Cu(II), VA-044	Absorbance at 532 nm due for formation of TBARS products	BSA	% inhibition		(Kuzmenko et al., 2004)
LCT	Lipid hydration with phosphate buffer pH 7.4, sonication in an ultrasonic cleaner	Fe(III)/ascorbate	Absorbance at 532 nm due for formation of TBARS products	α-tocopherol	% inhibition	Roasted coffe e residues	(Yen et al., 2005a)
Egg LCT	Lipid hydrated with phosphate buffer pH 7.4, sonication	Fe(III)/ascorbate	Absorbance at 532 nm due to MDA	n.a	% inhibition	Ipomoea aquatica Forsk	(Prasad et al., 2005)
Soybean PC	Sonication	Cu(II) acetate	Absorbance measurement at 234 nm due to conjugate dienes	n.a	% inhibition of conjugated diene hydroperoxides and hexanal production after 72 h of incubation	Isolated phenolic compounds of olive pulp and olive oil	(Morello et al., 2005)

Table 5 Methods for assessment of antioxidant capacity using SUVs (continuation).

Lipid	Preparation method	Oxidation Initiator	Principle of Measurement or Detection System	Calibrator	Data treatment	Applications	Reference
Egg PC	Lipid dissolution in organic solvents, hydration with Hepes buffer, ultrasonic irradiation	Fe(III) - chelate	The rate of **oxygen consumption** associated with lipid peroxidation, assuming an oxygen concentration of 217 nm/mol in the initial.	-	The amount of TBA-reactive substances (TBARS)	Series of vegetables, fruits, and commercial frozen pulps of fruits commonly consumed in Brazil	(Fukuzawa et al., 2005)
LCT	Lipid dissolution in organic solvents, solvents evaporation, hydration with 10 mM sodium phosphate buffer, sonication	DPPH; ABTS	Absorbance; percent inhibition of liposome oxidation compared to control, induced by copper acetate at 37 °C, for 2 h	-	Formation of thiobarbituric reactive compounds	The antioxidant activity of a series of vegetables, fruits, and commercial frozen pulps of fruits commonly consumed in Brazil	(Hassimotto et al., 2005)
Egg LC	Lipid hydrated with phosphate buffer, sonication	Fe(III)/ascorbate	Absorbance at 535 nm due for formation of TBARS products	n.a	% Inhibition	Extracts Hippophae rhamnoides L.	(Negi et al., 2005)
Soybean PC	Lipid dissolution in 0.12 M KCl and 5 mM histidine buffer (pH=6.8), sonication	Fe(III)/$ABTS^{\bullet+}$	Absorbance (λ not given)	Trolox	Inhibition of Lipid Oxidation in a Liposome System; hydrolysis time; [1 - (sample solution absorbance/blank solution absorbance)] *100; TEAC	Corn crop	(Kong and Xiong, 2006)
LCT	Lipid hydration with phosphate buffer pH 7.4, sonication	Fe(III)/ascorbate or ABTS	Absorbance at 700 nm Spectrophotometric	Trolox and α-tocopherol	% Inhibition	Extracts of Cordyceps sinensis (CSE) and Cordyceps militaris (CME)	(Yu et al., 2006)

Table 5 Methods for assessment of antioxidant capacity using SUVs (continuation).

Lipid	Preparation method	Oxidation Initiator	Principle of Measurement or Detection System	Calibrator	Data treatment	Applications	Reference
Lecithin	Suspended in deionized water, sonicated	n.s	Absorbance measurement at 234 nm due to formation of conjugated dienes	n.a	% inhibition	Extracts of R. nutkana, R. pisocarpa, R. woodsii and ascorbic acid	(Yi et al., 2007)
LCT	Lipid dissolution in deionized water and sonication	Cu(II) acetate	Absorbance measurement at 234 nm due to formation of conjugated dienes and Absorbance at 532 nm due for formation of TBARS products	n.a	% inhibition	HFIP60 and its fractions	(Thiansilakul et al., 2007)
Egg LC	Lipid hydration with phosphate buffer pH 7.4, sonication	Fe(III)/ascorbate	Absorbance at 532 nm due for formation of TBARS products	n.a	%inhibition (expressed as IC 50)	Sapota juice, gallic acid, catechin, ascorbic acid, β-carotener	(Kulkarni et al., 2007)
Egg LC	Lipid hydration with phosphate buffer pH 7.4, sonication	Fe(III)/ascorbate	Absorbance at 532 nm due for formation of TBARS products	n.a	%inhibition (expressed as IC 50)	Methanol extract, Dihydromonacolin-MV (Antioxidant properties), BHA	(Dhale et al., 2007)
LCT	Lipid dissolution in organic solvents, solvents evaporation, hydration with phosphate buffer saline pH 7.4, vortex agitation, sonication	n.s	Fluorescence	n.a	Fluorescence intensity	Flavonoids (quercetin and rutin)	(Xi and Guo, 2007)
DPPC	Lipid dissolution in organic solvents, solvents evaporation, hydration with HEPES buffer pH 7.4, sonication	n.s	n.s	n.a	Phase transition temperature	Epicatechin derivatives	(Lazaro et al., 2007)
LCT	Lipid hydration in doubly distilled, sonication	Cu(II)acetate	Absorbance measurement at 245 and 268 nm due to conjugated dienes hydroperoxides	Trolox	Time related changes in hydroperoxides content	Gallic, caffeic, sinapic, uric, and ascorbic acids and isoeugenol	(Nenadis et al., 2007)

Table 5 Methods for assessment of antioxidant capacity using SUVs (continuation).

Lipid	Preparation method	Oxidation Initiator	Principle of Measurement or Detection System	Calibrator	Data treatment	Applications	Reference
Egg PC in absence and presence of 3-HF	Lipid dissolution in organic solvents, solvents evaporation, hydration with water, vortex agitation and sonication	AAPH	Absorbance measurement at 245 and 268 nm due to conjugated dienes and absorbance at 532 nm due for formation of TBARS products	Trolox	% inhibition	3-hydroxyflavone (3-HF)	(Chaudhuri et al., 2008)
Total lipids (n.s)	Lipid dissolution in organic solvents, solvents evaporation, hydration with a saline solution, vortex agitation, sonication	Fe(II) or Fe(III)	Absorbance measurement at 234 and 270 nm due to conjugated dienes and trienes respectively and absorbance at 532 nm due for formation of TBARS products	n.a	Lag phase, slope	Bovine retina	(Fagali and Catala, 2009)
Soybean PC and dicetyl phosphate and chlolesterol	Lipid hydration with Tris HCl pH 7.4, sonication, extrusion	UV radiation	n.s	n.a	n.s	Resveratrol	(Kristl et al., 2009)
PC and α-tocopherol or β-carotene	Lipid dissolution in organic solvents, solvents evaporation, hydration with phosphate buffer pH 7.4, sonication	AMVN	Fluorescence at λ_{exc}=500 nm; λ_{em}=520 nm	n.a	Fluorescence increase (F.U/min)	Antioxidant nutrients	(Yeum et al., 2009)
EPC	Lipid dissolution in organic solvents, solvents evaporation, hydration with tris-HCl buffer, vortex agitation, sonication	Cu(II) ion	Absorbance at 535 nm due for formation of TBARS products	n.a	% inhibition	Plasmalogen	(Wang and Wang)
Soybean phosphatidylcholine	Dissolved in chloroform, dispersed in histidine buffer, vortex agitation, sonication	Fe(III)/ascorbate	Absorbance at 535 nm due for formation of TBARS products	n.a	% inhibition	CooKed pork patties	(Kong et al.)

(n.a – not applicable; n.g – not given)

Table 6 Methods for assessment of antioxidant capacity using other biomimetic systems.

Biomimetic System	Lipid	Preparation method	Oxidation Initiator	Principle of Measurement or Detection System	Calibrator	Data treatment	Applications	Reference
Suspension	DOPC suspension	Lipid dissolution in 20 nM Tris-HCl buffer pH 7.4	AMVN	Fluorescence decay of BODIPY 581/591 C11 (540 and 600 nm)	Trolox	AUC relative to Trolox	α-tocopherol, β-carotene	(Naguib, 1998)
Not specified	Soybean PC	Lipid dissolution organic solvent, evaporation of solvent, vortex agitation, centrifugation	Fe(III)/ascorbate -or AAPH	Measurement of TBARS (absorbance at 530 nm) and peroxides (SCN^- method)	1,1,3,3-tetraethoxypropane (TBARS); cumene hydroperoxide (peroxide)	% liposome oxidation, based on equivalents of calibrator	Water-soluble antioxidants in cereal extracts	(Baublis et al., 2000)
Small vesicles	Egg LC	Lipid dissolution organic solvent, evaporation of solvent, hydration with sodium phosphate buffer pH 7.4, sonication	Fe(III) /ascorbate or H_2O_2	Measurement of TBARS (absorbance at 530 nm) and peroxides (SCN^- method)	n.a	% inhibition of peroxidation	Water extracts of roasted and unrosasted Chinese herb; pure compounds	(Yen and Chuang, 2000)
Not specified/not characterized	Soybean PC	Lipid dissolution organic solvent, evaporation of solvent, hydration with KCl buffer pH 7.0, sonication	Fe(III)/ascorbate	Measurement of TBARS (absorbance at 532 nm)	n.a	TBARS value	Whey protein hydrolysates	(Pena-Ramos and Xiong, 2001)
Not known	Egg PC	Lipid dissolution in 2 mM NaCl solution, pH 6	γ irradiation	Measurement of hydroperoxides (HPLC and iodometric technique) and of deterioration of fatty acid residues (HPLC, λ=207 nm)	n.a	Evaluation of lipid hydroperoxide formation upon irradiation intensity	Pure compounds, including resveratrol	(Stojanovic et al., 2001)

Table 6 Methods for assessment of antioxidant capacity using other biomimetic systems (continuation).

Biomimetic System	Lipid	Preparation method	Oxidation Initiator	Principle of Measurement or Detection System	Calibrator	Data treatment	Applications	Reference
Not specified/not characterized	Egg PC and BhCL	Prepared by reverse-phase evaporation in KCl and Tris-HCl buffer pH 7.4	ADP/Fe(II)	Measurement of TBARS (absorbance at 532 nm); oxygen consumption by Clark-type probe	Tetraethoxypropane	Lag time and % inhibition,	Carotenoids (L-carotene and astaxanthin)	(Goto et al., 2001)
Not specified/not characterized	Soybean LCT	Lipid dissolution in PBS, sonication	AAPH	Measurement of absorbance at 500 nm	n.a	% inhibition	Ethanol extract derived from Rhus Verniciflua Stokes(RVS), Korean plant	(Lim et al., 2001)
Not specified	LC	Lipid hydration with phosphate buffer, sonication	Fe(III)/ascorbate	Measurement of TBARS (absorbance at 532 nm)	n.a	% inhibition	Ethanolic extracts of sesame coat (EESC)	(Chang et al., 2002)
Liposome models not specified	n.s	n.s	Fe(II)	Fluorescence decrease at 384 nm	Positive control: BHA, BHT, TBHQ	Evaluation of the decrease of relative fluorescence intensity along time	Antioxidant Compounds from the Mycelia of the Edible Mushroom Grifola frondosa	(Zhang et al., 2002)
Not specified	1-stearoyl-2-linoleoylsn-glyceryl-3-phosphocholine (SLPC)	Not given	Fe(II) or AAPH	Measurement of the fluorescence decrease (λ not given)	n.a	% inhibition	3-dehydroshikimic acid	(Chang et al., 2003)

Table 6 Methods for assessment of antioxidant capacity using other biomimetic systems (continuation).

Biomimetic System	Lipid	Preparation method	Oxidation Initiator	Principle of Measurement or Detection System	Calibrator	Data treatment	Applications	Reference
Not specified	Not specified	Lipid dissolution in organic solvents, solvent evaporation, hydration, vortex agitation, extrusion	Fe(III)/ascorbate	Cytoprotective effects of NO· against photoinitiated chain peroxidation and necrotic killing	n.a	PC-OOH (mM)	NO·	(Niziolek et al., 2003)
Model liposome	n.s	n.s	Fe(II)	Fluorescence decrease at 384 nm	n.a	Relative fluorescence	Antioxidant compounds of *Agrocybe aegerita*	(Zhang et al., 2003)
Monolayers	DLPC or Phospholipids	hexane/ethanol, evaporation	UV-irradiation	Absorbance (λ not given)	n.a	Area variation, lag phase, % oxidation UV induced	n.a	(Morandat et al., 2003)
Not specified	Egg PC	n.s	AAPH or AMVN	Absorbance (λ not given);	No control	Consumption of oxygen; Fluorescence decay; NADH oxidation by peroxyl radicals, DPBF fluorescence quenched by free radicals	n.a	(Olek et al., 2004)
Not specified	PLPC	Lipid dissolution in organic solvent, co-lyophilization and co-sonication	Cu(II) or AAPH	Absorbance at 245 nm (Mean initial optical density at 245 nm)	n.a	Evaluation of the Hydroperoxides formation	n.a	(Gal et al., 2003)

Table 6 Methods for assessment of antioxidant capacity using other biomimetic systems (continuation).

Biomimetic System	Lipid	Preparation method	Oxidation Initiator	Principle of Measurement or Detection System	Calibrator	Data treatment	Applications	Reference
Not specified	Egg PC	n.s	AAPH	n.s	α-tocopherol and L-ascorbic acid	n.a	Rhizomes of Zingiber officinale Roscoe	(Masuda et al., 2004)
Suspension	Egg PC	n.s	AAPH	Absorbance (λ not given) Spectrophotometric	n.a	% inhibition	Components of the Berries and Pimenta dioica	(Miyajima et al., 2004)
Not specified	n.s	n.s	Fe(III)/ ascorbate	Absorbance at 532 nm due for formation of TBARS products	n.a	% inhibition of peroxidation	Whey protein isolate (WPI)	(Pena-Ramos et al., 2004)
Not specified	n.s	n.s	DPPH Test	Absorbance at 532nm was measured by a Perkin Elmer Lambda 40 Spectrophotometry	n.a	Detect liposome lipid peroxidation (for estimation!) IC50; %inhibition	17 species of Sideritis L. species	(Guvenc et al., 2005)
Not specified	LCT	n.s	Cu(II)acetate	Absorbance measurement at 234 nm due to formation of conjugated dienes	n.a	% inhibition	Grap seeds (catechin and epicatechin)	(Hatzidimitriou et al., 2007)
Not specified	n.s	n.s	Fe(II)	Absorbance at 535 nm due for formation of TBARS products	n.a	% inhibition	Peel (flavedo and albedo) and juice of some commercially grown citrus fruit	(Guimaraes et al.)

(n.a – not applicable; n.g – not given)

1.7.2 Lipids employed

The lipids more used in biomimetic systems preparation are egg phosphatidylcholine and soybean phosphatidylcholine, however other lipids are used in biomimetic systems preparation, such as: 1,2-dihexadecanoyl-sn-glycero-3-phosphocholine (DPPC), 1,2-dilauroyl-sn-glycero-3-phosphocholine (DLPC), 1,2-dioctadecanoyl-sn-glycero-3-phosphocholine (DSPC), 1,2-dimyristoyl-sn-glycero-3-phosphocholine (DMPC), dioleoylphosphatidylcholine (POPC), 1-stearoyl-2-linoleoylsn-glyceryl-3-phosphocholine (SLPC) and linoleic acid.

The EPC is an phosphoslipid containing choline, also named as lecithin. It is the most abundant phospholipid in nature and the most frequently used in biomimetic strutures preparation. Indeed, it is ideal for use in studies as model biological membranes because it is a natural lipid found in these membranes. The lecithin can be extracted from the egg yolk or soybean, comprising a lipid mixture, with carbonyl chains bearing different lengths and different degrees of unsaturation. Typical lots of egg yolk phosphatidylcholine have fatty acid contents of approximately 33% 16:0 (palmitic, the most abundant in lecithin), 13% 18:0 (stearic), 31% 18:1 (oleic), and 15% 18:2 (linoleic), with other fatty acids being minor contributors, givening an average molecular weight of approximately 768. The liposomes from lecithin are zwitterionic, therefore, with neutral charge at physiologic pH. The main drawback of the application of natural lipids is in its complex composition, with consequences for interpretation of results.

DPPC is a semi-synthetic lipid, which can be easily characterized to concerning its phase transition, among other thermodynamic parameters comparatively to natural lipids.

The multilamellar vesicles are prepared by hydration of a lipid film, as referred previously, through an easy and fast method.

The hydration lipid film is a common step in MLVs, LUVs and SUVs preparation because the amphiphilic phospholipids, bearing a hydrophilic group, do not aggregate in micelles, when in aqueous solution, because instead, due to their large structure, they form vesicles, from bilayers that fold, forming closed spherical structures.

In the several examples taken from literature (Table 1.3) Unilamellar vesicles were formed from different mechanical agitation processes, starting from the suspension formed after lipid film hydration. Hence, for LUVs preparation, several techniques were employed namely: De-Rehydration, extrusion, detergente dialisys, reverse evaporation and freeze-thaw cycling. The technique most used is undoubtedly the extrusion because despite being slow and complex, it leads to the formation of the homogeneous structures with well

defined size range, with good stability and very similar to biological structures concerning their bilayer structure.

The SUVs preparation is possible through different techniques: sonication, extrusion, high-pressure homogenization and solvent injection. The first is the technique most used, but references found in the literature do not mention details about the amplitude, numbers of cycle for sonication in order to obtain structures with size ≤ 100 μm.

For preparation micelles a surfactant is used, because these types of molecules have a capacity to form aggregates in aqueous media. The interface area between the hydrocarbon chains of the surfactant and water decrease, consequently the monomers are associated and form aggregates. The polar head is in contact with the aqueous media and hydrophobic tail bears inside the micelle structure. Therefore, the micelles are prepared simply by dispersion in aqueous media.

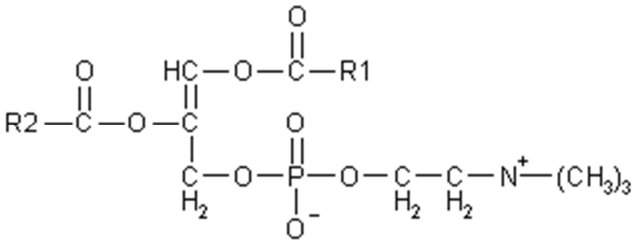

EPC

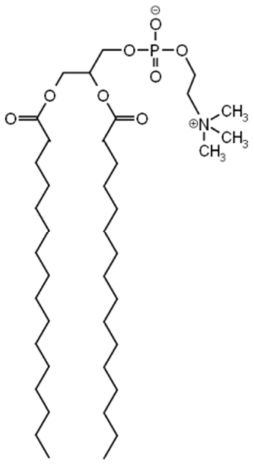

DPPC

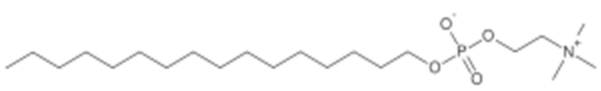

HePC

Figure 1.10: Structure of lipid used in different works. For R1, R2 composition please see text.

1.7.3 Initiator of oxidation

In many reports, the lipid peroxidation is induced by various biologically relevant inducers (e.g. transition metals and enzymes), from which the most commonly inducers are copper and iron ions (commonly applied in the presence of ascorbic acid). Moreover, synthetic radical generators are also often applied. Some of them are water-soluble (e.g. ABAP/AAPH) and others are lipid-soluble (e.g. AMVN) (Schnitzer et al., 2007b).
In fact AAPH is a water soluble azo compound which has been extensively as a free radical generator. In this case the free radicals are formed in solution and attack the external part of liposomes. The decomposition of AAPH produces molecular nitrogen and two carbon radicals. The carbon radicals may combine to produce stable products or react with molecular oxygen to give peroxyl radicals.

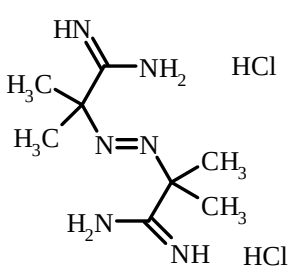

AAPH

2,2′-azobis(2-amidinopropane) dihydrochloride

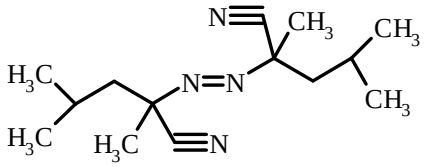

AMVN

2,2′-azobis(2,4-dimethylvaleronitrile)

Figure 1.11. Molecular structure of thermolabile azo-compounds used for generation of peroxyl radicals.

1.7.4 Measurement of oxidation

The measurement of oxidation extent can be performed directly, by measuring the products of oxidation or oxygen consumption, or indirectly, using fluorescent probes that are also prone to oxidation.
Malondialdehyde, arising from peroxidation of PUFAs with more them two double bonds (such as linoleic and arachidonic acids), is frequently determined by the Thiobarbituric

acid method. This method, also called TBARS (from thiobarbituric acid reactive substances), to generates a coloured product, a $(TBA)_2$-MDA adduct, measured spectrophotometrically. However, the application of this method has been disputed (Halliwell and Gutteridge, 2007) because other TBARS are formed along the quantification, biasing the final results.

Other common method of analysis, consist on the measurement of intermediates, namely conjugates dienes. The oxidation of PUFAs forms conjugated dienes that absorb UV light at 230 to 235 nm. Measurement of dienes is a useful index of peroxidation in pure lipids and isolated lipoprotein and has the advantage that it measures an early stage in peroxidation (Halliwell and Gutteridge, 2007). Diene conjugates measurements can rarely be carried out directly on tissues and body fluids because many others substances present absorb strongly in the UV. Extraction of lipids into organic solvents (e.g chloroform:methanol mixture) before measurement is a common approach to this problem.

Finally, measurement of peroxides as end-products of lipid peroxidation has also been carried out, using high performance liquid chromatography or gas chromatography. This approach allows the determination of different reaction products, as they are separated in the chromatographic colunn.

Several membrane-partioning probes, as indirect reports of oxidation, have been introduced to measure lipid peroxidation or reactive species within membranes: 1,6-Diphenyl-1,3,5-Hexatriene, diphenylhexatriene propionic acid, trimethylamine-diphenylhexatriene and another popular probe is C11 Bodipy $^{581/591}$ (upon oxidation, its fluorescence shifts from red to green, so that the green/(red+green) ratio can be used as an estimate of membrane oxidation.

1.7.5 Applications

Application towards aromatic plants, various medicinal and culinary herbs, food products were frequent. Some endemic species are of particular interest for small countries as products with important role as antioxidant. Plant extracts, rich in polyphenols and bioactive compounds, have also been tested.

1.8 References

Ames, B. N.; Shigenaga, M. K.; Hagen, T. M. Oxidants, antioxidants, and the degenerative diseases of aging. *Proceedings of the National Academy of Sciences of the United States of America* **1993,** *90*, 7915-7922.

Aruoma, O. I. Characterization of drugs as antioxidant prophylactics. *Free Radical Biology and Medicine* **1996,** *20*, 675-705.

Aruoma, O. I. Scavenging of hypochlorous acid by carvedilol and ebselen in vitro. *General Pharmacology* **1997,** *28*, 269-272.

Aruoma, O. I.; Deiana, M.; Jenner, A.; Halliwell, B.; Kaur, H.; Banni, S.; Corongiu, F. P.; Dessi, M. A.; Aeschbach, R. Effect of hydroxytyrosol found in extra virgin olive oil on oxidative DNA damage and oil low-density lipoprotein oxidation. *Journal of Agricultural and Food Chemistry* **1998,** *46*, 5181-5187.

Asanuma, M.; Nishibayashi-Asanuma, S.; Miyazaki, I.; Kohno, M.; Ogawa, N. Neuroprotective effects of non-steroidal anti-inflammatory drugs by direct scavenging of nitric oxide radicals. *Journal of Neurochemistry* **2001,** *76*, 1895-1904.

Balachandran, B.; Rao, A. V. Time-dependent uptake and antiperoxidative potential of lycopene in multilamellar liposomes. *Food Research International* **2003,** *36*, 611-616.

Barros, M. P.; Pinto, E.; Colepicolo, P.; Pedersen, M. Astaxanthin and peridinin inhibit oxidative damage in Fe2+-loaded liposomes: Scavenging oxyradicals or changing membrane permeability? *Biochemical and Biophysical Research Communications* **2001,** *288*, 225-232.

Baublis, A.; Decker, E. A.; Clydesdale, F. M. Antioxidant effect of aqueous extracts from wheat based ready-to-eat breakfast cereals. *Food Chemistry* **2000,** *68*, 1-6.

Becker, E. M.; Ntouma, G.; Skibsted, L. H. Synergism and antagonism between quercetin and other chain-breaking antioxidants in lipid systems of increasing structural organisation. *Food Chemistry* **2007,** *103*, 1288-1296.

Beninger, C. W.; Hosfield, G. L. Antioxidant activity of extracts, condensed tannin fractions, and pure flavonoids from Phaseolus vulgaris L. seed coat color genotypes. *Journal of Agricultural and Food Chemistry* **2003,** *51*, 7879-7883.

Benzie, I. F. F.; Strain, J. J. The ferric reducing ability of plasma (FRAP) as a measure of "antioxidant power": The FRAP assay. *Analytical Biochemistry* **1996,** *239*, 70-76.

Benzie, I. F. F.; Strain, J. J. Ferric reducing antioxidant power assay: Direct measure of total antioxidant activity of biological fluids and modified version for simultaneous

measurement of total antioxidant power and ascorbic acid concentration. *Methods in Enzymology* **1999,** *299*, 15-27.

Bittner, O.; Gal, S.; Pinchuk, I.; Danino, D.; Shinar, H.; Lichtenberg, D. Copper-induced peroxidation of liposomal palmitoyllinoleoylphosphatidylcholine (PLPC), effect of antioxidants and its dependence on the oxidative stress. *Chemistry and Physics of Lipids* **2002,** *114*, 81-98.

Broniowska, K. A.; Kirilyuk, I.; Wisniewska, A. Spin-labelled lutein as a new antioxidant in protection against lipid peroxidation. *Free Radical Research* **2007,** *41*, 1053-1060.

Brown, D. A.; London, E. Structure and origin of ordered lipid domains in biological membranes. *Journal of Membrane Biology* **1998,** *164*, 103-114.

Calliste, C. A.; Trouillas, P.; Allais, D. P.; Simon, A.; Duroux, J. L. Free radical scavenging activities measured by electron spin resonance spectroscopy and B16 cell antiproliferative behaviors of seven plants. *Journal of Agricultural and Food Chemistry* **2001,** *49*, 3321-3327.

Cantrell, A.; McGarvey, D. J.; Truscott, T. G.; Rancan, F.; Bohm, F. Singlet oxygen quenching by dietary carotenoids in a model membrane environment. *Archives of Biochemistry and Biophysics* **2003,** *412*, 47-54.

Cao, G. H.; Prior, R. L. Comparison of different analytical methods for assessing total antioxidant capacity of human serum. *Clinical Chemistry* **1998,** *44*, 1309-1315.

Caro, A. A.; Cederbaum, A. I. Antioxidant properties of S-adenosyl-L-methionme in Fe2+-initiated oxidations. *Free Radical Biology and Medicine* **2004,** *36*, 1303-1316.

Castelli, F.; Trombetta, D.; Tomaino, A.; Bonina, F.; Romeo, G.; Uccella, N.; Saija, A. Dipalmitoylphosphatidylcholine/linoleic acid mixed unilamellar vesicles as model membranes for studies on novel free-radical scavengers. *Journal of Pharmacological and Toxicological Methods* **1997,** *37*, 135-141.

Chan, W. K. M.; Faustman, C.; Yin, M.; Decker, E. A. Lipid oxidation induced by oxymyoglobin and metmyoglobin with involvement of H2O2 and superoxide anion. *Meat Science* **1997,** *46*, 181-190.

Chang, L. W.; Yen, W. J.; Huang, S. C.; Duh, P. D. Antioxidant activity of sesame coat. *Food Chemistry* **2002,** *78*, 347-354.

Chang, Y. C.; Almy, E. A.; Blamer, G. A.; Gray, J. I.; Frost, J. W.; Strasburg, G. M. Antioxidant activity of 3-dehydroshikimic acid in liposomes, emulsions, and bulk oil. *Journal of Agricultural and Food Chemistry* **2003,** *51*, 2753-2757.

Chaudhuri, S.; Pahari, B.; Sengupta, B.; Sengupta, P. K. Binding of the bioflavonoid robinetin with model membranes and hemoglobin: Inhibition of lipid peroxidation and protein glycosylation. *Journal of Photochemistry and Photobiology B-Biology 98*, 12-19.

Chaudhuri, S.; Basu, K.; Sengupta, B.; Banerjee, A.; Sengupta, P. K. Ground- and excited-state proton transfer and antioxidant activity of 3-hydroxyflavone in egg yolk phosphatidylicholine liposomes: absorption and fluorescence spectroscopic studies. *Luminescence* **2008,** *23*, 397-403.

Chaudhuri, S.; Pahari, B.; Sengupta, P. K. Ground and excited state proton transfer and antioxidant activity of 7-hydroxyflavone in model membranes: Absorption and fluorescence spectroscopic studies. *Biophysical Chemistry* **2009,** *139*, 29-36.

Chen, G.; Djuric, Z. Carotenoids are degraded by free radicals but do not affect lipid peroxidation in unilamellar liposomes under different oxygen tensions. *Febs Letters* **2001,** *505*, 151-154.

Christian, K. R.; Nair, M. G.; Jackson, J. C. Antioxidant and cyclooxygenase inhibitory activity of sorrel (Hibiscus sabdariffa). *Journal of Food Composition and Analysis* **2006,** *19*, 778-783.

Cimato, A. N.; Piehl, L. L.; Facorro, G. B.; Torti, H. B.; Hager, A. A. Antioxidant effects of water- and lipid-soluble nitroxide radicals in liposomes. *Free Radical Biology and Medicine* **2004,** *37*, 2042-2051.

Costantini, D.; Verhulst, S. Does high antioxidant capacity indicate low oxidative stress? *Functional Ecology* **2009,** *23*, 506-509.

Cullis, R. P.; Fenske, B. D.; Hope, J. M. Physical properties and functional roles of lipids in membranes. *Biochemistry of Lipids, Lipoproteins and Membranes* **1996**, 1-33.

Davies, M. J. Reactive species formed on proteins exposed to singlet oxygen. *Photochemical & Photobiological Sciences* **2004,** *3*, 17-25.

De Guidi, G.; Ragusa, S.; Cambria, M. T.; Belvedere, A.; Catalfo, A.; Cambria, A. Photosensitizing effect of some nonsteroidal antiinflammatory drugs on natural and artificial membranes: Dependence on phospholipid composition. *Chemical Research in Toxicology* **2005,** *18*, 204-212.

Deleu, M.; Paquot, M.; Nylander, T. Fengycin interaction with lipid monolayers at the air-aqueous interface - implications for the effect of fengycin on biological membranes. *Journal of Colloid and Interface Science* **2005,** *283*, 358-365.

Demel, R. A.; Vandeene.Ll; Pethica, B. A. Monolayer interactions of phospholipids and cholesterol. *Biochimica Et Biophysica Acta* **1967,** *135*, 11-&.

Dhale, M. A.; Divakar, S.; Kumar, S. U.; Vijayalakshmi, G. Isolation and characterization of dihydromonacolin-MV from Monascus purpureus for antioxidant properties. *Applied Microbiology and Biotechnology* **2007,** *73*, 1197-1202.

Diaz, M.; Decker, E. A. Antioxidant mechanisms of caseinophosphopeptides and casein hydrolysates and their application in ground beef. *Journal of Agricultural and Food Chemistry* **2004,** *52*, 8208-8213.

Dotan, Y.; Lichtenberg, D.; Pinchuk, I. Lipid peroxidation cannot be used as a universal criterion of oxidative stress. *Progress in Lipid Research* **2004,** *43*, 200-227.

Duh, P. D.; Yen, G. C.; Yen, W. J.; Chang, L. W. Antioxidant effects of water extracts from barley (Hordeum vulgare L.) prepared under different roasting temperatures. *Journal of Agricultural and Food Chemistry* **2001,** *49*, 1455-1463.

Duh, P. D.; Yen, G. C.; Yen, W. J.; Wang, B. S.; Chang, L. W. Effects of pu-erh tea on oxidative damage and nitric oxide scavenging. *Journal of Agricultural and Food Chemistry* **2004,** *52*, 8169-8176.

Dwiecki, K.; Neunert, G.; Polewski, P.; Polewski, K. Antioxidant activity of daidzein, a natural antioxidant, and its spectroscopic properties in organic solvents and phosphatidylcholine liposomes. *Journal of Photochemistry and Photobiology B-Biology* **2009,** *96*, 242-248.

Edidin, M. Timeline - Lipids on the frontier: a century of cell-membrane bilayers. *Nature Reviews Molecular Cell Biology* **2003,** *4*, 414-418.

Escribá, P. V.; González-Ros, J. M.; Goñi, F. M.; Kinnunen, P. K. J.; Vigh, L.; Sánchez-Magraner, L.; Fernández, A. M.; Busquets, X.; Horváth, I.; Barceló-Coblijn, G. Membranes: a meeting point for lipids, proteins and therapies. *Journal of Cellular and Molecular Medicine* **2008,** *12*, 829-875.

Esteves, M.; Siquet, C.; Gaspar, A.; Rio, V.; Sousa, J. B.; Reis, S.; Marques, M. P. M.; Borges, F. Antioxidant versus cytotoxic properties of hydroxycinnamic acid derivatives - A new paradigm in phenolic research. *Archiv Der Pharmazie* **2008,** *341*, 164-173.

Ezure, T.; Kanayama, T.; Nishino, C. Action of the novel antioxidants 4GBE43 and 2BBE43 against lipid peroxidation. *Biochemical Pharmacology* **2001,** *62*, 335-340.

Fabris, S.; Momo, F.; Ravagnan, G.; Stevanato, R. Antioxidant properties of resveratrol and piceid on lipid peroxidation in micelles and monolamellar liposomes. *Biophysical Chemistry* **2008,** *135*, 76-83.

Fagali, N.; Catala, A. Fe2+ and Fe3+ initiated peroxidation of sonicated and non-sonicated liposomes made of retinal lipids in different aqueous media. *Chemistry and Physics of Lipids* **2009,** *159*, 88-94.

Faria, A.; Oliveira, J.; Neves, P.; Gameiro, P.; Santos-Buelga, C.; de Freitas, V.; Mateus, N. Antioxidant properties of prepared blueberry (Vaccinium myrtillus) extracts. *Journal of Agricultural and Food Chemistry* **2005,** *53*, 6896-6902.

Fiorini, R.; Ragni, L.; Ambrosi, S.; Littarru, G. P.; Gratton, E.; Hazlett, T. Fluorescence studies of the interactions of ubiquinol-10 with Liposomes. *Photochemistry and Photobiology* **2008,** *84*, 209-214.

Frankel, E. N.; Meyer, A. S. The problems of using one-dimensional methods to evaluate multifunctional food and biological antioxidants. *Journal of the Science of Food and Agriculture* **2000,** *80*, 1925-1941.

Frias, J.; Miranda, M. L.; Doblado, R.; Vidal-Valverde, C. Effect of germination and fermentation on the antioxidant vitamin content and antioxidant capacity of Lupinus albus L. var. Multolupa. *Food Chemistry* **2005,** *92*, 211-220.

Fukuzawa, K.; Saitoh, Y.; Akai, K.; Kogure, K.; Ueno, S.; Tokumura, A.; Otagiri, M.; Shibata, A. Antioxidant effect of bovine serum albumin on membrane lipid peroxidation induced by iron chelate and superoxide. *Biochimica Et Biophysica Acta-Biomembranes* **2005,** *1668*, 145-155.

Gabbianelli, R.; Falcioni, G.; Lupidi, G.; Greci, L.; Damiani, E. Fluorescence study on rat epithelial cells and liposomes exposed to aromatic nitroxides. *Comparative Biochemistry and Physiology C-Toxicology & Pharmacology* **2004,** *137*, 355-362.

Gabrielska, J.; Soczynska-Kordala, M.; Przestalski, S. Quercetin reduces prooxidant action of organometallic compounds on liposome membranes irradiated with UV. *Polish Journal of Environmental Studies* **2004,** *13*, 509-514.

Gabrielska, J.; Soczynska-Kordala, M.; Hladyszowski, J.; Zylka, R.; Miskiewicz, J.; Przestalski, S. Antioxidative effect of quercetin and its equimolar mixtures with phenyltin compounds on liposome membranes. *Journal of Agricultural and Food Chemistry* **2006,** *54*, 7735-7746.

Gal, S.; Pinchuk, I.; Lichtenberg, D. Peroxidation of liposomal palmitoyllinoleoylphosphatidylcholine (PLPC), effects of surface charge on the oxidizability and on the potency of antioxidants. *Chemistry and Physics of Lipids* **2003,** *126*, 95-110.

Glazer, A. N. Phycoerythrin fluorescence-based assay for reactive oxygen species. *Methods in Enzymology* **1990,** *186*, 161-168.

Goto, S.; Kogure, K.; Abe, K.; Kimata, Y.; Kitahama, K.; Yamashita, E.; Terada, H. Efficient radical trapping at the surface and inside the phospholipid membrane is responsible for highly potent antiperoxidative activity of the carotenoid astaxanthin. *Biochimica Et Biophysica Acta-Biomembranes* **2001,** *1512*, 251-258.

Gregoris, E.; Stevanato, R. Correlations between polyphenolic composition and antioxidant activity of Venetian propolis. *Food and Chemical Toxicology 48*, 76-82.

Guimaraes, R.; Barros, L.; Barreira, J. C. M.; Sousa, M. J.; Carvalho, A. M.; Ferreira, I. Targeting excessive free radicals with peels and juices of citrus fruits: Grapefruit, lemon, lime and orange. *Food and Chemical Toxicology 48*, 99-106.

Gutierrez, M. E.; Garcia, A. F.; de Madariaga, M. A.; Sagrista, M. L.; Casado, F. J.; Mora, M. Interaction of tocopherols and phenolic compounds with membrane lipid components: Evaluation of their antioxidant activity in a liposomal model system. *Life Sciences* **2003,** *72*, 2337-2360.

Guvenc, A.; Houghton, P. J.; Duman, H.; Coskun, M.; Sahin, P. Antioxidant activity studies on selected Sideritis species native to Turkey. *Pharmaceutical Biology* **2005,** *43*, 173-177.

Halliwell, B.; Murcia, M. A.; Chirico, S.; Aruoma, O. I. Free-Radicals and Antioxidants in Food and in-Vivo - What They Do and How They Work. *Critical Reviews in Food Science and Nutrition* **1995,** *35*, 7-20.

Halliwell, B.; Gutteridge, J. M. C., *Free Radicals in Biology and Medicine*. 3rd ed.; Oxford University Press: Oxford, 1999.

Halliwell, B. Phagocyte-derived reactive species: salvation or suicide? *Trends in Biochemical Sciences* **2006,** *31*, 509-515.

Halliwell, B.; Gutteridge, J. M. C., *Free radicals in biology and medicine*. 4th ed.; Oxford University Press: Oxford, 2007.

Han, R. M.; Tian, Y. X.; Becker, E. M.; Andersen, M. L.; Zhang, J. P.; Skibsted, L. H. Puerarin and conjugate bases as radical scavengers and antioxidants: Molecular mechanism and synergism with beta-carotene. *Journal of Agricultural and Food Chemistry* **2007,** *55*, 2384-2391.

Han, R. M.; Tian, Y. X.; Liu, Y.; Chen, C. H.; Ai, X. C.; Zhang, J. P.; Skibsted, L. H. Comparison of Flavonoids and Isoflavonoids as Antioxidants. *Journal of Agricultural and Food Chemistry* **2009,** *57*, 3780-3785.

Hassimotto, N. M. A.; Genovese, M. I.; Lajolo, F. M. Antioxidant activity of dietary fruits, vegetables, and commercial frozen fruit pulps. *Journal of Agricultural and Food Chemistry* **2005,** *53*, 2928-2935.

Hatzidimitriou, E.; Nenadis, N.; Tsimidou, M. Z. Changes in the catechin and epicatechin content of grape seeds on storage under different water activity (a(w)) conditions. *Food Chemistry* **2007,** *105*, 1504-1511.

Hincha, D. K. Effects of alpha-tocopherol (vitamin E) on the stability and lipid dynamics of model membranes mimicking the lipid composition of plant chloroplast membranes. *Febs Letters* **2008,** *582*, 3687-3692.

Hirata, T.; Tanaka, M.; Ooike, M.; Tsunomura, T.; Sakaguchi, M. Antioxidant activities of phycocyanobilin prepared from Spirulina platensis. *Journal of Applied Phycology* **2000,** *12*, 435-439.

Hisamoto, M.; Kikuzaki, H.; Ohigashi, H.; Nakatani, N. Antioxidant compounds from the leaves of Peucedanum japonicum Thunb. *Journal of Agricultural and Food Chemistry* **2003,** *51*, 5255-5261.

Hu, C.; Kitts, D. D. Studies on the antioxidant activity of Echinacea root extract. *Journal of Agricultural and Food Chemistry* **2000,** *48*, 1466-1472.

Hu, C.; Kitts, D. D. Antioxidant, prooxidant, and cytotoxic activities of solvent-fractionated dandelion (Taraxacum officinale) flower extracts in vitro. *Journal of Agricultural and Food Chemistry* **2003,** *51*, 301-310.

Huang, C. H.; He, W. L.; Guo, J. K.; Chang, X. X.; Su, P. X.; Zhang, L. X. Increased sensitivity to salt stress in an ascorbate-deficient Arabidopsis mutant. *Journal of Experimental Botany* **2005,** *56*, 3041-3049.

Hunneche, C. S.; Lund, M. N.; Skibsted, L. H.; Nielsen, J. Antioxidant activity of a combinatorial library of emulsifier - Antioxidant bioconjugates. *Journal of Agricultural and Food Chemistry* **2008,** *56*, 9258-9268.

Jayasinghe, C.; Gotoh, N.; Aoki, T.; Wada, S. Phenolics composition and antioxidant activity of sweet basil (Ocimum basilicum L.). *Journal of Agricultural and Food Chemistry* **2003,** *51*, 4442-4449.

Kikuzaki, H.; Hisamoto, M.; Hirose, K.; Akiyama, K.; Taniguchi, H. Antioxidant properties of ferulic acid and its related compounds. *Journal of Agricultural and Food Chemistry* **2002,** *50*, 2161-2168.

Kinnunen, P. K. J. On the principles of functional ordering in biological-membranes. *Chemistry and Physics of Lipids* **1991,** *57*, 375-399.

Kinnunen, P. K. J.; Koiv, A.; Lehtonen, J. Y. A.; Rytomaa, M.; Mustonen, P. LIPID DYNAMICS AND PERIPHERAL INTERACTIONS OF PROTEINS WITH MEMBRANE SURFACES. *Chemistry and Physics of Lipids* **1994,** *73*, 181-207.

Koga, T.; Takahashi, I.; Yamauchi, R.; Piskula, M.; Terao, J. Kinetic studies on the formation of phosphatidylcholine hydroperoxides in large unilamellar vesicles by azo compounds. *Chemistry and Physics of Lipids* **1997,** *86*, 85-93.

Kojima, C.; Hirano, Y.; Yuba, E.; Harada, A.; Kono, K. Preparation and characterization of complexes of liposomes with gold nanoparticles. *Colloids and Surfaces B-Biointerfaces* **2008,** *66*, 246-252.

Kong, B. H.; Zhang, H. Y.; Xiong, Y. L. Antioxidant activity of spice extracts in a liposome system and in cooked pork patties and the possible mode of action. *Meat Science 85*, 772-778.

Kong, B. H.; Xiong, Y. L. L. Antioxidant activity of zein hydrolysates in a liposome system and the possible mode of action. *Journal of Agricultural and Food Chemistry* **2006,** *54*, 6059-6068.

Kristl, J.; Teskac, K.; Caddeo, C.; Abramovic, Z.; Sentjurc, M. Improvements of cellular stress response on resveratrol in liposomes. *European Journal of Pharmaceutics and Biopharmaceutics* **2009,** *73*, 253-259.

Kubo, K.; Sekine, S.; Saito, M. Primary aminophospholipids in the external layer of liposomes protect their component polyunsaturated fatty acids from 2,2 '-azobis(2-amidinopropane)dihydrochloride-mediated lipid peroxidation. *Journal of Agricultural and Food Chemistry* **2005,** *53*, 750-758.

Kulkarni, A. P.; Aradhya, S. M.; Divakar, S. Isolation and identification of a radical scavenging antioxidant - punicalagin from pith and carpellary membrane of pomegranate fruit. *Food Chemistry* **2004,** *87*, 551-557.

Kulkarni, A. P.; Policegoudra, R. S.; Aradhya, S. M. Chemical composition and antioxidant activity of sapota (Achras sapota Linn.) fruit. *Journal of Food Biochemistry* **2007,** *31*, 399-414.

Kuzmenko, A. I.; Wu, H.; Bridges, J. P.; McCormack, F. X. Surfactant lipid peroxidation damages surfactant protein A and inhibits interactions with phospholipid vesicles. *Journal of Lipid Research* **2004,** *45*, 1061-1068.

Lazaro, E.; Castillo, J. A.; Rafols, C.; Roses, M.; Clapes, P.; Torres, J. L. Interaction of antioxidant biobased epicatechin conjugates with biomembrane models. *Journal of Agricultural and Food Chemistry* **2007,** *55*, 2901-2905.

Lebedev, A. V.; Ivanova, M. V.; Levitsky, D. O. Echinochrome, a naturally occurring iron chelator and free radical scavenger in artificial and natural membrane systems. *Life Sciences* **2005,** *76*, 863-875.

Ledbetter, J. W.; Schaertel, S. Pyridinyl and ketyl radicals of pyridoxal-5 '-phosphate on micellar and liposomal surfaces. *Journal of Photochemistry and Photobiology B-Biology* **1998,** *47*, 12-21.

Li, X. L.; Zhou, A. G.; Han, Y. Anti-oxidation and anti-micro organism activities of purification polysaccharide from Lygodium japonicum in vitro. *Carbohydrate Polymers* **2006,** *66*, 34-42.

Liang, J.; Tian, Y. X.; Fu, L. M.; Wang, T. H.; Li, H. J.; Wang, P.; Han, R. M.; Zhang, J. P.; Skibsted, L. H. Daidzein as an Antioxidant of Lipid: Effects of the Microenvironment in Relation to Chemical Structure. *Journal of Agricultural and Food Chemistry* **2008,** *56*, 10376-10383.

Lim, K. T.; Hu, C.; Kitts, D. D. Antioxidant activity of a Rhus verniciflua Stokes ethanol extract. *Food and Chemical Toxicology* **2001,** *39*, 229-237.

Lipowsky, R.; Sackmann, E., *Handbook of Biological Physics* 1995.

Lotito, S. B.; Actis-Goretta, L.; Renart, M. L.; Caligiuri, M.; Rein, D.; Schmitz, H. H.; Steinberg, F. M.; Keen, C. L.; Fraga, C. G. Influence of oligomer chain length on the antioxidant activity of procyanidins. *Biochemical and Biophysical Research Communications* **2000,** *276*, 945-951.

Lu, Z. B.; Nie, G. J.; Belton, P. S.; Tang, H. R.; Zhao, B. L. Structure-activity relationship analysis of antioxidant ability and neuroprotective effect of gallic acid derivatives. *Neurochemistry International* **2006,** *48*, 263-274.

Lúcio, M.; Ferreira, H.; Lima, J. L. F. C.; Reis, S. Use of liposomes to evaluate the role of membrane interactions on antioxidant activity. *Analytica Chimica Acta* **2007,** *597*, 163-170.

Maeba, R.; Sawada, Y.; Shimasaki, H.; Takahashi, I.; Ueta, N. Ethanolamine plasmalogens protect cholesterol-rich liposomal membranes from oxidation caused by free radicals. *Chemistry and Physics of Lipids* **2002,** *120*, 145-151.

Magalhães, L. M.; Segundo, M. A.; Reis, S.; Lima, J. L. F. C. Methodological aspects about in vitro evaluation of antioxidant properties. *Analytica Chimica Acta* **2008,** *613*, 1-19.

Magalhães, L. M.; Lúcio, M.; Segundo, M. A.; Reis, S.; Lima, J. L. F. C. Automatic flow injection based methodologies for determination of scavenging capacity against

biologically relevant reactive species of oxygen and nitrogen. *Talanta* **2009,** , doi:10.1016/j.talanta.2009.02.006.

Marathe, D.; Mishra, K. P. Radiation-induced changes in permeability in unilamellar phospholipid liposomes (vol 157, pg 685, 2002). *Radiation Research* **2002,** *158*, 666-666.

Masuda, Y.; Kikuzaki, H.; Hisamoto, M.; Nakatani, N. Antioxidant properties of gingerol related compounds from ginger. *Biofactors* **2004,** *21*, 293-296.

Matsushita, Y.; Suzuki, R.; Nara, E.; Yokoyama, A.; Miyashita, K. Antioxidant activity of polar carotenoids including astaxanthin-beta-glucoside from marine bacterium on PC liposomes. *Fisheries Science* **2000,** *66*, 980-985.

Mattson, M. P. Metal-catalyzed disruption of membrane protein and lipid signaling in the pathogenesis of Neurodegenerative disorders. *Redox-Active Metals in Neurological Disorders* **2004,** *1012*, 37-50.

McNulty, H. P.; Byun, J.; Lockwood, S. F.; Jacob, R. F.; Mason, R. P. Differential effects of carotenoids on lipid peroxidation due to membrane interactions: X-ray diffraction analysis. *Biochimica Et Biophysica Acta-Biomembranes* **2007,** *1768*, 167-174.

Menez, C.; Legrand, P.; Rosilio, V.; Lesieur, S.; Barratt, G. Physicochemical characterization of molecular assemblies of miltefosine and amphotericin B. *Molecular pharmaceutics* **2007,** *4*, 281-288.

Miller, N. J.; Rice-Evans, C.; Davies, M. J.; Gopinathan, V.; Milner, A. A Novel Method for Measuring Antioxidant Capacity and Its Application to Monitoring the Antioxidant Status in Premature Neonates. *Clinical Science* **1993,** *84*, 407-412.

Miyajima, Y.; Kikuzaki, H.; Hisamoto, M.; Nakatani, N. Antioxidative polyphenols from berries of Pimenta dioica. *Biofactors* **2004,** *21*, 301-303.

Morandat, S.; Bortolato, M.; Anker, G.; Doutheau, A.; Lagarde, M.; Chauvet, J. P.; Roux, B. Plasmalogens protect unsaturated lipids against UV-induced oxidation in monolayer. *Biochimica Et Biophysica Acta-Biomembranes* **2003,** *1616*, 137-146.

Morello, J. R.; Vuorela, S.; Romero, M. P.; Motilva, M. J.; Heinonen, M. Antioxidant activity of olive pulp and olive oil phenolic compounds of the arbequina cultivar. *Journal of Agricultural and Food Chemistry* **2005,** *53*, 2002-2008.

Murata, Y.; Osaki, K.; Shimoishi, Y.; Baba, N.; Tada, M. Degradation of ethyl docosahexaenoate by gamma-ray irradiation and suppression of this degradation by antioxidants. *Bioscience Biotechnology and Biochemistry* **2004,** *68*, 743-745.

Naguib, Y. M. A. A fluorometric method for measurement of peroxyl radical scavenging activities of lipophilic antioxidants. *Analytical Biochemistry* **1998,** *265*, 290-298.

Negi, P. S.; Chauhan, A. S.; Sadia, G. A.; Rohinishree, Y. S.; Ramteke, R. S. Antioxidant and antibacterial activities of various seabuckthorn (Hippophae rhamnoides L.) seed extracts. *Food Chemistry* **2005,** *92*, 119-124.

Nenadis, N.; Lazaridou, O.; Tsimidou, M. Z. Use of reference compounds in antioxidant activity assessment. *Journal of Agricultural and Food Chemistry* **2007,** *55*, 5452-5460.

Nicolescu, A. C.; Zavorin, S. I.; Turro, N. J.; Reynolds, J. N.; Thatcher, G. R. J. Inhibition of lipid peroxidation in synaptosomes and liposomes by nitrates and nitrites. *Chemical Research in Toxicology* **2002,** *15*, 985-998.

Niziolek, M.; Korytowski, W.; Girotti, A. W. Chain-breaking antioxidant and cytoprotective action of nitric oxide on photodynamically stressed tumor cells. *Photochemistry and Photobiology* **2003,** *78*, 262-270.

Olek, R. A.; Ziolkowski, W.; Kaczor, J. J.; Greci, L.; Popinigis, J.; Antosiewicz, J. Antioxidant activity of NADH and its analogue - An in vitro study. *Journal of Biochemistry and Molecular Biology* **2004,** *37*, 416-421.

Ou, B. X.; Hampsch-Woodill, M.; Prior, R. L. Development and validation of an improved oxygen radical absorbance capacity assay using fluorescein as the fluorescent probe. *Journal of Agricultural and Food Chemistry* **2001,** *49*, 4619-4626.

Pacher, P.; Beckman, J. S.; Liaudet, L. Nitric oxide and peroxynitrite in health and disease. *Physiological Reviews* **2007,** *87*, 315-424.

Panya, A.; Laguerre, M.; Lecomte, J.; Villeneuve, P.; Weiss, J.; McClements, D. J.; Decker, E. A. Effects of Chitosan and Rosmarinate Esters on the Physical and Oxidative Stability of Liposomes. *Journal of Agricultural and Food Chemistry 58*, 5679-5684.

Pena-Ramos, E. A.; Xiong, Y. L. Antioxidative activity of whey protein hydrolysates in a liposomal system. *Journal of Dairy Science* **2001,** *84*, 2577-2583.

Pena-Ramos, E. A.; Xiong, Y. L. L.; Arteaga, G. E. Fractionation and characterisation for antioxidant activity of hydrolysed whey protein. *Journal of the Science of Food and Agriculture* **2004,** *84*, 1908-1918.

Pinchuk, I.; Shoval, H.; Dotan, Y.; Lichtenberg, D. Evaluation of antioxidants: Scope, limitations and relevance of assays. *Chemistry and Physics of Lipids* **2012,** *165*, 638-47.

Poon, H. F.; Calabrese, V.; Scapagnini, G.; Butterfield, D. A. Free radicals and brain aging. *Clinics in Geriatric Medicine* **2004a,** *20*, 329-+.

Poon, H. F.; Calabrese, V.; Scapagnini, G.; Butterfield, D. A. Free radicals: Key to brain aging and heme oxygenase as a cellular response to oxidative stress. *Journals of Gerontology Series a-Biological Sciences and Medical Sciences* **2004b,** *59*, 478-493.

Prasad, K. N.; Divakar, S.; Shivamurthy, G. R.; Aradhya, S. M. Isolation of a free radical-scavenging antioxidant from water spinach (Ipomoea aquatica Forsk). *Journal of the Science of Food and Agriculture* **2005,** *85*, 1461-1468.

Pryor, W. A. Free-radical biology - xenobiotics, cancer, and aging. *Annals of the New York Academy of Sciences* **1982,** *393*, 1-22.

Rangel-Yagui, C. O.; Pessoa, A.; Tavares, L. C. Micellar solubilization of drugs. *Journal of Pharmacy and Pharmaceutical Sciences* **2005,** *8*, 147-163.

Rengel, D.; Diez-Navajas, A.; Serna-Rico, A.; Veiga, P.; Muga, A.; Milicua, J. C. G. Exogenously incorporated ketocarotenoids in large unilamellar vesicles. Protective activity against peroxidation. *Biochimica Et Biophysica Acta-Biomembranes* **2000,** *1463*, 179-187.

Roberts, W. G.; Gordon, M. H. Determination of the total antioxidant activity of fruits and vegetables by a liposome assay. *Journal of Agricultural and Food Chemistry* **2003,** *51*, 1486-1493.

Samuni, A. M.; Lipman, A.; Barenholz, Y. Damage to liposomal lipids: protection by antioxidants and cholesterol-mediated dehydration. *Chemistry and Physics of Lipids* **2000,** *105*, 121-134.

Santos, N. C. A Bala mágica acertou? *Química Nova* **2002,** *25*, 1181-1185.

Sarkar, S.; Das, N. Mannosylated liposomal flavonoid in combating age-related ischemia-reperfusion induced oxidative damage in rat brain. *Mechanisms of Ageing and Development* **2006,** *127*, 391-397.

Schnitzer, E.; Pinchuk, I.; Bor, A.; Leikin-Frenkel, A.; Lichtenberg, D. Oxidation of liposomal cholesterol and its effect on phospholipid peroxidation. *Chemistry and Physics of Lipids* **2007a,** *146*, 43-53.

Schnitzer, E.; Pinchuk, I.; Lichtenberg, D. Peroxidation of liposomal lipids. *European Biophysics Journal with Biophysics Letters* **2007b,** *36*, 499-515.

Schroeder, M. T.; Becker, E. M.; Skibsted, L. H. Molecular mechanism of antioxidant synergism of tocotrienols and carotenoids in palm oil. *Journal of Agricultural and Food Chemistry* **2006,** *54*, 3445-3453.

Severcan, F.; Durmus, H. O.; Eker, F.; Akinoglu, B. G.; Haris, P. I. Vitamin D-2 modulates melittin-membrane interactions. *Talanta* **2000,** *53*, 205-211.

Shi, J.; Kakuda, Y.; Yeung, D. Antioxidative properties of lycopene and other carotenoids from tomatoes: Synergistic effects. *Biofactors* **2004,** *21*, 203-210.

Sies, H. Biochemistry of oxidative stress. *Angewandte Chemie-International Edition in English* **1986,** *25*, 1058-1071.

Singer, S. J., Nicolson, G.L. The fluid mosaic model of the structure of cell membranes. *Science* **1993**, 175:720-31.

Singleton, V. L.; Rossi, J. A. Colorimetry of total phenolics with phosphomolybdic-phosphotungstic acid reagents. *American Journal of Enology and Viticulture* **1965,** *16*, 144-158.

Singleton, V. L.; Orthofer, R.; Lamuela-Raventos, R. M. Analysis of total phenols and other oxidation substrates and antioxidants by means of Folin-Ciocalteu reagent. *Methods in Enzymology* **1999,** *299*, 152-178.

Stojanovic, S.; Sprinz, H.; Brede, O. Efficiency and mechanism of the antioxidant action of trans-resveratrol and its analogues in the radical liposome oxidation. *Archives of Biochemistry and Biophysics* **2001,** *391*, 79-89.

Tang, S. Z.; Kerry, J. P.; Sheehan, D.; Buckley, D. J. Antioxidative mechanisms of tea catechins in chicken meat systems. *Food Chemistry* **2002,** *76*, 45-51.

Thiansilakul, Y.; Benjakul, S.; Shahidi, F. Antioxidative activity of protein hydrolysate from round scad muscle using alcalase and flavourzyme. *Journal of Food Biochemistry* **2007,** *31*, 266-287.

Tirmenstein, M. A.; Ge, X. K.; Elkins, C. R.; Fariss, M. W. Administration of the tris salt of alpha-tocopheryl hemisuccinate inactivates CYP2E1, enhances microsomal alpha-tocopherol levels and protects against carbon tetrachloride-induced hepatotoxicity. *Free Radical Biology and Medicine* **1999,** *26*, 825-835.

Tournaire, C.; Croux, S.; Maurette, M. T.; Beck, I.; Hocquaux, M.; Braun, A. M.; Oliveros, E. Antioxidant Activity of Flavonoids - Efficiency of Singlet Oxygen (1(Delta)G) Quenching. *Journal of Photochemistry and Photobiology B-Biology* **1993,** *19*, 205-215.

Troszynska, A.; Estrella, I.; Lopez-Amores, M. L.; Hernandez, T. Antioxidant activity of pea (Pisum sativum L.) seed coat acetone extract. *Lebensmittel-Wissenschaft Und-Technologie-Food Science and Technology* **2002,** *35*, 158-164.

Tsao, R.; Yang, R.; Young, J. C. Antioxidant isoflavones in Osage orange, Maclura pomifera (Raf.) Schneid. *Journal of Agricultural and Food Chemistry* **2003,** *51*, 6445-6451.

Udilova, N.; Jurek, D.; Marian, B.; Gille, L.; Schulte-Hermann, R.; Nohl, H. Induction of lipid peroxidation in biomembranes by dietary oil components. *Food and Chemical Toxicology* **2003,** *41*, 1481-1489.

Vereb, G.; Szollosi, J. M. J.; Nagy, P.; Farkas, T.; Vigh, L.; Matyus, L.; Waldmann, T. A.; Damjanovich, S.-. Dynamic, yet structured: the cell membrane three decades aflter the singer-Nicolson model. *Proc Natl Acad Sci USA* **2003**, 100: 8053-8.

Verstraeten, S. V.; Keen, C. L.; Schmitz, H. H.; Fraga, C. G.; Oteiza, P. I. Flavan-3-ols and procyanidins protect liposomes against lipid oxidation and disruption of the bilayer structure. *Free Radical Biology and Medicine* **2003,** *34*, 84-92.

Viljanen, K.; Kivikari, R.; Heinonen, M. Protein-lipid interactions during liposome oxidation with added anthocyanin and other phenolic compounds. *Journal of Agricultural and Food Chemistry* **2004,** *52*, 1104-1111.

Vuorela, S.; Meyer, A. S.; Heinonen, M. Impact of isolation method on the antioxidant activity of rapeseed meal phenolics. *Journal of Agricultural and Food Chemistry* **2004,** *52*, 8202-8207.

Wang, G.; Wang, T. The Role of Plasmalogen in the Oxidative Stability of Neutral Lipids and Phospholipids. *Journal of Agricultural and Food Chemistry 58*, 2554-2561.

Wayner, D. D. M.; Burton, G. W.; Ingold, K. U.; Locke, S. Quantitative Measurement of the Total, Peroxyl Radical-Trapping Antioxidant Capability of Human-Blood Plasma by Controlled Peroxidation - the Important Contribution Made by Plasma-Proteins. *Febs Letters* **1985,** *187*, 33-37.

Wilkinson, F.; Helman, W. P.; Ross, A. B. Rate Constants for the Decay and Reactions of the Lowest Electronically Excited Singlet-State of Molecular-Oxygen in Solution - an Expanded and Revised Compilation. *Journal of Physical and Chemical Reference Data* **1995,** *24*, 663-1021.

Wrona, M.; Korytowski, W.; Rozanowska, M.; Sarna, T.; Truscott, T. G. Cooperation of antioxidants in protection against photosensitized oxidation. *Free Radical Biology and Medicine* **2003,** *35*, 1319-1329.

Xi, J. Q.; Guo, R. Interactions between flavonoids and hemoglobin in lecithin liposomes. *International Journal of Biological Macromolecules* **2007,** *40*, 305-311.

Yen, G. C.; Chuang, D. Y. Antioxidant properties of water extracts from Cassia tora L. in relation to the degree of roasting. *Journal of Agricultural and Food Chemistry* **2000,** *48*, 2760-2765.

Yen, W. J.; Chang, L. W.; Lee, C. P.; Duh, P. D. Inhibition of lipid peroxidation and nonlipid oxidative damage by carnosine. *Journal of the American Oil Chemists Society* **2002,** *79*, 329-333.

Yen, W. J.; Chang, L. W.; Duh, P. D. Antioxidant activity of peanut seed testa and its antioxidative componet, ethyl protocatechuate. *Lwt-Food Science and Technology* **2005,** *38*, 193-200.

Yeum, K. J.; Beretta, G.; Krinsky, N. I.; Russell, R. M.; Aldini, G. Synergistic interactions of antioxidant nutrients in a biological model system. *Nutrition* **2009,** *25*, 839-846.

Yi, O.; Jovel, E. M.; Towers, G. H. N.; Wahbe, T. R.; Cho, D. Antioxidant and antimicrobial activities of native Rosa sp from British Columbia, Canada. *International Journal of Food Sciences and Nutrition* **2007,** *58*, 178-189.

Yin, M. C.; Chan, K. C. Nonenzymatic antioxidative and antiglycative effects of oleanolic acid and ursolic acid. *Journal of Agricultural and Food Chemistry* **2007,** *55*, 7177-7181.

Yu, H. M.; Wang, B. S.; Huang, S. C.; Duh, P. D. Comparison of protective effects between cultured Cordyceps militaris and natural Cordyceps sinensis against oxidative damage. *Journal of Agricultural and Food Chemistry* **2006,** *54*, 3132-3138.

Zhang, Y.; Mills, G. L.; Nair, M. G. Cyclooxygenase inhibitory and antioxidant compounds from the fruiting body of an edible mushroom, Agrocybe aegerita. *Phytomedicine* **2003,** *10*, 386-390.

Zhang, Y. J.; Mills, G. L.; Nair, M. G. Cyclooxygenase inhibitory and antioxidant compounds from the mycelia of the edible mushroom Grifola frondosa. *Journal of Agricultural and Food Chemistry* **2002,** *50*, 7581-7585.

Zielinski, H.; Kozlowska, H. Antioxidant activity and total phenolics in selected cereal grains and their different morphological fractions. *Journal of Agricultural and Food Chemistry* **2000,** *48*, 2008-2016.

Zou, Y. P.; Lu, Y. H.; Wei, D. Z. Antioxidant activity of a flavonoid-rich extract of Hypericum perforatum L. in vitro. *Journal of Agricultural and Food Chemistry* **2004,** *52*, 5032-5039.

CHAPTER 2

Materials and methods

2. Material and Methods

2.1. Introduction

In this chapter, reagents and general steps for preparation of solutions that were used throughout this work are described. Furthermore, several aspects related to the ORAC methodology for evaluation of antioxidant capacity of various compounds, the comparative study among of biomimetic lipid aggregates (micelles and vesicles) as *in vitro* models to assess antioxidant capacity against peroxidation, dynamic light scattering (DLS) characterization of the structures used, microplate fluorimetric methodologies to assess antioxidant activity at different locations (hydrophilic medium, interface and lipophilic medium) on phospholipid membranes with optimization procedures and the expression of this parameters and the study of antioxidants (biological and reference) effect at air-water interface for biophysical approach to membrane peroxidation.

2.2. Reagents, solutions and samples

All chemicals used were of analytical reagent grade with no further purification, purchased from several suppliers and stored according to the product information. For the preparation of all solutions, water from Milli-Q system (resistivity > 18 MΩ cm), ethanol, methanol and chloroform pro analysis were used throughout the work.

Standard stock solutions were obtained by rigorous weighing the respective reagent in a Mettler Toledo analytical balance (model AG 285), followed by dissolution in the appropriate solvent (namely water, buffer solution, ethanol, methanol, chloroform, or combinations of these liquids).

The working standards were obtained by rigorous dilution of the stock solution using Gilson micropipettes with disposable tips, volumetric flasks (class A) of different volumes. Micropipettes (models P100, P200, P1000, and P5000, with corresponding maximum capacities of 100, 200, 1000, and 5000 μL) were regularly calibrated with deionised water.

Whenever necessary, pH of solutions was measured using a pH-meter GLP-21 equipped with a combined reference-glass pH electrode (Crison 52-02), namely the phosphate buffer at pH 7.4.
The phosphate buffer volume was heated to 37ºC before the dissolution of the AAPH, allowing the formation of radicals generation in the work described in Chapters 3 and 4.
In all experiments, aqueous/buffer solutions were prepared for water soluble compounds. For compounds that are sparingly soluble in water, solutions containing up to 50% of ethanol (or chloroform:methanol (3:1)) were prepared. For compounds, including antioxidants and fluorimetric probes, with low/very low solubility in water, prior incorporation into the biomimetic structures was performed by dissolving the compound in the organic solvent containing the lipids for monolayer or vesicle preparation.

2.3. Fluorimetric measurements

In this thesis, the ORAC method(Ou et al., 2001) was used in the presence of biomimetic lipid structures. The ORAC method consists on the generation of peroxyl radicals in the presence of a probe, fluorescein, that upon oxidation has its fluorescence quenched. The presence of antioxidants removes peroxyl radicals from the reaction media, avoiding or delaying the oxidation of the probe. This assay was performed using a microplate reader (MR), model Synergy HT, from Bio-Tek Instruments Inc. (Winooski, VT, USA). This MR allowed fluorescence, absorbance and luminescence measurements. In this work the fluorimetric measurements were performed using a tungsten halogen lamp with interference filters for wavelength specificity, λ_{exc}=485±20; λ_{exc}=528±20 and λ_{exc}=360±40; λ_{exc}=460±40 in conjunction with a photomultiplier tube. The tungsten halogen lamp produces a large amount of light at a constant intensity, providing increased sensitivity and repeatability. Moreover, specially designed fluorescent interference filters prevent light leakage from excitation wavelength to the emission wavelength, particularly important with fluorescent compounds with small Stoke's shifts. Disposable 96-wells microplates were obtained from Orange Scientific.

2.4. ORAC method – quantification

The quantification of antioxidant capacity in the ORAC method is based on the area under the curve (AUC, depicted in Figure 8) that represents the oxidation of the probe along time. The protective effect of antioxidants is evaluated from the net integrated area under the fluorescence decay curves ($AUC_{sample} - AUC_{blank}$) and results are generally expressed as μM of trolox equivalents (Equation 1). The advantage of the AUC approach is that it can be applied for antioxidants that exhibit distinct lag phases and also to those samples that have no lag phases. Moreover, it takes into account the initial reaction rate and the total extent of probe attack, which includes the action of slow-reacting or secondary antioxidant products formed.

$$[(AUC_{sample} - AUC_{Blank})/(AUC_{Trolox} - AUC_{Blank})] \times [(\text{moles of Trolox/moles of sample})]$$

Equation 1.

All experiments were carried out in triplicate and using some wells for different control experiments (microplate self-fluorescence, probe alone, with and without radicals generator or antioxidant) for all assays. The reactions were performed at 37°C as the reaction was started by thermal decomposition of AAPH in 75 mM phosphate buffer, pH 7.4. Data acquisition was performed by Gen 5 software, with data stored as readings of fluorescence intensity for every minute during total time periods between 30 min and three hours.

2.5. Preparation of biomimetic lipid systems

Various models of biomembranes, including 2D (monolayers) and 3D (micelles and vesicles) were selected for the studies performed in this thesis. The steps required for their preparation are schematically depicted in Figure 1.

The hexadecylphosphocholine (HePC) micelles were prepared in a round flask, for addition of the surfactant, in 75 mM phosphate buffer, pH 7.4 at 2.304 mM, then the solution was vortexed during 10 minutes, followed by 2-3 passages through filters with

pore size of 100 μm, placed on an extruder. The classical methodology for micelles preparation described in the literature(Menez et al., 2007) was modified, because with the previous procedure did not fostered the production of micelles with size characteristic - 6.79/181.0±2.2

For MLV preparation, the lipid (EPC in generally) is dissolved in chloroform:methanol (3:1) in round-bottomed flask, later the solvent was removed under reduced pressure on a rotary evaporator with the water bath set at 30°C. N_2 is introduced to re-establish atmospheric pressure and the flask was covered in aluminum foil to avoid lipid oxidation. A pump is then used to keep the flask under a pressure of < 0.5 mmHg during at least 1 h.

After solvent evaporation, the resulting lipidic film was hydrated with a given volume of phosphate buffer (75 mM, pH = 7.4) and vortexed during 10-15 minutes. The final preparation was a whitish homogeneous liquid.

For preparation of LUVs, this suspension was submitted to extrusion, comprising two passages through a polycarbonate filter with a pore size of 200 μm, followed by ten passages through a filter with pore size of 100 μm into extruder.

For SUVs preparation, the suspension containing MLVs was sonicated with a sonication probe (Sonics Vibracell model CV18), during 20 cycles of 1 minute each, with an amplitude of 85%. The preparation was performed with attention of the lipid volume, because with sonication of volume larger of lipid solutions not possible obtainer the solution with uniform size vesicles.

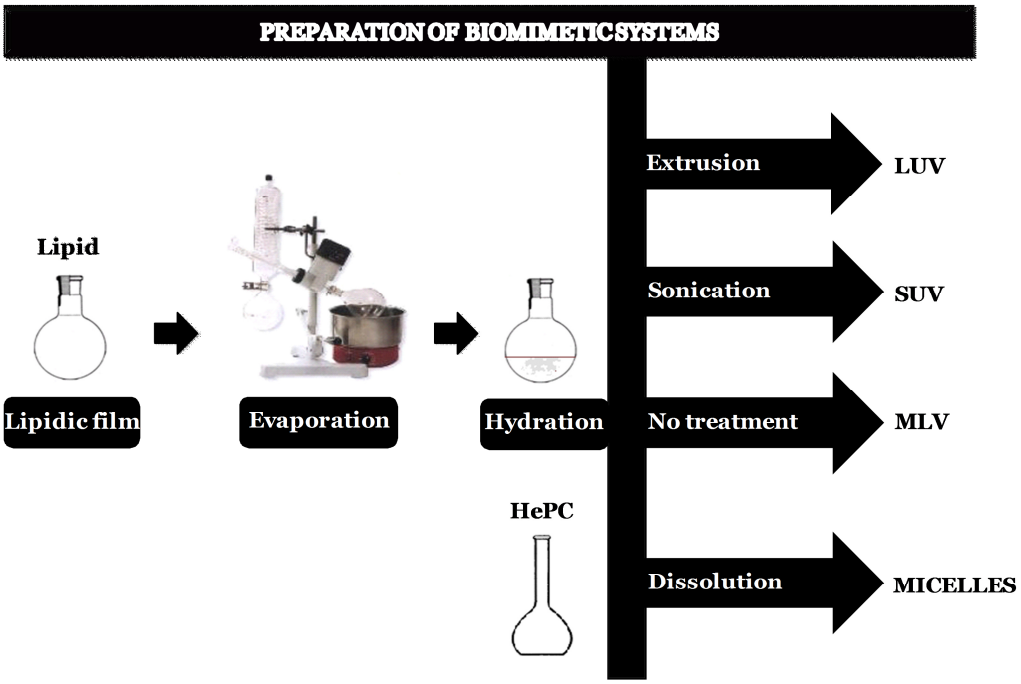

Figure 2.1: Schematic representation of techniques used in this work for preparation of biomimetic systems.

The characterization of the micelles and vesicles used in this thesis was performed in a BI-MAS DLS instrument (Brookhaven Instruments, USA) containing a controlled temperature cell holder - Dynamic Light Scattering Instrument.
The samples were placed in a quartz cuvette at 37ºC (the same temperature applied for all assays) for measurement of the mean size, the size distribution of particles, and a potential zeta.

2.6. Surface pressure – area measurements in monolayers

Langmuir monolayers at the liquid-air interface are well-defined interfacial systems and, therefore, excellent model systems to give information about the lipid phases and the phase transitions, which are both dependent on the temperature, the pressure, and the pH (Nunes et al., 2011; Wustneck et al., 2005). The surface pressure-area (π/A) isotherms (depicted in Figure 2) give information about the phases, the type of phase transition (first or second) of a lipid monolayer, the minimum area per molecule and the compressibility. The minimum area per molecule (A_{min}) is the mean area occupied for one molecule in the surface layer and it indicates the molecular packing and the interactions between the monolayer components. This parameter was determined by extrapolation from the isotherm. Elastic modulus (C_s^{-1}) was calculated from the π/A isotherms by the following equation:

$$C_s^{-1} = -A\,(d\pi/dA),$$

where A is the area per lipid molecule, and π is the surface pressure. C_s^{-1} describes the relationship between the surface pressure increase and the area per molecule decrease. A higher value of C_s^{-1} is indicative of a less compressible monolayer (Nunes et al., 2011; Wang and Yang, 2009).
The lipid DPPC, DPPC+α-linolenic acid, EPC were prepared for dissolution in Chloroform. The spreading solutions were deposited onto the aqueous subphase with a Hamilton microsyringe, precise to 2.0 μL. After spreading, the monolayers were left to equilibrate for ca. 10 min for solvent evaporation prior to film compression (barrier speed of 20 cm^2 min^{-1}).
The π–A isotherms of DPPC, DPPC+α-linolenic acid and EPC, expressed for the absolute molecular area ($Å^2$ per molecule) of DPPC or of EPC, were recorded with a NIMA 601 (Nima Technology, Coventry, UK) Langmuir trough (total area = 600 cm^2; subphase volume c.a. 400 mL).

The concentration of the lipid simple or mixture surface pressure was measured, before beginning compression, with the accuracy of ± 0.1 mN m^{-1} using a Wilhelmy type dynamometric system with a strip of filter paper. All measurements were performed at 21 °C (controlled room temperature). Π–A isotherms were measured at least twice to collapse monolayer. Before each measurement, the trough was cleaned thoroughly with chloroform and double deionized water.

Parameters pertaining to each isotherm (elastic modulus C_s^{-1}, $\pi_{collapse}$, $A_{collapse}$, A_{min}) were assessed.

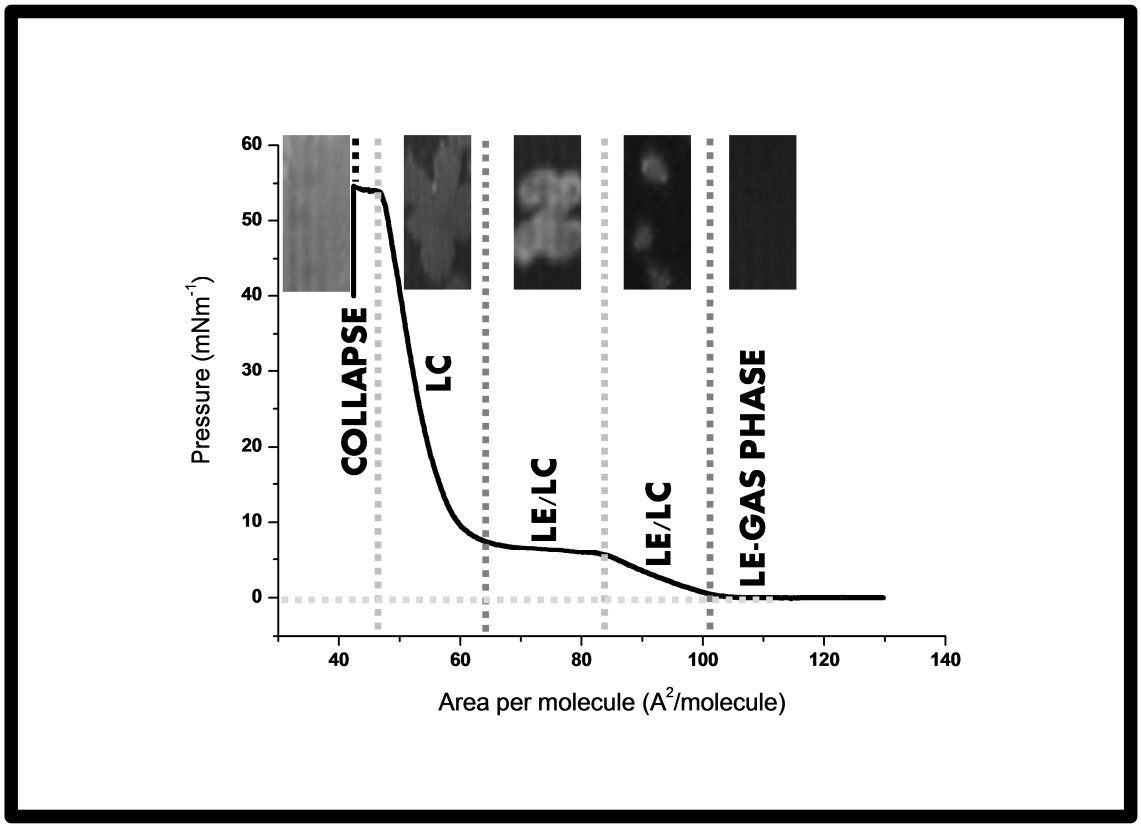

Figure 2.2: Isotherm representation, of DPPC monolayer obtained with a NIMA 601 (Nima Technology, Coventry, UK) Langmuir trough (total area = 600 cm^2; subphase volume c.a. 400 mL of the phosphate buffer) and BAM images at different pressures and lipid phases (LE-lipid expanded; LE/LC-lipid expanded/lipid condensed; LC – lipid condensed and monolayer collapse).

2.7 Brewster angle microscopy (BAM) in monolayers

Brewster angle microscopy (BAM) is a powerful tool that enables the visualization of the morphological changes (depicted in Figure 2): beginning of domains formation, domains shape in different phases (LE and LC), domains shape disappearance and collapse that occur during the compression of the monolayers. Moreover, BAM also gives some information on the fluidity of the film in relation to the geometry of the domains observed at the water interface (Allouche et al., 2007). The contrast in BAM images is due to local differences in the monolayer refractivity index, caused by differences in local molecular density or packing (Alonso et al., 2004; Bringezu et al., 2002; Goncalves da Silva and Romao, 2005).

Brewster angle microscopy (BAM) images were obtained from a I-Elli 2000 apparatus (supplied by Nanofilm Technologies, Göttingen, Germany) using a Nd:YAG diode laser, which were recorded with a lateral resolution of 2 μm. The image processing procedure included a geometrical correction of the image, as well as a filtering operation to reduce interference fringes and noise. Furthermore, the brightness of each image was scaled to improve contrast. The size of the images is 430 μm in width. The microscope and film balance were located on a table with vibration isolation (antivibration system MOD-2 S, Halcyonics, Göttingen, Germany) in a large class 100 clean room.

BAM images were obtained from the $\pi \pm 0.1$ mN m^{-1} (before compression) to monolayer collapse (variable with different assay conditions) for monitoring different aspects: namely, the initial images, beginning of domains formation, domains shape in different phases (LE and LC), domains shape disappearance and collapse.

2.8 References

Allouche, M.; Castano, S.; Colin, D.; Desbat, B.; Kerfelec, B. Structure and orientation of pancreatic colipase in a lipid environment: PM-IRRAS and Brewster angle microscopy studies. *Biochemistry* **2007,** *46*, 15188-97.

Alonso, C.; Alig, T.; Yoon, J.; Bringezu, F.; Warriner, H.; Zasadzinski, J. A. More than a monolayer: relating lung surfactant structure and mechanics to composition. *Biophys J* **2004,** *87*, 4188-202.

Bringezu, F.; Ding, J.; Brezesinski, G.; Waring, A. J.; Zasadzinski, J. A. Influence of Pulmonary Surfactant Protein B on Model Lung Surfactant Monolayers. *Langmuir* **2002,** *18*, 2319-2325.

Goncalves da Silva, A. M.; Romao, R. I. Mixed monolayers involving DPPC, DODAB and oleic acid and their interaction with nicotinic acid at the air-water interface. *Chem Phys Lipids* **2005,** *137*, 62-76.

Menez, C.; Legrand, P.; Rosilio, V.; Lesieur, S.; Barratt, G. Physicochemical characterization of molecular assemblies of miltefosine and amphotericin B. *Molecular pharmaceutics* **2007,** *4*, 281-288.

Nunes, C.; Brezesinski, G.; Pereira-Leite, C.; Lima, J. L.; Reis, S.; Lucio, M. NSAIDs interactions with membranes: a biophysical approach. *Langmuir* **2011,** *27*, 10847-58.

Ou, B. X.; Hampsch-Woodill, M.; Prior, R. L. Development and validation of an improved oxygen radical absorbance capacity assay using fluorescein as the fluorescent probe. *Journal of Agricultural and Food Chemistry* **2001,** *49*, 4619-4626.

Wang, Z.; Yang, S. Effects of fullerenes on phospholipid membranes: a langmuir monolayer study. *Chemphyschem* **2009,** *10*, 2284-9.

Wustneck, R.; Perez-Gil, J.; Wustneck, N.; Cruz, A.; Fainerman, V. B.; Pison, U. Interfacial properties of pulmonary surfactant layers. *Adv Colloid Interface Sci* **2005,** *117*, 33-58.

CHAPTER 3

Insights about α-tocopherol and Trolox interaction with phosphatidylcholine monolayers under peroxidation conditions through Brewster Angle Microscopy

3.Insights about α-tocopherol and Trolox interaction with phosphatidylcholine monolayers under peroxidation conditions through Brewster Angle Microscopy

3.1 Introduction

Biological membranes are not only a remarkable barrier to keep the cell intact, but they also allow exchange of substances required for or produced from the cell metabolism (Edidin, 2003). The membranes are centrally involved in the control and execution of a great variety of cellular processes, thus requiring the maintenance of their proper structure and function (Mueller et al., 2012; Nugent and Jones, 2012). Hence, any perturbation of the bilayer structure may lead to modifications of membrane properties and, consequently, changes on its physiological role. Phospholipids are the main components of the biological membranes, liable to free radical attack that induces lipid peroxidation. This uncontrolled oxidative reaction generates cytotoxic compounds and disrupts the various important structural and protective functions associated with biomembranes, and it has been implicated in the etiology of many diseases, including cancer, cardiovascular and neurological diseases, and other oxidative stress mediated dysfunctions (Halliwell and Gutteridge, 2007).

In fact, several biophysical changes and associated kinetic features have been identified on membrane models under peroxidation conditions through either experimental or theoretical approaches. For instance, peroxidation of liposomes was shown to be faster when the oxidizable lipids reside in the relatively rigid gel phase bilayers than in the less tightly-packed liquid crystalline bilayers(Cubillos et al., 2006; McLean and Hagaman, 1992; Mowri et al., 1984). Moreover, exposure of liposomes comprising dilinoleoylphosphatidylcholine (DLPC) and cholesterol to conditions of spontaneous oxidation caused the formation of moderate levels of hydroperoxides and a concentration-dependent formation of discrete immiscible cholesterol-rich domains, as observed by small angle X-ray scattering (SAXS) (Jacob and Mason, 2005). This technique also allowed the observation of a marked reduction of the width of the hydrocarbon core, a similar decrease of the overall width of the membrane, and a decrease of the molecular volume of the bilayers as a consequence of iron(II)/ascorbate-induced peroxidation of liposomal DLPC (Mason et al., 1997). Theoretical molecular dynamics simulations led to similar conclusions concerning the changes on organized lipid structures (Cwiklik and

Jungwirth, 2010; Khabiri et al., 2012; Leekumjorn et al., 2009; Wong-Ekkabut et al., 2007).

The deleterious consequences of membranes peroxidation have stimulated numerous studies on the efficacy and mechanisms of action of biologically relevant antioxidants (Cuzzocrea et al., 2001; KamalEldin and Appelqvist, 1996; Niki, 1987; Valko et al., 2007; Valko et al., 2006). Lipidic biomimetic models, namely large unilamellar vesicles (LUVs), have been applied to assessment of antioxidant activity of compounds upon peroxidation conditions(Lúcio et al., 2009; Reis et al., 2010; Schnitzer et al., 2007; Tsuchiya et al., 2010). Langmuir monolayers formed by phosphatidylcholines bearing different acyl chains, with and without unsaturations, have also been applied for studying of rosmarinic acid interaction with this biomimetic model, showing that cholesterol decreases the penetration of rosmarinic acid (Fadel et al., 2011). More recently, by using Brewster angle microscopy (BAM) and Langmuir monolayer compression isotherms, the presence of an oxidatively modified phosphatidylcholine in monolayers was shown to efficiently oppose the miscibility transition and to stabilize micron-sized domain separation at lipid lateral packing densities corresponding to the equilibrium lateral pressure of c.a. 32 mN m^{-1} that is suggested to prevail in bilayer membranes (Volinsky et al., 2012). Despite these examples, information about mechanistic details, especially those concerning the role of interactions between antioxidant compounds and membranes, are still to be unveiled.

Hence, the objective of the present work is to evaluate the interaction between antioxidants and the organized monolayer formed by phosphatidylcholine molecules at air/water interface upon peroxidation conditions. For this, a biophysical approach will be implemented, by profiling the changes of surface pressure (π) and molecular area (A) upon monolayer compression and by monitoring monolayer features and domain formation through BAM. Peroxidation conditions will be fostered by the presence of peroxyl radicals generated by previous thermal decomposition of 2,2'-azobis(2-methylpropionamidine) dihydrochloride (AAPH) in the aqueous buffered subphase. The role of α-tocopherol, a relevant natural antioxidant, and of its water soluble analogue Trolox will be assessed through modifications in the π-A isotherms profile and changes on formation of lipid domains obtained by BAM.

3.2 Reagents and solutions

Egg yolk L-α-phosphatidylcholine (EPC), potassium phosphate monobasic, 2,2'-azobis(2-methylpropionamidine) dihydrochloride (AAPH), α-linolenic acid (LA), and α-tocopherol

were purchased from Sigma-Aldrich (St. Louis, MO). 1,2-dihexadecanoyl-*sn*-glycero-3-phosphocholine (DPPC) was purchased from Avanti Polar Lipids Inc. 6-Hydroxy-2,5,7,8-tetramethylchromane-2-carboxylic acid (Trolox) was obtained from Fluka (Buchs, Switzerland). Chloroform from Landilab (Porto, Portugal) was used as co-spreading solvent. The subphase used, 75 mM hydrogen phosphate/phosphate buffer (pH 7.4), was prepared using Milli-Q water (resistivity > 18.2 MΩ cm, Millipore, Billerica, MA).
Lipid solutions were prepared in chloroform and they contained DPPC (0.734 mg mL^{-1}), DPPC + LA (9:1, w/w; 0.642 mg mL^{-1} of DPPC) or EPC (0.751 mg mL^{-1}). Trolox was added to the subphase buffer at 20 μM. For generation of peroxyl radicals, AAPH (12 mM) was dissolved in hydrogen phosphate buffer at 37 °C and kept at this temperature during 10 minutes. Whenever necessary, Trolox was dissolved in this solution immediately before it was poured into the trough. α-Tocopherol (20 μM) was incorporated onto lipid solutions prior to monolayer spreading.

3.3 Results

3.3.1 π-A measurements

The isotherm obtained for DPPC spread on aqueous phosphate buffer pH 7.4 (Fig. 3.1) presents the characteristic shape reported before(Duncan and Larson, 2008) for other subphases, with a marked plateau between 63 to 80 $Å^2$ per molecule at surface pressure of ca. 6-7 mN m^{-1}, corresponding to the transition of expanded liquid (LE) to condensed liquid (LC). Other parameters, including A_{min} (57 Å), $\pi_{collapse}$ (53 ± 1 mN m^{-1}), $A_{collapse}$ (47.1 ± 1.0 Å) and the elastic modulus C_s^{-1} (248 mN m^{-1}) are also in agreement with values described in the literature (Duncan and Larson, 2008; Nunes et al., 2011). (Table 3.1).

Table 3.1. Characteristic parameters (elastic modulus, collapse pressure and collapse area) of the Langmuir monolayers tested on aqueous subphases containing the peroxidation inducer (AAPH) and antioxidants (Trolox and α-tocopherol)

Lipid system	Subphase	C_s^{-1} (mN m^{-1})	$\pi_{collapse}$ (mN m^{-1})	$A_{collapse}$ (Å per molecule)
DPPC	Phosphate buffer pH 7.4	248	53 ± 1	47.1 ± 1.0
	AAPH	142	62 ± 1	33.6 ± 0.3
	Trolox	450	60 ± 2	34.4 ± 2.5
	Trolox + AAPH	145	63 ± 1	32.9 ± 1.3
	α-tocopherol	195	59 ± 1	34.9 ± 1.9
	α-tocopherol + AAPH	110	64 ± 1	27.3 ± 0.3
DPPC + LA	Phosphate buffer pH 7.4	117	49 ± 1	47.8 ± 1.1
	AAPH	160	63 ± 1	34.7 ± 1.3
	Trolox	216	60 ± 1	37.8 ± 1.3
	Trolox + AAPH	159	64 ± 1	29.5 ± 0.3
	α-tocopherol	152	51 ± 1	50.5 ± 1.1
	α-tocopherol + AAPH	175	59 ± 1	27.2 ± 0.7
EPC	Phosphate buffer pH 7.4	93.3	42 ± 1	46.1 ± 2.8
	AAPH	96.3	45 ± 1	46.1 ± 1.1
	Trolox	95.2	44 ± 1	59.6 ± 1.7
	Trolox + AAPH	103	45 ± 1	61.8 ± 3.4
	α-tocopherol	108	45 ± 1	50.4 ± 2.4
	α-tocopherol + AAPH	133	43 ± 1	62.6 ± 1.6

The addition of linolenic acid to the DPPC monolayer caused a decrease in the elastic modulus C_s^{-1} (117 mN m^{-1}) and in the $\pi_{collapse}$ (49 ± 1 mN m^{-1}). At the same time, $A_{collapse}$ (47.8 ± 1.1 Å) was the same, but A_{min} increased to 79 Å. Furthermore, the plateau corresponding to LE/LC phase transition observed for the DPPC disappeared when linolenic acid was present (Fig. 1).

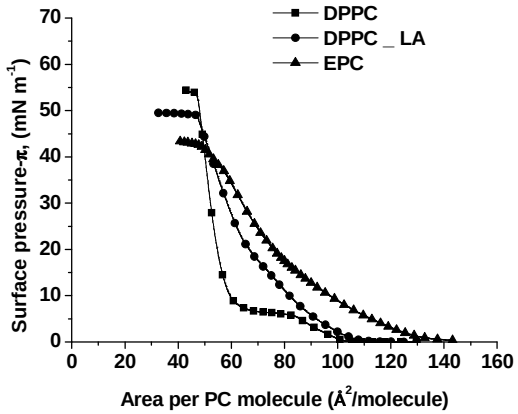

Figure 3.1. Surface pressure-area isotherms of monolayers formed by DPPC (■), DPPC + LA (●) and EPC (▲) upon a phosphate buffer (pH 7.4) subphase.

For EPC, no plateau corresponding to LE-LC phase transition was observed (Fig. 3.1). $\pi_{collapse}$ (42 ± 1 mN m^{-1}) and the elastic modulus C_s^{-1} (93.3 mN m^{-1}) were lower than the values obtained for DPPC monolayers (Table 1). Moreover, $A_{collapse}$ (46.1 ± 2.8 Å) was not significantly different, and A_{min} was further increased to 97 Å. These observations are in agreement with EPC isotherms given in the literature.(Mitsche et al., 2010; Rigoletto et al., 2011)

The addition of AAPH to the subphase or the incorporation of α-tocopherol did not cause significant changes in the shape of DPPC isotherm but an increase of $\pi_{collapse}$ (c.a. 60 mN m^{-1}) and a decrease of $A_{collapse}$ (c.a. 34 Å) were observed. These changes were also observed for DPPC isotherms obtained for other subphases (Fig. 3.2 and 3.3, A), with a concomitant shift of the isotherm towards higher values of area per molecule. This shift was more pronounced for monolayers tested with α-tocopherol + AAPH, followed by Trolox + AAPH.

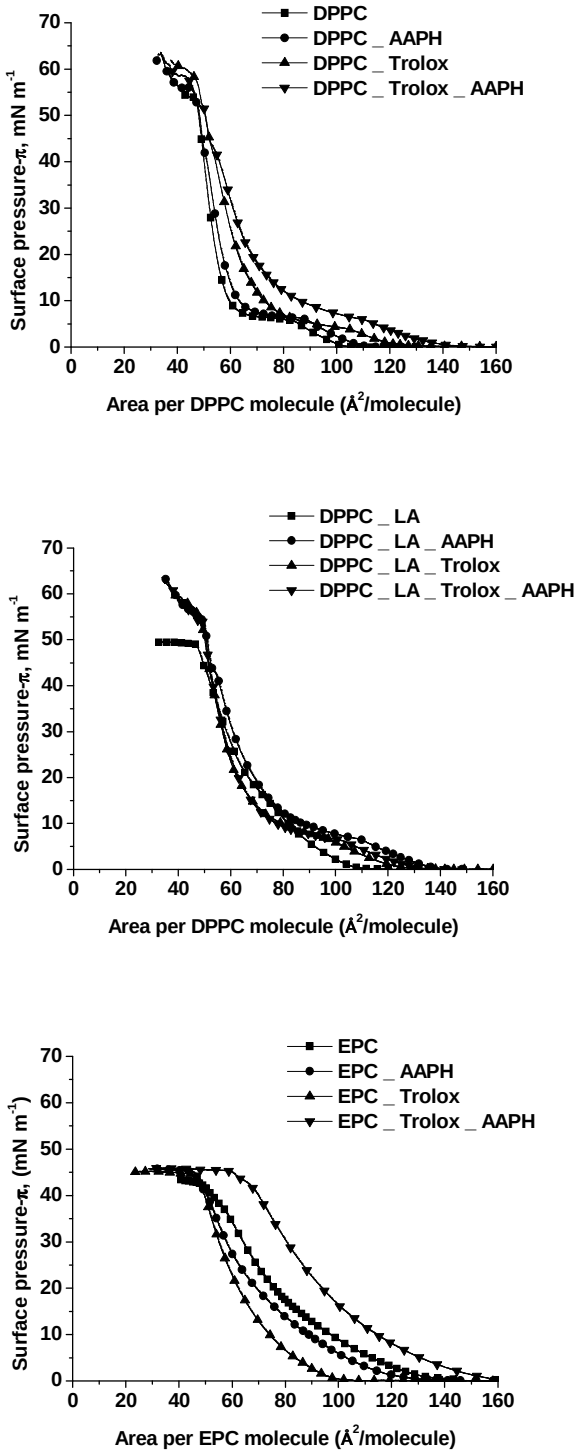

Figure 3.2. Surface pressure-area isotherms for different lipid systems, with monolayers formed and compressed above subphases containing phosphate buffer pH 7.4 (■), AAPH solution (●), Trolox solution (▲) and AAPH + Trolox solution (▼). A: DPPC; B: DPPC + LA; C: EPC.

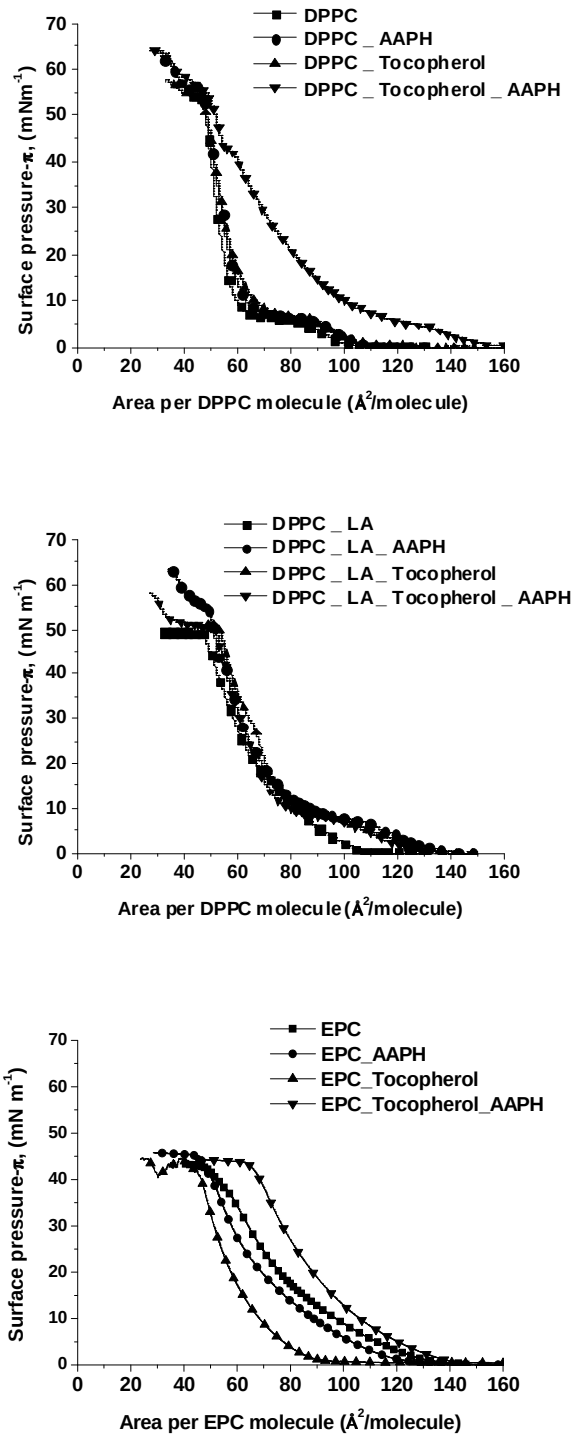

Figure 3.3. Surface pressure-area isotherms for lipid systems containing α-tocopherol, with monolayers formed and compressed above subphases containing phosphate buffer pH 7.4 (without α-tocopherol: ■; with α-tocopherol: ▲) or AAPH solution (without α-tocopherol: ●; with α-tocopherol: ▼). A: DPPC ; B: DPPC + LA; C: EPC.

For DPPC + LA monolayer (Fig. 3.2 and 3.3, B), the addition of AAPH to the subphase restored the plateau corresponding to the LE/LC phase transition and this was shifted towards higher areas per DPPC molecule when compared to the DPPC isotherm. In fact, this behavior was observed for all DPPC + LA monolayers containing either the antioxidants or their combination with AAPH in the subphase.

When the antioxidants (α-tocopherol or Trolox) were present with AAPH, a decrease of $A_{collapse}$ was also observed (from 47 to 28 Å) for both DPPC and DPPC + LA monolayers. This observation was accompanied by a less steep increase of surface pressure for values above 53 mN m^{-1} (which corresponds to $\pi_{collapse}$ of monolayers spread over phosphate buffer).

For EPC, the addition of AAPH provided $\pi_{collapse}$ and $A_{collapse}$ similar to those obtained for the phosphate buffer subphase, but a slight displacement of the whole isotherm towards lower molecular areas (c.a. –10 $Å^2$ per molecule) was observed (Fig. 3.2 and 3.3, C). This displacement was further exaggerated when Trolox was present in the subphase (c.a. –20 $Å^2$ per molecule at 10 mN m^{-1}) or when α-tocopherol was incorporated to the monolayer (c.a. –30 $Å^2$ per molecule). However, when both AAPH and antioxidants were present, the isotherm was shifted to the opposite direction towards larger areas per molecule (c.a. + 10 to 15 $Å^2$ per molecule).

3.3.2 BAM observation

The morphology of all monolayers was directly visualized by BAM simultaneously to the π–A isotherm recording. Light gray structures appeared upon compression of the DPPC monolayer spread over a phosphate buffer subphase (Fig. 3.4B) and they became organized into bean and two-lobed shaped domains against a black matrix at 6.3 mN m^{-1} (Fig. 3.4C); these structures evolved to more complex multilobed domains (Fig. 3.4D) within a small change of surface pressure, corresponding to LE/LC transition (Klopfer and Vanderlick, 1996). Up to 10 mN m^{-1}, the domains became larger, occupying a larger area than the dark background. The light gray domains became less organized with smoother contours as soon as the surface pressure increases above 10 mN m^{-1} (Fig. 3.4E and 3.4F) and the observation area was completely gray when $\pi_{collapse}$ was reached.

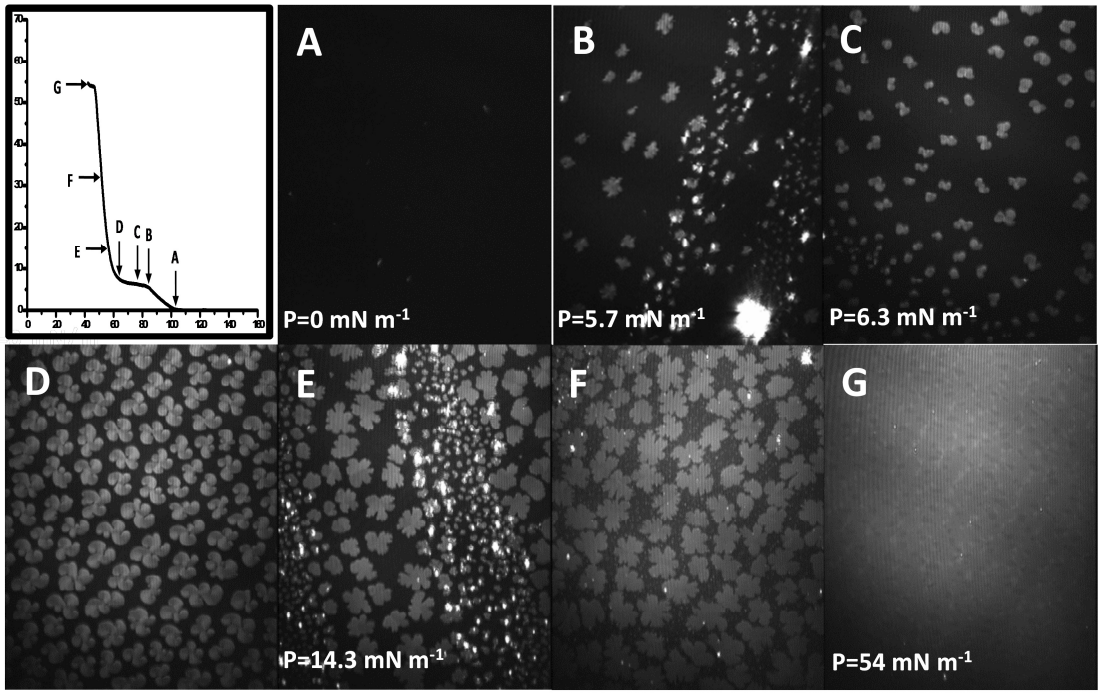

Figure 3.4. Brewster angle micrographs of DPPC monolayer at different surface pressures upon monolayer compression.

For DPPC + LA monolayer spread on phosphate buffer pH 7.4, the formation of domains was not observed. In fact, small white aggregates can be seen as soon as monolayer compression started. The number and size of aggregates increased as surface pressure increased, as depicted in Fig. 3.5A-C. The same behavior was observed for EPC monolayer (Fig. 3.5D-F).

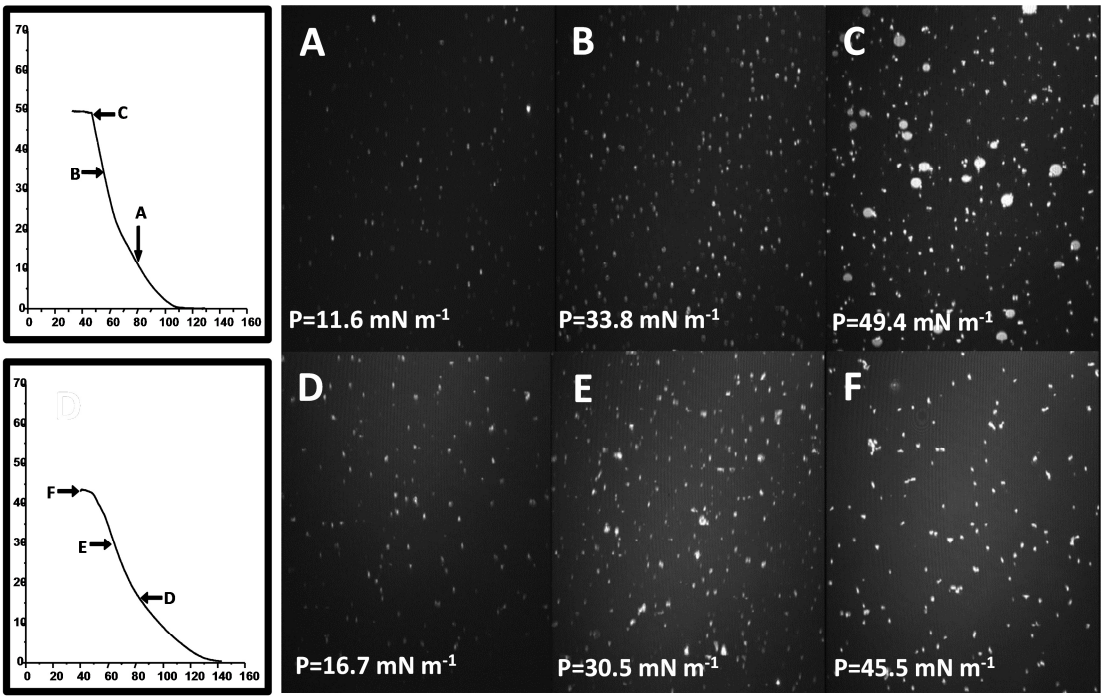

Figure 3.5. Brewster angle micrographs of DPPC + LA (A-C) and EPC (D-F) monolayers at different surface pressures upon monolayer compression.

For DPPC monolayer containing AAPH in the subphase, small round gray structures appeared at 6.8 mN m^{-1} and progressed towards more complex, multilobed structures (Fig. 3.6A) that became less organized around 12 mN m^{-1} and merged at 14 mN m^{-1}. The addition of Trolox to the subphase of DPPC monolayer also allowed the formation of multilobed domains that started to appear at similar surface pressures and remained organized up to higher pressure values (up to 30 mN m^{-1}) as shown in Fig. 3.6B. This effect disappeared when Trolox and AAPH were both present. In fact, small round white dots appeared at low surface pressures (c.a. 1 mN m^{-1}) and remained throughout the experiment. The formation of light gray structures was observed from 6.4 to 15.3 mN m^{-1}, and their lobes were less defined (Fig. 3.6C) when compared to those of DPPC only. At $\pi_{collapse}$, the small round white dots could be still seen against a completely light gray background (Fig. 3.6D).

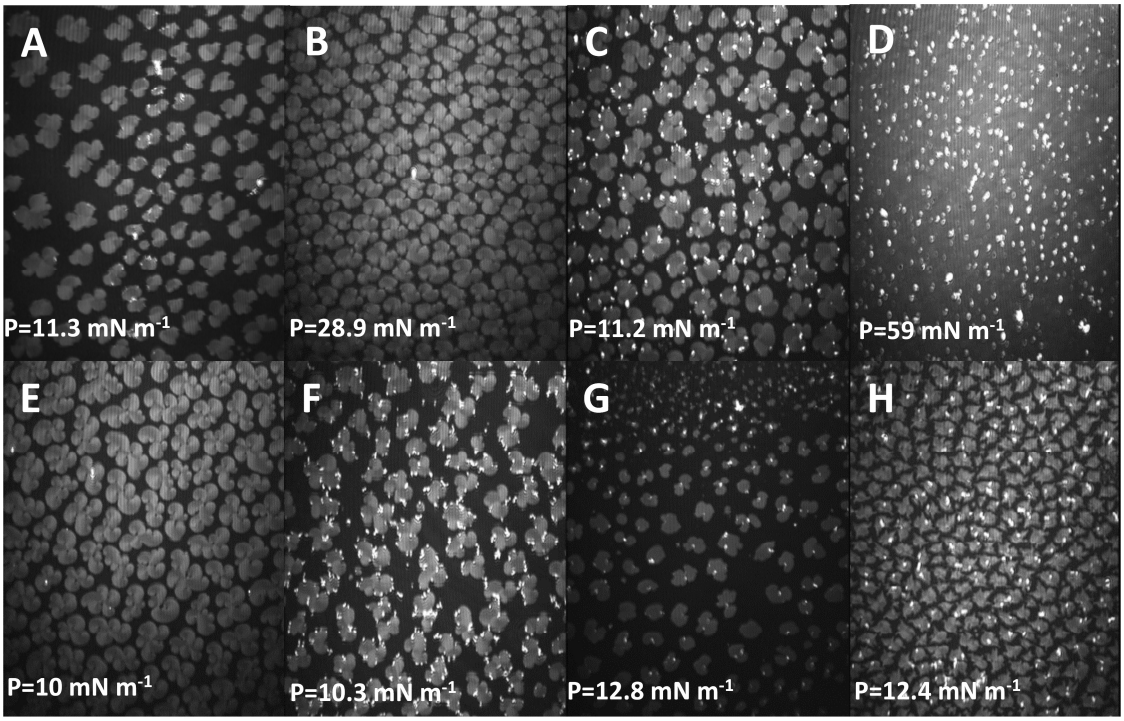

Figure 3.6. Brewster angle micrographs showing representative features for monolayers of DPPC and DPPC + LA. A, DPPC monolayer with AAPH in the subphase; B, DPPC monolayer with Trolox in the subphase; C, D, DPPC monolayer with AAPH and Trolox in the subphase; E, DPPC monolayer with α-tocopherol; F, DPPC monolayer with α-tocopherol and AAPH in the subphase; G, DPPC + LA monolayer with AAPH in the subphase; H, DPPC + LA monolayer with AAPH and Trolox in the subphase.

The addition of α-tocopherol to the DPPC monolayer allowed the formation of domains at a slightly lower surface pressure (c.a. 5.9 mN m^{-1}). Upon compression, the small structures evolved to a multilobed pattern, presenting more complex features (more lobes) as shown in Fig. 3.6E, which collapsed into a light gray background at 14 mN m^{-1}. When both α-tocopherol and AAPH were present, small round white dots were also formed at low surface pressures. The formation of light gray domains was observed for pressures above 7.3 mN m^{-1}, but they presented a less smooth, slightly irregular contour as shown in Fig. 3.6F, that merged for surface pressures above c.a. 23 mN m^{-1} (image not shown).

For DPPC + LA monolayers, domain formation was again visible for all monolayers where antioxidants and/or AAPH were added (Fig. 3.6G and H, Fig. 3.7). Moreover, small round white dots were present for all experiments containing AAPH, Trolox or both compounds in the subphase. For experiments with α-tocopherol, branched structures could be seen from surface pressures above 6 mN m^{-1} (Fig. 3.7). These structures were white and not associated to the light gray domains. Furthermore, the format of the light gray domains was different, showing rounded borders for all experiments containing AAPH and for the

monolayer containing α-tocopherol. For DPPC + LA monolayer, the light gray domains presented irregular borders as shown in Fig. 3.6H.

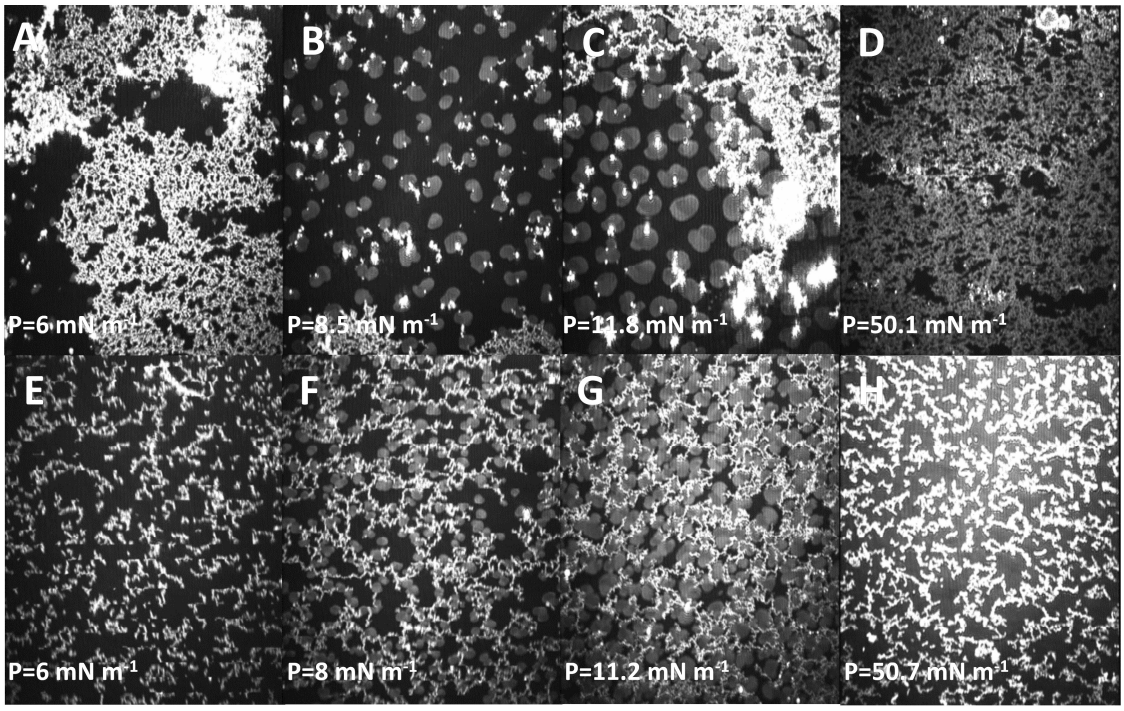

Figure 3.7. Brewster angle micrographs showing representative features for monolayers of DPPC + LA and α-tocopherol in phosphate buffer subphase (A-D) or with AAPH in the subphase (E-H).

For EPC monolayers, slight changes could be observed by BAM, namely the appearance of small rounded light gray lipid aggregates near $\pi_{collapse}$.

3.4 Discussion and conclusions

The idea behind this work was to exploit lipid monolayers as a 2D system to provide insight about the effect of peroxidation, the role and interaction of antioxidants (α-tocopherol and Trolox) with membranes, and the interaction of peroxidation products with lipidic domains of cell membrane. Initially, α-linolenic acid was targeted as a possible structure prone to peroxidation as it contains 3 double bonds (18:3;*(cis)*9,12,15). Preliminary experiments have shown that monolayer formation exclusively from this compound was hindered by the phosphate buffer subphase. Previous reports have established the feasibility of α-linolenic acid monolayer formation above a water subphase at 20 °C (Hac-Wydro and Wydro, 2007). However, the pKa of this fatty acid was determined as 8.28 in aqueous solution/dispersion, below the values of 9.24 and 9.85

reported for linoleic and oleic acids (Kanicky and Shah, 2002). For these two fatty acids, the apparent surface pKa was estimated as three units lower, namely 5.94 and 6.22, respectively (Tomoaiacotisel et al., 1987). This decrease on pKa value might be the result of the shift of pH scale in the monolayer compared to the bulk or it might also reflect an actual decrease of the acidity constants in monomolecular films. Hence, a similar decrease can be expected for linolenic acid. Therefore, for our experimental conditions, the apparent surface pKa of linolenic acid was probably surpassed, causing the ionization and dissolution of this fatty acid in the pH 7.4 subphase.

Therefore, L-α-DPPC monolayers were chosen for further experiments. As this phosphatidylcholine does not possess any oxidable unsaturation on its acyl chains, mixed monolayers containing both DPPC and linolenic acid were evaluated as a model for performing the peroxidation studies. Moreover, EPC was also tested in order to evaluate if the DPPC + α-linolenic acid (LA) monolayer would provide a behavior similar to a more complex lipid mixture pertaining to biological systems.

In fact, the addition of linolenic acid caused fluidification of DPPC monolayer, evidenced by the absence of any plateau in the isotherms corresponding to the LE to LC phase transition, by the decrease of C_s^{-1} and it was confirmed by BAM images, where formation of the typical multilobed domains from DPPC was not observed. The DPPC + LA isotherm was displaced towards higher areas per molecule when compared with DPPC isotherm, which seems opposite to the observations reported by Hac-Wydro and Wydro (Hac-Wydro and Wydro, 2007). Although a similar temperature was applied (20 °C), the pH of our experimental conditions was controlled and fostered the ionization of carboxylic group of linolenic acid, promoting the interaction between the negatively charged group with the positively charged N from the choline moiety of DPPC, with the inclusion of the linolenic acid hydrophobic chain among the acyl chains of DPPC (Fig. 3.8, scheme 1).

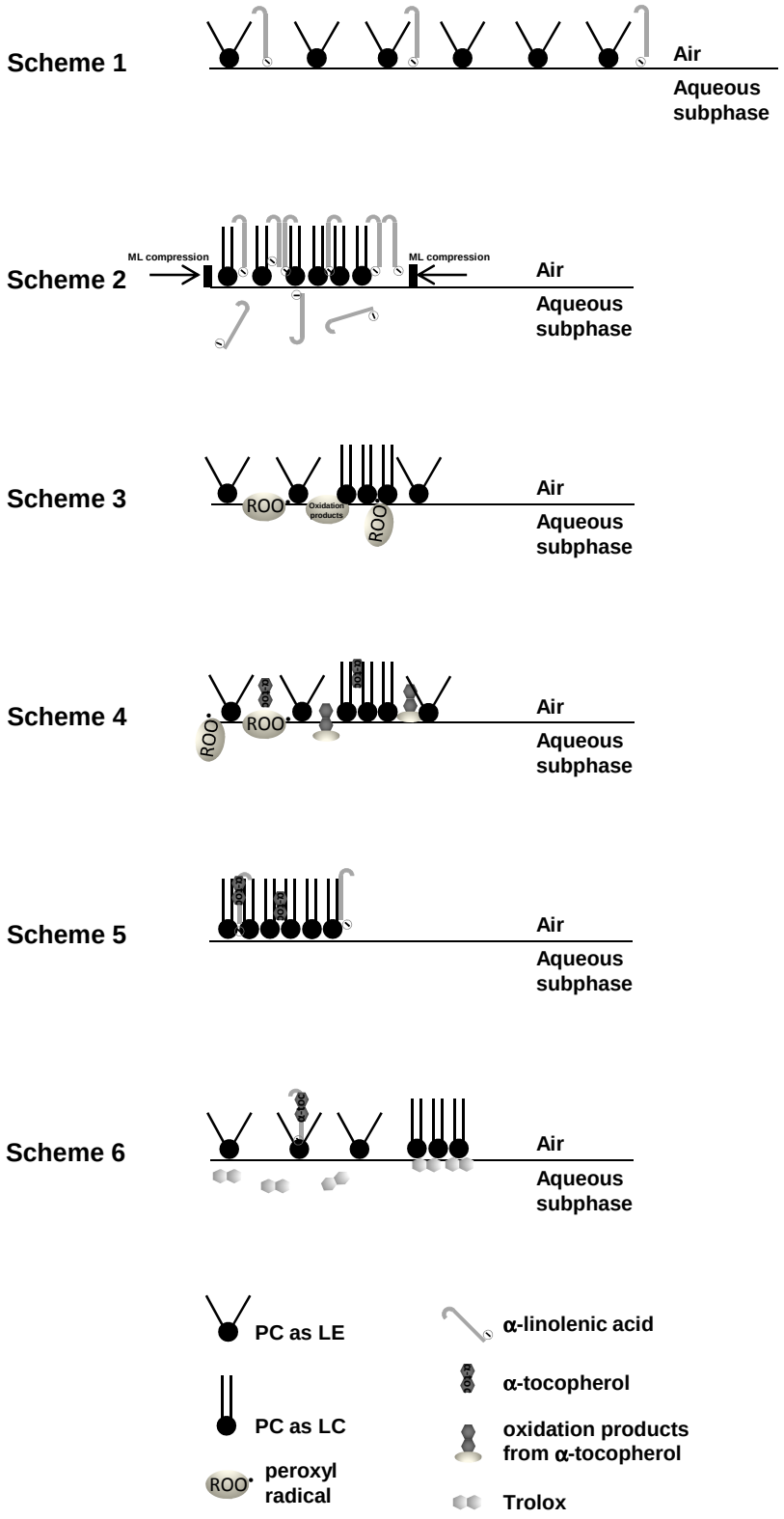

Figure 3.8. Schematic representations of interaction between monolayer and aqueous phase components.

Compared to DPPC and DPPC + LA monolayers, EPC provided an even more fluid monolayer, with the lowest value of C_s^{-1}, and the highest value of A_{min}, existing as an expanded liquid. According to theoretical (Martinez-Seara et al., 2007) and experimental (Marsh, 1999; Murzyn et al., 2006) studies, the presence (and position) of double bonds affects the properties of monolayers/bilayers in the LE state, causing an increase on surface area per lipid. Knowing that typical lots of egg yolk phosphatidylcholine have esterified fatty acid contents of approximately 33% 16:0 (palmitoyl), 13% 18:0 (stearoyl), 31% 18:1 (oleoyl) and 15% 18:2 (linoleoyl), we can consider that half of the acyl chains presented unsaturated bonds, justifying the features of the EPC monolayer.

Nevertheless, DPPC, DPPC + LA and EPC monolayers presented similar $A_{collapse}$, about 47 Å per molecule, which means that the large phosphocholine headgroup present in all phospholipids tested was the limiting factor of molecular area upon monolayer compression (Brezesinski et al., 1996; Vaknin et al., 1991). For the DPPC + LA monolayer, this means that the linolenic acid will be located among the acyl chains of DPPC (Hac-Wydro and Wydro, 2007) or it may be squeezed out of the monolayer, going into the subphase (Fig. 3.8, scheme 2).

Several changes were observed upon the addition of AAPH to the subphase and/or antioxidants to the monolayer (α-tocopherol) or to its aqueous subphase (Trolox). Concerning the presence of AAPH in the subphase, no significant change in the isotherm was observed and this was expected because DPPC acyl chains do not possess any unsaturated bond prone to oxidative attack. However, BAM images show a clear interaction between components of AAPH subphase with the monolayer through the change of domain shape and the appearance of white dots, located mainly at the frontier between LC and LE phases. In previous reports, these white structures have been associated to salt crystals (Benitez and Talham, 2004) or to packing defects created where adjacent domain edges with conflicting molecular orientations grow together during the LE/LC phase transition (Schief et al., 2000). In our case, these structures may derive from AAPH itself or from its decomposition products. The decomposition of AAPH produces molecular nitrogen and two carbon radicals. The carbon radicals may combine to produce stable products or react with molecular oxygen to give peroxyl radicals. The carbon radicals are formed in pairs in close proximity, some recombining to give nonreactive stable products (Betigeri et al., 2005). Our BAM results show that AAPH molecules and derivatives clearly interact with all monolayers, fostering the existence of peroxyl radicals in its vicinity (Fig. 3.8, scheme 3).

One of the most important aspects was the verification that peroxyl radicals were present in the experimental conditions employed when the monolayer was compressed. Considering that the rate of free radical generation can be calculated as $1.36 \times 10^{-6} \times$

[AAPH] × time and expressed as M s^{-1},(Niki, 1990) we have estimated the production of 0.98 μmol min^{-1} of radical during the 10 min incubation period prior transferring AAPH/buffer solution to the trough. Peroxyl radicals are rather instable, starting chain reactions that will generate autoxidation products (peroxides and alcohols) in the absence of other substrates/oxidable species (Werber et al., 2011). Hence, as experiments were carried out at 21 °C, for which the rate of formation from AAPH is about ten times lower than at 37 °C, we did not expect a significant production of this radical during monolayer stabilization and compression. Analyzing the results shown in Fig. 3.3A, it is possible to ascertain that peroxyl radicals were present because a significant change in the isotherm of DPPC was noticed when α-tocopherol was present in the monolayer and AAPH (along with derived decomposition products) were in the subphase concomitantly, while no significant change in the isotherms was noticed when these species were added separately. This means that their interaction took place along the experiment in the Langmuir trough, in presence of peroxyl radicals that reached the monolayer.

In fact, it has been shown that α-tocopherol intercalates into phospholipid bilayers with the long axis of the molecule oriented parallel to the lipid hydrocarbon chains, with the α-tocopherol molecule able to rotate about its long axis and diffuse laterally within fluid lipid bilayers (Wang and Quinn, 1999). Moreover, previous studies of binary mixtures of DPPC (Quinn, 1995) or EPC (Naumowicz and Figaszewski, 2005) and α-tocopherol have shown that complexes of 10:1 stoichiometry (phospholipid:α-tocopherol) are formed. Our BAM results corroborate such observations as a clear change in the complexity of LC domains (Fig. 3.6E) was observed upon α-tocopherol incorporation into the DPPC monolayer.

Moreover, α-tocopherol reacts with a peroxyl radical either by concerted hydrogen transfer or by sequential electron followed by proton transfer to form a lipid hydroperoxide and the tocopheroxyl radical. The stability of the tocopheroxyl radical is attributed to the delocalization of the unpaired electron about the fully substituted chromanol ring system. Reaction of the tocopheroxyl radical with a peroxyl radical yields two groups of products, namely 8α-substituted tocopherones and epoxy-8α-hydroperoxytocopherones, also prone to interact with membrane bilayers (Liebler et al., 1990; Wang and Quinn, 1999). From our results, the LC domains presented less organized, less defined shapes with a high number of white dots associated to the LC domains when both AAPH and α-tocopherol were present (Fig. 3.6F). These features undeniably provide further evidence of the interaction and formation of oxidation products that also interact with the phospholipid monolayer (Fig. 3.8, scheme 3.4).

In Fig. 3.9 selected BAM images are presented, corresponding to the effect of α-tocopherol and Trolox in the DPPC monolayer at two different pressures (10 and 30 mN m^{-1}). These images confirm the different interaction of each antioxidant with the monolayer, which is

putatively related with their location within the membrane as discussed above. In fact, for lower pressures (10 mN m^{-1}), despite the maintenance of the multilobed shape of the lipid domains, the fluidification of the monolayer and smaller lipid domains were observed in the presence of Trolox. In the presence of α-tocopherol, a more complex pattern may be recognized, and the size of the lipid domains is similar when compared to that of DPPC monolayers without antioxidants. Nevertheless, for higher pressures (30 mN m^{-1}), a more pronounced effect in the lipid domains was observed for α-tocopherol. Indeed, the lipid domains are due to the arrangement of the alkyl chains of the phospholipids, being the alkyl chains of the lipid in closer contact with the prenyl chains of the antioxidant. Contrastingly, the interaction of DPPC with Trolox is confined to the phospholipid headgroups, which is confirmed by the presence of a multilobed pattern even at high pressures.

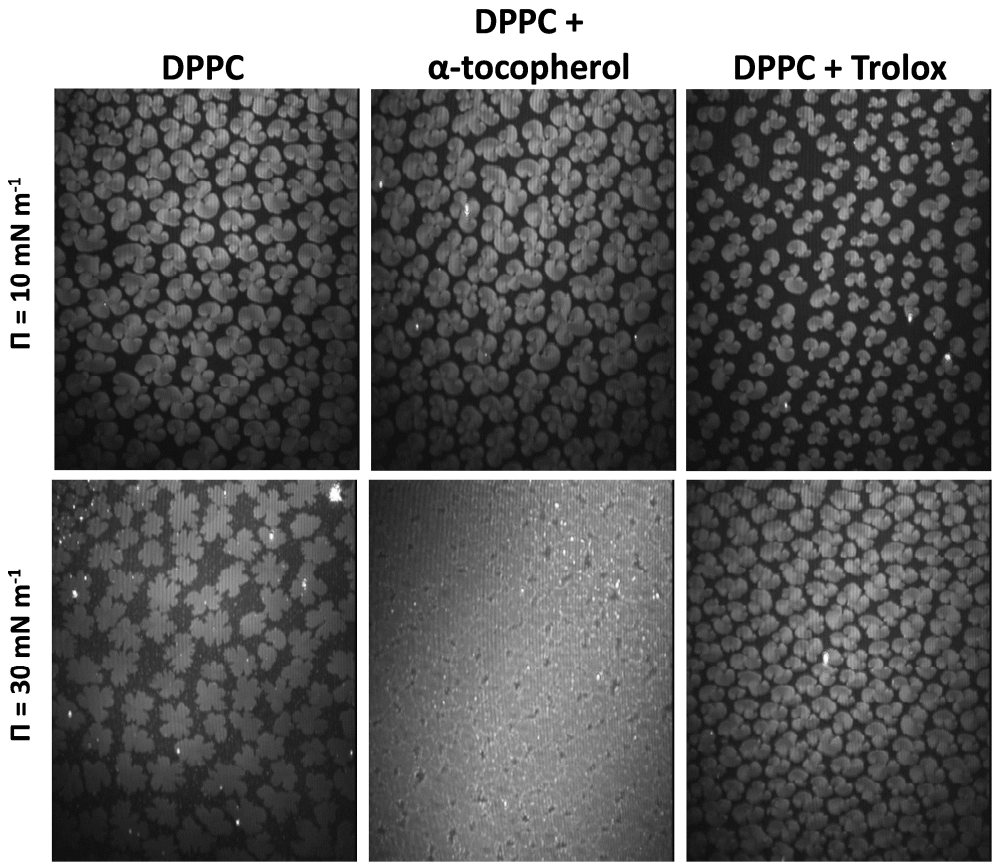

Figure 3.9. Domain patterns formed in DPPC monolayers for surface pressures of 10 and 30 mN m^{-1} in absence of antioxidants and in presence of either α-tocopherol or Trolox.

For DPPC + LA monolayers, the addition of any other component, AAPH or antioxidant, caused the reappearance of the plateau associated to the LE/LC transition of DPPC in the isotherms and the corresponding formation of domains observed by BAM. As all isotherms are similar, even in the absence of AAPH, the oxidation of LA by peroxyl

radicals is not the cause of LC domain formation. In fact, the absence of a plateau for DPPC + LA isotherm obtained for the buffer subphase indicates the miscibility between these two lipids, which was surpassed by the electrostatic interactions of Trolox, AAPH and oxidation products with the charged head groups of DPPC, causing phase segregation upon monolayer compression. The existence of this electrostatic interaction is further supported by the decrease of $A_{collapse}$ observed for those experiments. The presence of LA (and its oxidation products) in the monolayer can be inferred by the atypical shape of DPPC domains (Fig. 3.6, G and H) whenever AAPH and/or Trolox were present.

The BAM technique also allowed the observation of a white branched structure, whenever α-linolenic acid and α-tocopherol were present (Fig. 3.7), indicating a separation of these components. These branched structures are formed through van de Waals interactions, as described previously for a calix[8]arene derivative (Miguel et al., 2005). Association of α-tocopherol to fatty acids have been reported before,(Kagan and Quinn, 1988; Quinn, 2012) bearing formation of complexes between the 3 methyl groups of the chromanol ring of α-tocopherol and the unsaturated residues of the fatty acids (rather than the prenyl side chain) (Urano et al., 1993). From our BAM micrographs and known hydrophobicity of these compounds, the α-tocopherol-α-linolenic acid complexes seem to be located above or within the monolayer (Fig. 3.8, scheme 3.5), which may be considered an evidence for location of these complexes between the two lipidic layers that comprises the biological membrane or in lateral PUFA-rich segregated domains, as previously suggested by other authors (Atkinson et al., 2010; Quinn, 2012).

Trolox, a soluble analogue of α-tocopherol as it possess the chroman head (including a hydroxyl-bearing aromatic system) and lacks the saturated hydrocarbon tail present in α-tocopherol, has been extensively applied as standard compound in antioxidant assessment (Magalhães et al., 2008) and frequently in methods comprising lipidic biomimetic structures (Nenadis et al., 2007). Generally, Trolox is considered as an aqueous phase antioxidant. Our results indicate a significant interaction of Trolox with the monolayers, promoting the expansion of DPPC and the compression of the EPC monolayer. Moreover, it also promoted the stabilization of DPPC domains over a larger π range (Fig. 3.6B) without changing their shape, which indicates that Trolox interacts with the surface of DPPC monolayer (Fig. 3.8, scheme 3.6). In fact, under the experimental conditions applied, Trolox will present a negative charge on the carboxylic group (pKa 3.89), (Barclay et al., 1995) fostering its interaction with the positively charged choline group of the phospholipids, which justifies our observations.

BAM images for the concomitant presence of Trolox and AAPH in the subphase of DPPC and DPPC + LA monolayers also showed significant differences from those taken when only one substance was present. Isotherms were also different for DPPC and EPC

monolayers. Recent work has demonstrated that Trolox reacts by adding one or two oxygen atoms to its phenoxyl radical, and none or little molecular rearrangement is undertaken. Besides, other minor by-products have been described, including those derived from the bond of the phenoxyl radical with the peroxyl radicals derived from AAPH (Bentayeb et al., 2012). These molecules can further interact with the phospholipid monolayer, in a way similar to Trolox because the carboxylic group is kept in the majority of reaction products.

For EPC monolayers, BAM images were not useful to ascertain peroxidation/antioxidant protection effects. As it comprises a mixture of phosphatidylcholines that form a homogenous monolayer throughout the experimental conditions, domain formation was not observed. Nevertheless, the interaction with AAPH subphase caused a slight compression of the monolayer (Fig. 3.2 and 3.3, C) probably due to oxidation of the unsaturated acyl chains.

The addition of either Trolox (subphase) or α-tocopherol (monolayer) promoted even more the monolayer compression, in this case due to the Trolox interaction with the polar headgroups of phosphatidylcholines (seen also here for DPPC) or due to the hydrophobic α-tocopherol interaction with the unsaturated acyl chains in the phospholipid through van der Waals forces.

The EPC monolayer expansion observed in the presence of both AAPH and antioxidants may indicate a depletion of each antioxidant through competition with the EPC double bonds as targets of oxidation by peroxyl radicals, which can be interpreted as a protective effect. Nevertheless, the isotherm profile does not coincide with the initial EPC isotherm, surpassing it towards larger areas per EPC molecule, indicating also the interaction of Trolox and α-tocopherol oxidation products with the monolayer (also verified for DPPC monolayers).

In conclusion, the combination of π-A isotherms and BAM imaging is a suitable biophysical approach to evaluate the effect of peroxidation conditions on phosphatidylcholine monolayers in the presence of antioxidants and oxidation targets. The interaction of Trolox, α-tocopherol and their peroxidation products was clearly ascertain, which is a relevant result when considering the current application of Trolox as standard in methodologies aiming the assessment of antioxidant capacity in the presence of lipidic structures, such as liposomes. Undeniably, it is necessary to take into consideration the partition between antioxidants and biomimetic lipidic structures as an "effective" concentration, lower than the initial aqueous concentration will be available in both aqueous and lipidic phases. Furthermore, the presence of peroxidation products in the monolayer indicates that, in methodologies where these products are measured in the aqueous phase, results may be biased, accounting for a lower extension of peroxidation.

Finally, the formation of segregated, branched shaped domains of α-tocopherol and linolenic acid observed for DPPC monolayers is of highly significance for biological systems, providing microscopic imaging evidence of the association between α-tocopherol and unsaturated fatty acids.

3.5 References

Atkinson, J.; Harroun, T.; Wassall, S. R.; Stillwell, W.; Katsaras, J. The location and behavior of alpha-tocopherol in membranes. *Molecular Nutrition & Food Research* **2010,** *54*, 641-651.

Barclay, L. R. C.; Artz, J. D.; Mowat, J. J. Partitioning and antioxidant action of the water-soluble antioxidant, trolox, between the aqueous and lipid phases of phosphatidylcholine membranes: 14C tracer and product studies. *Biochimica Et Biophysica Acta-Biomembranes* **1995,** *1237*, 77-85.

Benitez, I. O.; Talham, D. R. Brewster angle microscopy of calcium oxalate monohydrate precipitation at phospholipid monolayer phase boundaries. *Langmuir* **2004,** *20*, 8287-8293.

Bentayeb, K.; Rubio, C.; Nerin, C. Study of the antioxidant mechanisms of Trolox and eugenol with 2,2 '-azobis (2-amidinepropane)dihydrochloride using ultra-high performance liquid chromatography coupled with tandem mass spectrometry. *Analyst* **2012,** *137*, 459-470.

Betigeri, S.; Thakur, A.; Raghavan, K. Use of 2,2 '-Azobis(2-amidinopropane) dihydrochloride as a reagent tool for evaluation of oxidative stability of drugs. *Pharmaceutical Research* **2005,** *22*, 310-317.

Brezesinski, G.; Thoma, M.; Struth, B.; Mohwald, H. Structural changes of monolayers at the air/water interface contacted with n-alkanes. *Journal of Physical Chemistry* **1996,** *100*, 3126-3130.

Cubillos, M.; Lissi, E.; Abuin, E. Lipid peroxidation rates of DPPC liposomes containing different amounts of oxidable lipids show opposite dependence with the temperature. *Journal of the Chilean Chemical Society* **2006,** *51*, 825-828.

Cuzzocrea, S.; Riley, D. P.; Caputi, A. P.; Salvemini, D. Antioxidant therapy: A new pharmacological approach in shock, inflammation, and ischemia/reperfusion injury. *Pharmacological Reviews* **2001,** *53*, 135-159.

Cwiklik, L.; Jungwirth, P. Massive oxidation of phospholipid membranes leads to pore creation and bilayer disintegration. *Chemical Physics Letters* **2010,** *486*, 99-103.

Duncan, S. L.; Larson, R. G. Comparing experimental and simulated pressure-area isotherms for DPPC. *Biophysical Journal* **2008,** *94*, 2965-2986.

Edidin, M. Timeline - Lipids on the frontier: a century of cell-membrane bilayers. *Nature Reviews Molecular Cell Biology* **2003,** *4*, 414-418.

Fadel, O.; El Kirat, K.; Morandat, S. The natural antioxidant rosmarinic acid spontaneously penetrates membranes to inhibit lipid peroxidation in situ. *Biochimica Et Biophysica Acta-Biomembranes* **2011,** *1808*, 2973-2980.

Hac-Wydro, K.; Wydro, P. The influence of fatty acids on model cholesterol/phospholipid membranes. *Chemistry and Physics of lipids* **2007,** *150*, 66-81.

Halliwell, B.; Gutteridge, J. M. C., *Free radicals in biology and medicine*. 4th ed.; Oxford University Press: Oxford, 2007.

Jacob, R. F.; Mason, R. P. Lipid peroxidation induces cholesterol domain formation in model membranes. *Journal of Biological Chemistry* **2005,** *280*, 39380-39387.

Kagan, V. E.; Quinn, P. J. The interaction of alpha-tocopherol and homologs with shorter hydrocarbon chains with phospholipid-bilayer dispersions - a fluorescence probe study. *European Journal of Biochemistry* **1988,** *171*, 661-667.

KamalEldin, A.; Appelqvist, L. A. The chemistry and antioxidant properties of tocopherols and tocotrienols. *Lipids* **1996,** *31*, 671-701.

Kanicky, J. R.; Shah, D. O. Effect of degree, type, and position of unsaturation on the pK(a) of long-chain fatty acids. *Journal of Colloid and Interface Science* **2002,** *256*, 201-207.

Khabiri, M.; Roeselova, M.; Cwiklik, L. Properties of oxidized phospholipid monolayers: An atomistic molecular dynamics study. *Chemical Physics Letters* **2012,** *519-20*, 93-99.

Klopfer, K. J.; Vanderlick, T. K. Isotherms of dipalmitoylphosphatidylcholine (DPPC) monolayers: Features revealed and features obscured. *Journal of Colloid and Interface Science* **1996,** *182*, 220-229.

Leekumjorn, S.; Cho, H. J.; Wu, Y. F.; Wright, N. T.; Sum, A. K.; Chan, C. The role of fatty acid unsaturation in minimizing biophysical changes on the structure and local effects of bilayer membranes. *Biochimica Et Biophysica Acta-Biomembranes* **2009,** *1788*, 1508-1516.

Liebler, D. C.; Baker, P. F.; Kaysen, K. L. Oxidation of vitamin-e - evidence for competing autoxidation and peroxyl radical trapping reactions of the tocopheroxyl radical. *Journal of the American Chemical Society* **1990,** *112*, 6995-7000.

Lúcio, M.; Nunes, C.; Gaspar, D.; Ferreira, H.; Lima, J. L. F. C.; Reis, S. Antioxidant Activity of Vitamin E and Trolox: Understanding of the Factors that Govern Lipid Peroxidation Studies In Vitro. *Food Biophysics* **2009,** *4*, 312-320.

Magalhães, L. M.; Segundo, M. A.; Reis, S.; Lima, J. L. F. C. Methodological aspects about in vitro evaluation of antioxidant properties. *Analytica Chimica Acta* **2008,** *613*, 1-19.

Marsh, D. Thermodynamic analysis of chain-melting transition temperatures for monounsaturated phospholipid membranes: Dependence on cis-monoenoic double bond position. *Biophysical Journal* **1999,** *77*, 953-963.

Martinez-Seara, H.; Rog, T.; Pasenkiewicz-Gierula, M.; Vattulainen, I.; Karttunen, M.; Reigada, R. Effect of double bond position on lipid bilayer properties: Insight through atomistic simulations. *Journal of Physical Chemistry B* **2007,** *111*, 11162-11168.

Mason, R. P.; Walter, M. F.; Mason, P. E. Effect of oxidative stress on membrane structure: Small-angle x-ray diffraction analysis. *Free Radical Biology and Medicine* **1997,** *23*, 419-425.

McLean, L. R.; Hagaman, K. A. Effect of lipid physical state on the rate of peroxidation of liposomes. *Free Radical Biology and Medicine* **1992,** *12*, 113-119.

Miguel, G.; Pedrosa, J. M.; Martin-Romero, M. T.; Munoz, E.; Richardson, T. H.; Camacho, L. Conformational changes of a calix[8]arene derivative at the air-water interface. *Journal of Physical Chemistry B* **2005,** *109*, 3998-4006.

Mitsche, M. A.; Wang, L. B.; Small, D. M. Adsorption of egg phosphatidylcholine to an air/water and triolein/water bubble interface: use of the 2-dimensional phase rule to estimate the surface composition of a phospholipid/triolein/water surface as a function of surface pressure. *Journal of Physical Chemistry B* **2010,** *114*, 3276-3284.

Mowri, H.; Nojima, S.; Inoue, K. Effect of lipid-composition of liposomes on their sensitivity to peroxidation. *Journal of Biochemistry* **1984,** *95*, 551-558.

Mueller, N. S.; Wedlich-Soeldner, R.; Spira, F. From mosaic to patchwork: Matching lipids and proteins in membrane organization. *Molecular Membrane Biology* **2012,** *29*, 186-196.

Murzyn, K.; Zhao, W.; Karttunen, M.; Kurdziel, M.; Rog, T. Dynamics of water at membrane surfaces: Effect of headgroup structure. *Biointerphases* **2006,** *1*, 98-105.

Naumowicz, M.; Figaszewski, Z. A. Impedance analysis of phosphatidylcholine/alpha-tocopherol system in bilayer lipid membranes. *Journal of Membrane Biology* **2005,** *205*, 29-36.

Nenadis, N.; Lazaridou, O.; Tsimidou, M. Z. Use of reference compounds in antioxidant activity assessment. *Journal of Agricultural and Food Chemistry* **2007,** *55,* 5452-5460.

Niki, E. Antioxidants in relation to lipid-peroxidation. *Chemistry and Physics of lipids* **1987,** *44*, 227-253.

Niki, E. Free-radical initiators as source of water-soluble or lipid-soluble peroxyl radicals. *Methods in Enzymology* **1990,** *186*, 100-108.

Nugent, T.; Jones, D. T. Membrane protein structural bioinformatics. *Journal of Structural Biology* **2012,** *179*, 327-337.

Nunes, C.; Brezesinski, G.; Pereira-Leite, C.; Lima, J. L. F. C.; Reis, S.; Lúcio, M. NSAIDs interactions with membranes: a biophysical approach. *Langmuir* **2011,** *27*, 10847-58.

Quinn, P. J. Characterization of clusters of alpha-tocopherol in gel and fluid phases of dipalmitoylglycerophosphocholine. *European Journal of Biochemistry* **1995,** *233,* 916-925.

Quinn, P. J. Lipid-lipid interactions in bilayer membranes: Married couples and casual liaisons. *Progress in Lipid Research* **2012,** *51*, 179-198.

Reis, S.; Lúcio, M.; Segundo, M.; Lima, J. L. F. C., Use of Liposomes to Evaluate the Role of Membrane Interactions on Antioxidant Activity. In *Liposomes: Methods and Protocols, Vol 2: Biological Membrane Models*, Weissig, V., Ed. Humana Press Inc: Totowa, 2010; Vol. 606, pp 167-188.

Rigoletto, T. d. P.; Zaniquelli, M. E. D.; Santana, M. H. A.; de la Torre, L. G. Surface miscibility of EPC/DOTAP/DOPE in binary and ternary mixed monolayers. *Colloids and surfaces. B, Biointerfaces* **2011,** *83*, 260-9.

Schief, W. R.; Touryan, L.; Hall, S. B.; Vogel, V. Nanoscale topographic instabilities of a phospholipid monolayer. *Journal of Physical Chemistry B* **2000,** *104*, 7388-7393.

Schnitzer, E.; Pinchuk, I.; Lichtenberg, D. Peroxidation of liposomal lipids. *European Biophysics Journal with Biophysics Letters* **2007,** *36*, 499-515.

Tomoaiacotisel, M.; Zsako, J.; Mocanu, A.; Lupea, M.; Chifu, E. Insoluble mixed monolayers .3. The ionization characteristics of some fatty-acids at the air-water-interface. *Journal of Colloid and Interface Science* **1987,** *117*, 464-476.

Tsuchiya, H.; Ueno, T.; Tanaka, T.; Matsuura, N.; Mizogami, M. Comparative study on determination of antioxidant and membrane activities of propofol and its related compounds. *European Journal of Pharmaceutical Sciences* **2010,** *39*, 97-102.

Urano, S.; Matsuo, M.; Sakanaka, T.; Uemura, I.; Koyama, M.; Kumadaki, I.; Fukuzawa, K. Mobility and molecular-orientation of vitamin E in liposomal membranes as determined by 19F NMR and fluorescence polarization techniques. *Archives of Biochemistry and Biophysics* **1993,** *303*, 10-14.

Vaknin, D.; Kjaer, K.; Alsnielsen, J.; Losche, M. Structural-properties of phosphatidylcholine in a monolayer at the air-water-interface - neutron reflection study and reexamination of X-ray reflection measurements. *Biophysical Journal* **1991,** *59*, 1325-1332.

Valko, M.; Rhodes, C. J.; Moncol, J.; Izakovic, M.; Mazur, M. Free radicals, metals and antioxidants in oxidative stress-induced cancer. *Chemico-Biological Interactions* **2006,** *160*, 1-40.

Valko, M.; Leibfritz, D.; Moncol, J.; Cronin, M. T. D.; Mazur, M.; Telser, J. Free radicals and antioxidants in normal physiological functions and human disease. *International Journal of Biochemistry & Cell Biology* **2007,** *39*, 44-84.

Volinsky, R.; Paananen, R.; Kinnunen, P. K. J. Oxidized Phosphatidylcholines Promote Phase Separation of Cholesterol-Sphingomyelin Domains. *Biophysical Journal* **2012,** *103*, 247-254.

Wang, X. Y.; Quinn, P. J. Vitamin E and its function in membranes. *Progress in Lipid Research* **1999,** *38*, 309-336.

Werber, J.; Wang, Y. J.; Milligan, M.; Li, X. H.; Ji, J. A. Analysis of 2,2 '-Azobis (2-Amidinopropane) Dihydrochloride Degradation and Hydrolysis in Aqueous Solutions. *Journal of Pharmaceutical Sciences* **2011,** *100*, 3307-3315.

Wong-Ekkabut, J.; Xu, Z. T.; Triampo, W.; Tang, I. M.; Tieleman, D. P.; Monticelli, L. Effect of lipid peroxidation on the properties of lipid bilayers: A molecular dynamics study. *Biophysical Journal* **2007,** *93*, 4225-4236.

CHAPTER 4

Interaction of soluble biological antioxidants with phosphatidylcholine monolayers

4. Interaction of soluble biological antioxidants with phosphatidylcholine monolayers

4.1 Introduction

Membranes of eukaryotic cells act as barriers between separate functional compartments and, at the same time, the cell-surface membrane is the frontier between the cell and its environment. Exploration of this frontier has revealed its physical and functional properties. The plasma membrane is a lipid bilayer, the composition of which regulates frontier crossing by molecules between the cell surroundings and its interior, and the properties of the bilayer are different from those of any of its components alone (Edidin, 2003). Over the years the study of the bilayer has aroused much interest in order to better understand the possible structural, physical and chemical changes due to interactions between the bilayer components and other compounds.

Biological membranes generally contain mixtures of lipids that vary with respect to both their polar headgroups and their acyl chains. It has been admitted that the primary organizing force in the formation of these systems is dominated by the contribution of hydrophobic and hydrophilic effects (Gzyl-Malcher et al., 2009).

Lipid peroxidation has been a central aspect of studies about the nature of free radical species and their origin in biological systems (Sevanian and Ursini, 2000), once the free radicals and other so-called “reactive species” are constantly produced *in vivo* by all body tissues (Halliwell, 2001). Moreover, there has been a growing interest in lipid peroxidation based on evidence that biologically active products are formed that influence cell function and the course of major human diseases (Sevanian and Ursini, 2000). This uncontrolled reaction generates cytotoxic compounds and disrupts the various important structural and protective function associated with biomembranes, being implicated in the etiology of many diseases, including cancer, cardiovascular and neurological diseases, and other oxidative stress mediated dysfunctions.

Free radicals and reactive nonradical species derived from radicals exist in biological cells and tissues at low but measurable concentrations. Their concentrations are determined by the balance between their rates of production and their rates of clearance by various antioxidant compounds and enzymes (Droge, 2002).

Over the years biomimetic models and new techniques were used to understand the biological membranes and the role of the antioxidants (defined as an inhibitor of lipid peroxidation, namely biological antioxidants including glutathione, ascorbic acid and uric

acid). These molecules have a relevant role on protecting membranes from peroxidation and lipid peroxidation propagation (promoted by attack of lipid molecules), either by the capability to scavenge free radicals, or by interacting with membranes and changing their biophysical properties in a way that favors their interaction with lipid radicals (Reis et al., 2010). The relatively high intracellular concentrations of glutathione and other antioxidative compounds provide a strong basal scavenging capacity (Droge, 2002).

Glutathione is currently one of the most studied antioxidant because it is endogenously synthesized all throughout the body and found in all cells, sometimes in rather high concentrations. For example, the response of glutathione has been frequently studied during intense exercise, because the oxidized glutathione levels increased in the blood after exercise, suggesting an increase in oxidative stress. A decreased level of glutathione in the plasma is the result of an increased utilization of it inside the muscle, presumably to fight or "quench" any circulating free radicals (Kerksick and Willoughby, 2005).

The ascorbic acid is a key water-soluble antioxidant due to its ability to interact with ROS and to reduce the radicals formed from α-tocopherol and β-carotene (Sharma and Buettner, 1993). The participation in various free-radical processes is a likely cause of the known immunomodulating and antiviral properties of ascorbic acid (Furuya et al., 2008; Jariwalla et al., 2007; Uchide and Toyoda, 2011). Its aqueous solutions are easily oxidized (Capuzzi et al., 1996) but it is widely used as vitaminous, regenerative and antiviral medication in the treatment of various respiratory viral infections including influenza, herpetic infections, viral hepatitis and other infectious diseases (Brinkevich et al., 2012).

At physiological pH almost all uric acid is ionized to urate (Halliwell and Gutteridge, 2007). Urate is a powerful scavenger of ROS *in vitro*. Indeed, it was proposed that it works as a biological antioxidant and it was also further suggested that loss of urate oxidase was advantageous to primates since it simultaneously removed a source of H_2O_2 (from urate oxidase) and allowed a powerful antioxidant to accumulate (Ames et al., 1981).

In this context, the present work aims to provide a biophysical approach to assess the effect of peroxyl radicals resulting from a hydrophilic generator, 2,2′-azobis (2-amidinopropane) dihydrochloride (AAPH), and natural antioxidants with relevant role in biological systems: glutathione, ascorbic acid and uric acid. Biomembranes were mimicked using lipid monolayers as membrane model systems, since this provides a convenient model for understanding bilayer structures. Furthermore, since monolayers can be studied in a Langmuir trough, where both the temperature and the mean molecular area can be controlled, we were able to probe some aspects of the liquid expanded to liquid condensed phase transition. Different lipid compositions characteristic of the biomembranes were used: DPPC (L-α-dipalmitoylphosphatidylcholine), DPPC:linolenic acid (9:1), and EPC (L-α-phosphatidylcholine). The extensive range of peroxidation related

phenomena and monolayer structural changes were analyzed both by π/A isotherms and Brewster Angle Microscopy (BAM).

4.2 Reagents and solutions

Egg yolk phosphatidylcholine (EPC), potassium phosphate monobasic, 2,2'-azobis(2-methylpropionamidine) dihydrochloride (AAPH), uric acid, glutathione, ascorbic acid and α-linolenic acid (LA) were purchased from Sigma-Aldrich (St. Louis, MO). L-α-dipalmitoylphosphatidylcholine (DPPC) was purchased from Avanti Polar Lipids Inc. Chloroform from Landilab (Porto, Portugal) was used as co-spreading solvent. The subphase used, 75 mM hydrogen phosphate/phosphate buffer (pH 7.4), was prepared using Milli-Q water (resistivity > 18.2 MΩ cm, Millipore, Billerica, MA).
Lipid solutions were prepared in chloroform and they contained DPPC (0.734 mg mL^{-1}), DPPC + LA (9:1, w/w; 0.642 mg mL^{-1} of DPPC) or EPC (0.751 mg mL^{-1}). Uric acid, glutathione, ascorbic acid were added to the subphase buffer at 20 μM. For generation of peroxyl radicals, AAPH (12 mM) was dissolved in hydrogen phosphate buffer at 37 °C and kept at this temperature during 10 minutes. Whenever necessary, uric acid, glutathione, and ascorbic acid were dissolved in this solution immediately before its transfer into the trough.

4.3 Results

4.3.1 π-A measurements

The isotherms of DPPC, DPPC + LA and EPC spread above subphases containing AAPH, antioxidant (glutathione, ascorbic acid or uric acid) or these two compounds concomitantly are given in Fig. 4.1-4.3. DPPC isotherms present the typical plateau at 5 – 8 mN m^{-1}, corresponding to the first order phase transition from LE to LC. This plateau was displaced towards higher areas per molecule for subphases containing the antioxidant and AAPH. This effect was further enhanced for glutathione, where the transition pressure was also higher (9.4 mN m^{-1} compared to 6.2 mN m^{-1} observed for phosphate buffer subphase).

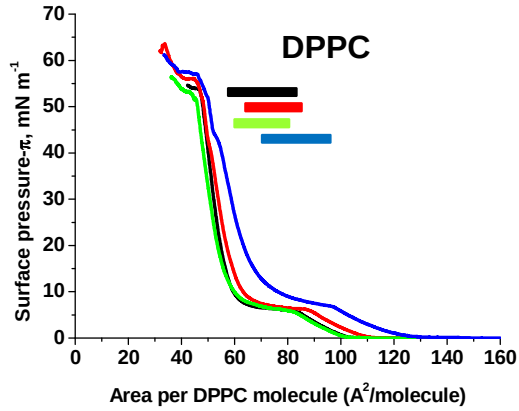

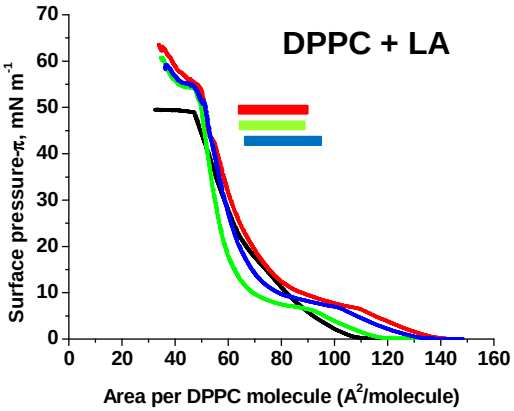

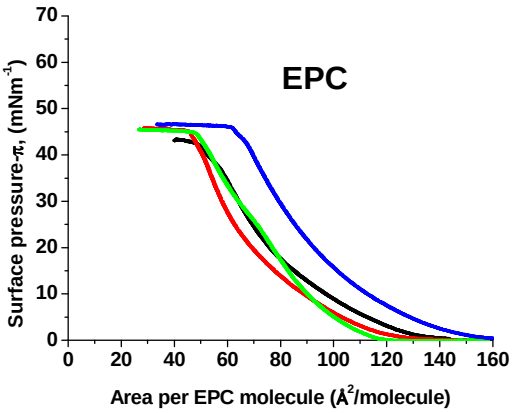

Figure 4.1. Surface pressure-area isotherms for different lipid systems, with monolayers formed and compressed above subphases containing phosphate buffer pH 7.4 (—), AAPH solution (—), glutathione solution (—), and AAPH + glutathione solution (—). The solid bars represent the area per DPPC molecule where LC domains can be visualized by BAM.

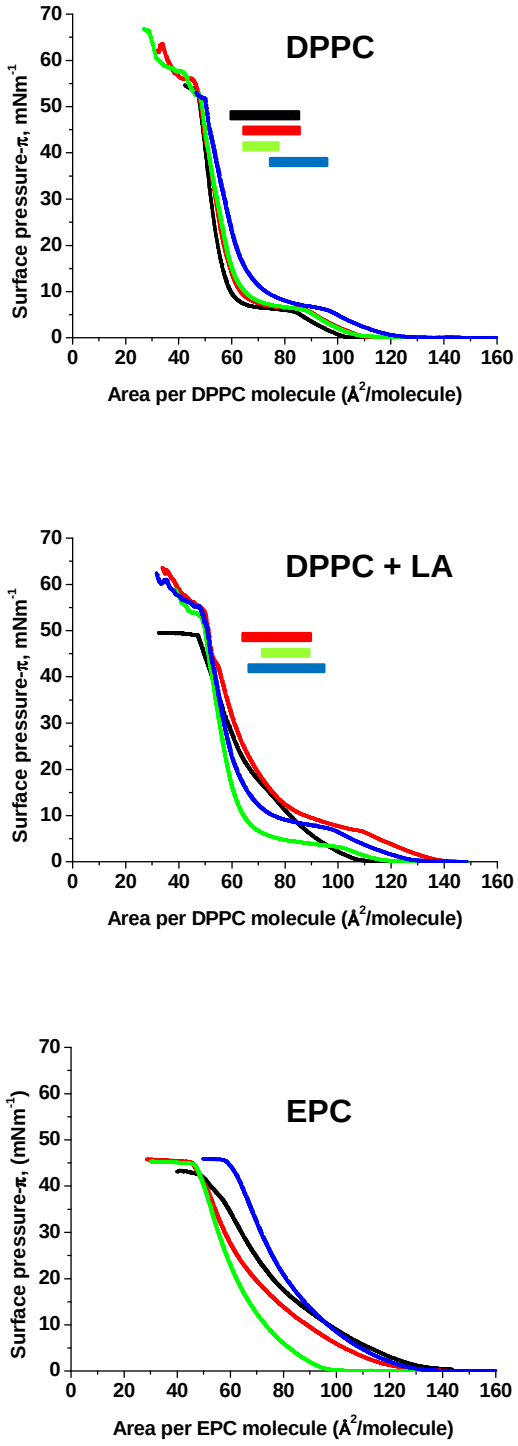

Figure 4.2. Surface pressure-area isotherms for different lipid systems, with monolayers formed and compressed above subphases containing phosphate buffer pH 7.4 (—), AAPH solution (—), ascorbic acid solution (—), and AAPH + ascorbic acid solution (—). The solid bars represent the area per DPPC molecule where LC domains can be visualized by BAM.

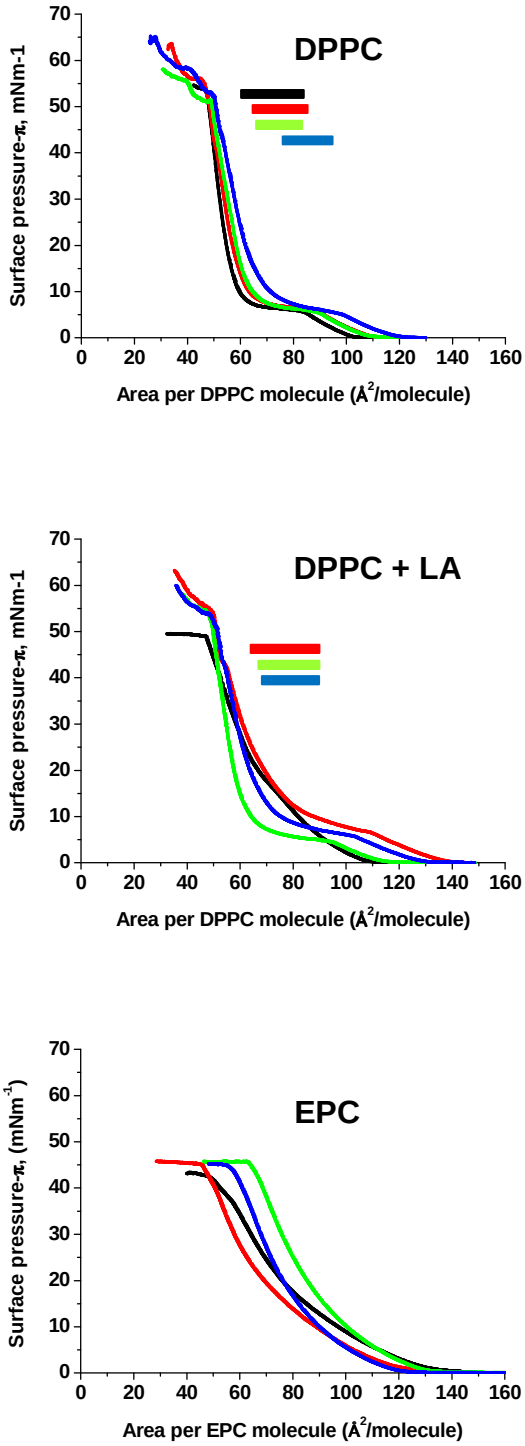

Figure 4.3. Surface pressure-area isotherms for different lipid systems, with monolayers formed and compressed above subphases containing phosphate buffer pH 7.4 (—), AAPH solution (—), uric acid solution (—), and AAPH + uric acid solution (—). The solid bars represent the area per DPPC molecule where LC domains can be visualized by BAM.

The DPPC + LA isotherm for the phosphate buffer subphase does not show any plateau corresponding to phase transition. However, when any of the tested compounds is added to the subphase, a plateau similar to that observed for monolayers containing DPPC only is achieved. For subphases containing each of the antioxidants tested, the isotherm for low π values (up to 95 $Å^2$ per molecule) is similar to that obtained for the phosphate buffer subphase. For lower areas per molecule, a plateau is observed up to 68 $Å^2$ per molecule, from which the area per molecule changes much less upon monolayer compression. Whenever AAPH was present in the subphase of DPPC + LA monolayer, the surface pressure starts to rise from larger areas per molecule (140 $Å^2$ per molecule) when compared to other subphases without this component (110 – 120 $Å^2$ per molecule). Moreover, the whole isotherm profile is shifted towards large areas per molecule, while the plateau zone is less evident when only AAPH is present. The concomitant addition of AAPH and any antioxidant to the subphase makes the isotherm shift slightly towards larger areas per molecule before the LE/LC transition and towards lower areas per molecule when the phosphatidylcholine exists as LC, compared to the DPPC + LA isotherm. In fact, isotherms from subphases containing AAPH and antioxidant are placed between the isotherms from subphases containing only one of these components.

$\pi_{collapse}$ and $A_{collapse}$ are similar for DPPC and DPPC + LA systems for all experiments when any of the compounds tested were added to the monolayer subphase, with values of c.a. 60 mN m^{-1} and 30 $Å^2$ per molecule, respectively (Table 4.1). These values are different from those attained for the monolayers spread above phosphate buffer, for which $\pi_{collapse}$ and $A_{collapse}$ were c.a. 51 mN m^{-1} and 47 $Å^2$ per molecule, respectively. Addition of AAPH in particular caused Cs^{-1} to converge to a similar value in both systems (142 and 160 mN m^{-1}), resulting in a more compressible monolayer for DPPC + LA and less compressible for DPPC.

Table 4.1. Characteristic parameters (elastic modulus, collapse pressure and collapse area) of the Langmuir monolayers tested on aqueous subphases containing the peroxidation inducer (AAPH) and antioxidants (glutathione, ascorbic acid, uric acid)

Lipid system	Subphase	C_s^{-1} (mN m^{-1})	$\pi_{collapse}$ (mN m^{-1})	$A_{collapse}$ (Å per molecule)
DPPC	Phosphate buffer pH 7.4 [a]	248	53 ± 1	47.1 ± 1.0
	AAPH [a]	142	62 ± 1	33.6 ± 0.3
	Glutathione	240	60 ± 6	33.0 ± 5.2
	Glutathione + AAPH	285	61 ± 1	34.6 ± 0.0
	Ascorbic acid	219	62 ± 6	31.3 ± 5.7
	Ascorbic acid + AAPH	179	62 ± 3	29.5 ± 2.4
	Uric acid	242	59 ± 2	29.3 ± 1.8
	Uric acid + AAPH	211	62 ± 3	29.5 ± 2.7
DPPC + LA	Phosphate buffer pH 7.4 [a]	117	49 ± 1	47.8 ± 1.1
	AAPH [a]	160	63 ± 1	34.7 ± 1.3
	Glutathione	223	61 ± 1	34.7 ± 0.7
	Glutathione + AAPH	213	60 ± 1	35.2 ± 2.6
	Ascorbic acid	203	61 ± 5	33.4 ± 0.4
	Ascorbic acid + AAPH	176	63 ± 1	31.3 ± 0.1
	Uric acid	185	59 ± 2	29.3 ± 1.8
	Uric acid + AAPH	218	62 ± 3	29.5 ± 2.7
EPC	Phosphate buffer pH 7.4 [a]	93	42 ± 1	46.1 ± 2.8
	AAPH [a]	96	45 ± 1	46.1 ± 1.1
	Glutathione	91	45 ± 1	55.7 ± 8.5
	Glutathione + AAPH	95	46 ± 1	59.2 ± 1.8
	Ascorbic acid	80	45 ± 1	46.2 ± 1.0
	Ascorbic acid + AAPH	129	46 ± 1	57.5 ± 2.7
	Uric acid	146	45 ± 1	66.4 ± 5.4
	Uric acid + AAPH	138	45 ± 1	56.4 ± 2.3

For EPC monolayers, no plateau corresponding to phase transitions is observed in the isotherms. $A_{collapse}$ values are increased for all subphases (56 – 66 Å^2 per molecule), except

for that containing ascorbic acid, where $A_{collapse}$ was similar to that observed for EPC placed above phosphate buffer (46 Å² per molecule).
Addition of AAPH causes the isotherm to shift towards lower area per molecule, they have similar shape to EPC isotherm for phosphate buffer.
Whenever AO was present, the shape of isotherm changed slightly with apparently higher slopes at higher π. The behavior for each AO was different. For glutathione subphase, the initial area per molecule is slightly lower (115 Å² vs 140 Å² for phosphate buffer), but from π = 15 mN m⁻¹ the two isotherms coincided. When AAPH was added with glutathione, the initial area per molecule was increased to 160 Å² per molecule and the whole isotherm was shifted towards higher areas.
For ascorbic acid subphase, the initial area per molecule is even lower (95 Å²) and the isotherm is completely shifted towards lower areas per molecule. Addition of AAPH to ascorbic acid subphase originated an isotherm with a similar shape of that with ascorbic acid subphase, starting at an area per molecule similar to that of phosphate buffer isotherm and ending at a higher $A_{collapse}$ (57 Å² per molecule).
For uric acid subphase, an opposite behavior was observed because all isotherms started at similar area per molecule values and the isotherm from the subphase containing uric acid is more displaced towards larger areas per molecule than that containing both uric acid and AAPH.

4.3.2 BAM observation

For DPPC monolayers, domain formation during the phase transition between LE and LC was observed for all subphases. Nevertheless, their formation began at larger areas per molecule for subphases containing both antioxidant and AAPH (c.a. 95 Å² per molecule compared to 78 to 86 Å² per molecule for other subphases). Moreover, the shape and surface pressure interval where they exist changed for different subphases. In Fig. 4.4 BAM images showing typical domain features are given for all subphases and monolayers tested. For DPPC monolayer spread on phosphate buffer subphase, typical multilobed domains, with four lobes, were seen for areas per molecule between 57 and 65 Å² (π between 7 and 14 mN m⁻¹) and they merged in a light gray background for π over 33 mN m⁻¹. When AAPH was added to the subphase, similar domains were observed at larger π values (12 – 16 mN m⁻¹), which formed a complete light gray background for π over 27 mN m⁻¹. When glutathione was added to DPPC monolayer subphase, multilobed domains were also formed, along with simpler two lobed structures. They also incorporate small white

dots associated to the contour of the domains, corresponding to the interface between LE and LC phases. They became less organized at lower π values (10 mN m^{-1}), forming a homogeneous background from 15 mN m^{-1}. When both glutathione and AAPH were present in the subphase, the white dots became larger and the domain contours became less defined.

For the subphase containing ascorbic acid, multilobed domains bearing 3 lobes can be seen among branched white structures. In opposition to the white dots observed for glutathione subphase, these branched structures are not clearly associated to the DPPC domains, but they existed in π and area per molecule intervals similar to that observed for the glutathione subphase. The concomitant presence of AAPH and ascorbic acid provided domains with less defined contour and the branched structures were still observed. Similar results were obtained for the uric acid subphase, with longer white branched structures that appeared as long as π became larger than zero.

For DDPC + LA monolayers, typical domain formation from DPPC is not observed. In fact, some round white lipid aggregates could be seen at high π (c.a. 40 mN m^{-1}, Fig. 4.4). As observed for the isotherms, the addition of any component (AAPH or antioxidants or both) to the subphase allowed the appearance of domain structures from DPPC. These structures were quite similar to those observed for DPPC monolayers when glutathione or glutathione and AAPH were present in the subphase. For ascorbic acid, the white branched forms disappeared and the domain shape had sharp edges, with lower size and multiple configurations (Fig. 4.4). When both ascorbic acid and AAPH were present, the domain shape looks more similar to that of DPPC concerning the existence of a round contour, but without the multilobed shape.

The opposite behavior was presented when uric acid was present in the subphase because round, multilobed domains were observed for DDPC + LA monolayers. When uric acid and AAPH were both present in the subphase, the domain shape changed, showing sharp edges, as observed for ascorbic acid subphase.

For EPC, domain formation was not observed. Small white aggregates could also be seen at large π (c.a. 30 mN m^{-1}), for all subphases. When AAPH was added to subphases containing either ascorbic or uric acid, the small white branched structures disappeared.

	DPPC	DPPC+LA	EPC	DPPC+AAPH	DPPC+LA+AAPH	EPC+AAPH
Phosphate buffer	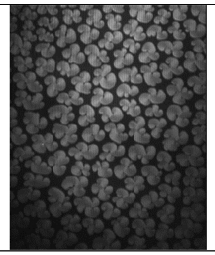			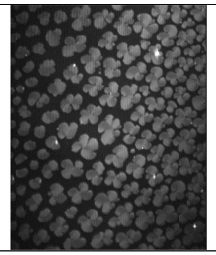	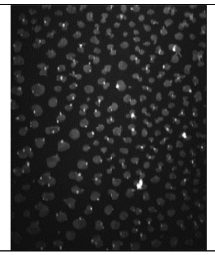	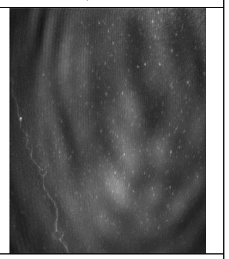
	(60.6; 9)	(49.3; 42.2)	(67.1; 32.3)	(65; 12.5)	(86.9; 8.9)	(56.7; 31.5)
Glutathione	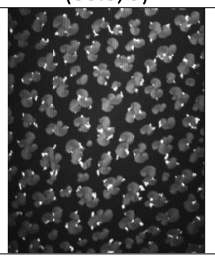	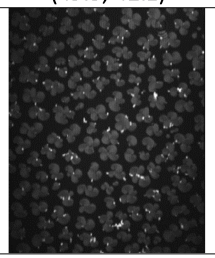	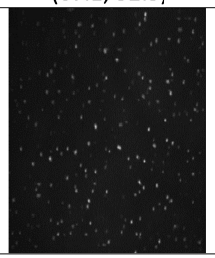	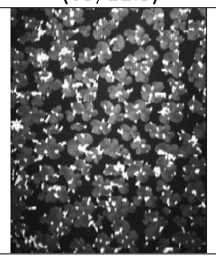	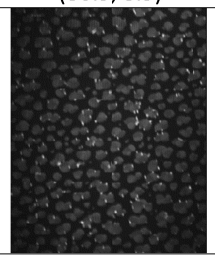	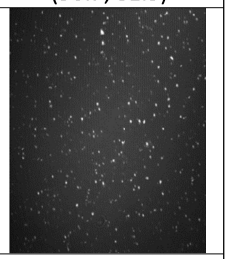
	(65.8; 7.4)	(73; 8.8)	(60.2; 33.2)	(76.1; 10)	(78.8; 10.0)	(79.0; 30.3)
Ascorbic acid	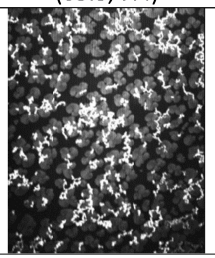	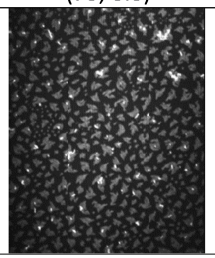		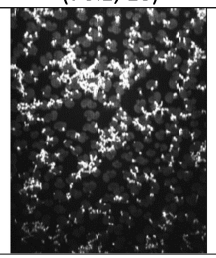	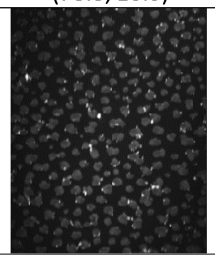	
	(76.7; 6.9)	(72.7; 8.5)	(53.7; 33.1)	(83.8; 8)	(81.6; 9)	(71.4; 30)
Uric acid	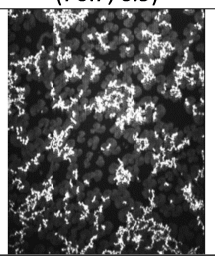	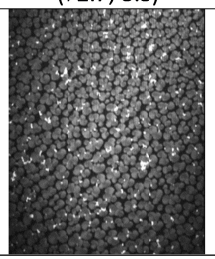		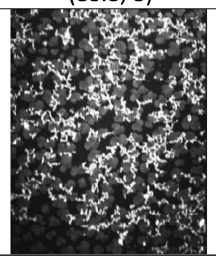	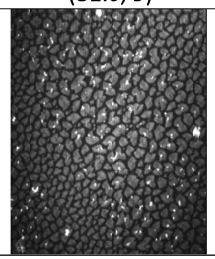	
	(68.6; 8.6)	(66.6; 7.5)	(57.6; 30.9)	(81.2; 9)	(71.6; 9.6)	(67.1; 30.9)

Figure 4. BAM images obtained for different monolayers (DPPC, DPPC + LA and EPC), with AAPH and/or antioxidants in the subphase (glutathione, ascorbic acid or uric acid).

4.4 Discussion

The addition of glutathione, ascorbic acid or uric acid to the subphase of DPPC monolayers did not cause any changes in the shape of π-A isotherms but a clear interaction with the monolayer can be seen in the BAM micrographs (Fig. 4.4). Glutathione presented the formation of white dots, corresponding to centers where formation of DPPC at condensed liquid state took place (Benitez and Talham, 2004; Schief et al., 2000). For ascorbic and uric acid, the brightest structures are more complex and do not seem to be particularly associated to any specific place of the condensed DPPC domains. These results may be justified by the different charges presented by these molecules. DPPC, bearing the phosphatidylcholine head in contact with the aqueous subphase, presents a positive charge in the choline group and a negative charge in the phosphatidyl moiety. Glutathione at pH 7.4 present a neutral net charge, with a positive charge on its glutamic acid residue and a negative charge on its carboxylic group from the glycine residue (Bieri and Burgi, 2005). This aspect can foster strong association between this molecule and the polar heads of DPPC. Concerning ascorbic and uric acids, both molecules present a negative net charge at our experimental pH. Ascorbic acid has two ionizable hydroxyl groups, with pKa of 4.25 and 11.5, respectively, resulting in the predominance of its monoanion form at physiological pH. In the case or uric acid, it presents a single negative charge at physiological pH as its pKa is 5.4 (Bieri and Burgi, 2005; Halliwell and Gutteridge, 2007). Hence, these molecules can only interact with the choline moiety of the PC, originating similar BAM micrographs.

When linolenic acid was added to the DPPC monolayer, the two components were miscible during monolayer compression with formation of brighter round aggregates, corresponding to linolenic acid segregation, only at high surface pressures. In fact, the collapse pressure was lower, with a value probably corresponding to the weighted average of values for monolayers with DPPC or LA only.

The addition of antioxidants changed the miscibility between the two lipids because the plateau corresponding to the LE/LC phase transition of DPPC reappeared and the formation of DPPC domains was again visible by BAM. Furthermore, their interaction with the monolayer seems to be more consolidated as the white bright structure appeared less frequently when compared to BAM micrographs taken in the absence of linolenic acid. The shape of domains was similar for glutathione and uric acid, with the multilobed pattern observed for DPPC monolayers. For ascorbic acid, the shape was different, with elongated borders, and larger, empty spaces near the center of the domain. These can be

caused due to electrostatic interaction between ascorbate and the positively charged choline moiety present on the polar head of DPPC.

The addition of AAPH to subphases containing the antioxidant compounds generated oxidation products from the antioxidants that also interacted with the DPPC monolayer. This observation is supported by the shift of isotherms towards higher areas per DPPC molecule, indicating a stronger interaction, even an intercalation in the monolayer as the change towards higher areas occur also for the highest surface pressures attained. For glutathione this interaction is even stronger, probably caused by the formation of larger dimer molecules (oxidized glutathione) formed when two glutathione molecules join together as the thiol groups of cysteine oxidize to form a disulfide bridge. These aspects are also supported by the BAM micrographs, as white structures are also visible, along with DPPC domains (light gray structures).

For ascorbic acid, oxidation products are mainly a dehydroascorbic derivative, whose ring is opened in aqueous solution and further oxidized to form a dicarboxylic compound. Uric acid is oxidized by peroxyl radicals, forming the urate radical, which is considerably more stable than peroxyl radicals (Domazou et al., 2012). All these oxidation products are known to interact with lipidic or hydrophobic structures and here we have biophysical evidence of these interactions.

For EPC monolayers, which bear a more close resemblance to biological membranes, peroxyl radicals formed from AAPH induced oxidation of the unsaturated bonds as shown by the displacement of isotherm towards lower molecular areas, caused by formation of shorter chains and the elimination of unsaturated acyl chains bearing kinks. These two features make phospholipid molecules to be placed close to each other.

When glutathione was added to the subphase of EPC, changes in the isotherm indicate a superficial interaction of this molecule with the polar heads of phospholipids because of monolayer expansion only for lower superficial pressures. Upon peroxidation, this interaction was changed because the whole isotherm was displaced, indicating the intercalation of glutathione oxidation products (dimeric molecules, as mentioned before) in the EPC monolayer.

Ascorbic acid also showed interaction with the polar head groups of EPC, with a stronger character than that shown by glutathione because the interaction was maintained for higher surface pressures and originated a more compact monolayer (lower area per molecule).

The interaction of uric acid, that exists predominantly as urate under our experimental conditions, and EPC monolayer is different considering the isotherm displacement. This is probably caused by the intercalation of urate molecules deeper into the monolayer, through interaction of its negative charge with the choline group of the PCs heads and also

through van der Waals interaction between the purine moiety and the double bonds present in EPC acyl chains. When AAPH is added to this subphase, the isotherm has a similar shape but shifts towards lower areas per molecule. This may occur for two reasons. Firstly, there is a depletion of the urate pool, oxidized by peroxyl radicals, reducing the presence of urate in the monolayer and originating a lower expansion. Secondly, urate radicals formed from the reaction between urate and peroxyl radicals can also attack the double bonds of EPC, causing monolayer compression as explained above.

In conclusion, the biological significance of our observations resides on the fact that typically aqueous antioxidants also interact with the 2D lipidic model studied here. Hence, this interaction should always be regarded when evaluating antioxidant capacity using biomimetic models of the membrane. Furthermore, different types of interaction were observed, comprising intercalation into the monolayer or adsorption into its surface. For all antioxidants, interactions with the monolayer surface were typically seen for pure compounds, while evidence for a higher degree of monolayer penetration was gathered for oxidation products. This aspect deserves further study as it hints to a possible accumulation of oxidation/peroxidation products in cell membranes.

4.5 References

Ames, B. N.; Cathcart, R.; Schwiers, E.; Hochstein, P. Uric-acid provides an antioxidant defense in humans against oxidant-caused and radical-caused aging and cancer - a hypothesis. *Proceedings of the National Academy of Sciences of the United States of America-Biological Sciences* **1981,** *78*, 6858-6862.

Benitez, I. O.; Talham, D. R. Brewster angle microscopy of calcium oxalate monohydrate precipitation at phospholipid monolayer phase boundaries. *Langmuir* **2004,** *20*, 8287-8293.

Bieri, M.; Burgi, T. L-Glutathione chemisorption on gold and acid/base induced structural changes: A PM-IRRAS and time-resolved in situ ATR-IR spectroscopic study. *Langmuir* **2005,** *21*, 1354-1363.

Brinkevich, S. D.; Boreko, E. I.; Savinova, O. V.; Pavlova, N. I.; Shadyro, O. I. Radical-regulating and antiviral properties of ascorbic acid and its derivatives. *Bioorganic & Medicinal Chemistry Letters* **2012,** *22*, 2424-2427.

Capuzzi, G.; LoNostro, P.; Kulkarni, K.; Fernandez, J. E. Mixtures of stearoyl-6-O-ascorbic acid and alpha-tocopherol: A monolayer study at the gas/water interface. *Langmuir* **1996,** *12*, 3957-3963.

Domazou, A. S.; Zhu, H.; Koppenol, W. H. Fast repair of protein radicals by urate. *Free Radical Biology and Medicine* **2012,** *52*, 1929-1936.

Droge, W. Free radicals in the physiological control of cell function. *Physiological Reviews* **2002,** *82*, 47-95.

Edidin, M. Timeline - Lipids on the frontier: a century of cell-membrane bilayers. *Nature Reviews Molecular Cell Biology* **2003,** *4*, 414-418.

Furuya, A.; Uozaki, M.; Yamasaki, H.; Arakawa, T.; Arita, M.; Koyama, A. H. Antiviral effects of ascorbic and dehydroascorbic acids in vitro. *International Journal of Molecular Medicine* **2008,** *22*, 541-545.

Gzyl-Malcher, B.; Filek, M.; Brezesinski, G. Influence of Cadmium and Selenate on the Interactions between Hormones and Phospholipids. *Langmuir* **2009,** *25*, 13071-13076.

Halliwell, B. Role of free radicals in the neurodegenerative diseases - Therapeutic implications for antioxidant treatment. *Drugs & Aging* **2001,** *18*, 685-716.

Halliwell, B.; Gutteridge, J. M. C., *Free radicals in biology and medicine*. 4th ed.; Oxford University Press: Oxford, 2007.

Jariwalla, R. J.; Roomi, M. W.; Gangapurkar, B.; Kalinovsky, T.; Niedzwiecki, A.; Rath, M. Suppression of influenza A virus nuclear antigen production and neuraminidase activity by a nutrient mixture containing ascorbic acid, green tea extract and amino acids. *Biofactors* **2007,** *31*, 1-15.

Kerksick, C.; Willoughby, D. The Antioxidant Role of Glutathione and N-Acetyl-Cysteine Supplements and Exercise-Induced Oxidative Stress. *Journal of the International Society of Sports Nutrition* **2005,** *2*.

Reis, S.; Lúcio, M.; Segundo, M. A.; Lima, J. L. F. C., Use of liposomes to evaluate the role of membrane interactions on antioxidant activity. In *Liposomes Methods and Protocols, Volume 2: Biological Membrane Models*, Weissig, V., Ed. Springer, Humana Press: Clifton, N.J., 2010; Vol. 606, pp 167-188.

Schief, W. R.; Touryan, L.; Hall, S. B.; Vogel, V. Nanoscale topographic instabilities of a phospholipid monolayer. *Journal of Physical Chemistry B* **2000,** *104*, 7388-7393.

Sevanian, A.; Ursini, F. Lipid peroxidation in membranes and low-density lipoproteins: Similarities and differences. *Free Radical Biology and Medicine* **2000,** *29*, 306-311.

Sharma, M. K.; Buettner, G. R. Interaction of vitamin C and vitamin E during free radical stress in plasma: An ESR study. *Free Radical Biology and Medicine* **1993,** *14*, 649-653.

Uchide, N.; Toyoda, H. Antioxidant Therapy as a Potential Approach to Severe Influenza-Associated Complications. *Molecules* **2011,** *16*, 2032-2052.

CHAPTER 5

Evaluation of antioxidant capacity using lipidic biomimetic structures

5.Evaluation of antioxidant capacity using lipidic biomimetic structures

5.1Introduction

The assessment of antioxidant capacity is frequently required in different situations, namely for evaluation of nutritional composition of food products (Prior et al., 2005; Tabart et al., 2009), for evaluation of biological redox status (Valko et al., 2007) or for assessment of pharmacological effects of drugs (Fernandes et al., 2004; Magalhães et al., 2007). According to Halliwell and co-workers (Halliwell and Gutteridge, 2007), an antioxidant in a biological system is "any substance that when present at low concentrations, compared to those of an oxidizable substrate significantly delays or prevents oxidation of that substrate". Hence, according to this definition, not all reductants involved in a chemical reaction are antioxidants; only those compounds which are capable of protecting a biological target meet these criteria. This protection may be based on several mechanisms of action, namely: i) inhibition of generation and scavenging capacity against reactive species of oxygen or nitrogen; ii) reducing capacity; iii) metal chelating capacity; iv) activity as antioxidative enzyme; v) and inhibition of oxidative enzymes.

Generally, the in vitro analytical methods for determination of antioxidant capacity aims at the first two mechanisms, relying on two different approaches, using competitive or non-competitive schemes (Magalhães et al., 2008). In the non-competitive assays, the antioxidant compounds interact with a reactive species, without any other competing target molecule in the reaction media. Therefore, these assays involve two components in the initial reaction mixture: the antioxidant compound(s) and the reactive species, which may also be the probe for reaction monitoring, as it happens for ABTS and DPPH assays (Brand-Williams et al., 1995; Re et al., 1999). These methods are quite popular for a primary screening of reducing capacity but they do not provide any information about real protection of biological targets.

On the other hand, in assays based on competitive schemes, the target species, defined as a compound that represents a biomolecule which may be attacked in vivo, and the antioxidant compounds compete for the reactive species (radical or nonradicals). The assessment of antioxidant capacity is based on the quantification of a compound that facilitates the analytical measurement (probe). For instance, in the ORAC assay (Cao et al.,

1993), the probe is fluorescein, that is also the competing target species. Although this assay is frequently acknowledged as a suitable tool for evaluation of antioxidant capacity concerning the scavenging against peroxyl radical, fluorescein is not a biological target of oxidation.

Moreover, recent work focusing on the evaluation of scavenging capacity against hydrogen peroxide (Ribeiro et al., 2010) showed that the direct reactivity towards hydrogen peroxide was higher for antioxidant compounds (glutathione and pyruvate) than for biological targets (cysteine, taurine and adenine). However, when a competitive scheme was applied, the scavenging effectiveness against hydrogen peroxide depended on the biological molecule present, showing that antioxidant assessment should also take into consideration the concomitant reactivity of biological molecules or structures that are prone to oxidative damage.

Therefore, the aim of this work was to develop a methodology based on a competitive scheme with a biologically relevant target for assessment of scavenging capacity against peroxyl radicals. At the present time, no experimental model system has emerged yet as a "gold standard" using biomimetic structures for evaluation of antioxidative capacity (Prior et al., 2005; Schnitzer et al., 2007) Until now, several lipidic structures have been assessed as potential targets for oxidation under competitive schemes, namely MLVs (Chaudhuri et al., 2009; Yin and Chan, 2007), LUVs (Dwiecki et al., 2009; Han et al., 2009), and SUVs (Fukuzawa et al., 2005; Hassimotto et al., 2005). However, no study comparing these structures under similar reaction conditions have been done so far to the best of our knowledge. Hence, we propose here the evaluation of EPC vesicles and hexadecylphosphocholine micelles as biological targets in a competitive adaptation of the ORAC assay.

5.2 Reagents and solutions

All chemicals used were of analytical reagent grade with no further purification. All chemicals used were of analytical reagent grade with no further purification. 2,2´-Azobis(2-methylpropionamidine) dihydrochloride (AAPH), egg L-α-phosphatidylcholine (EPC), hexadecylphosphocholine, glutathione ascorbic acid and uric acid were from Sigma-Aldrich (St. Louis, MO). Fluorescein sodium salt and Trolox (6-hydroxy-2,5,7,8-tetramethylchromane-2-carboxylic acid) were obtained from Fluka (Buchs, Switzerland). Water from Milli-Q system (resistivity > 18 MΩ cm) and absolute ethanol pro analysis (Panreac) was used for the preparation of all solutions. For preparation of vesicles,

methanol pro analysis from Merck (Darmstadt, Germany) and chloroform from Landilab (Porto, Portugal) were also used.
The stock solution of uric acid (1000 μM) was prepared by dissolving 16.81 mg in 20 mL of 0.01M NaOH. The excess of base was then neutralized with dropwise addition of 0.01M HCl until reaching pH 7.0. Finally, the volume was completed to 100 mL with water. Stock solutions of glutathione (1000 μM), ascorbic acid (1000 μM), and Trolox (500 μM) were prepared by dissolving the respective compound in water. Working standard solutions were prepared by rigorous dilution of the respective stock solution in buffer.

5.3 Preparation of lipid structures

For preparation of vesicles, the appropriate amount of EPC was dissolved in 10 mL of chloroform/methanol (3:1). This solvent was further evaporated under a nitrogen stream, where the resulting lipid film was left during at least 3 h to remove traces of the organic solvents. The dried lipid film was then dispersed in phosphate buffer (75 mM, pH 7.4) and the resulting mixture was vortexed to yield multilamellar vesicles (MLVs). This suspension was then extruded through polycarbonate filters using an extruder apparatus (Lipex Biomembranes, Vancouver, BC, Canada) to convert MLVs to LUVs.

5.4 Assessment of antioxidant capacity

The ORAC assay was implemented as a high-throughput 96-well microplate method. A microplate reader (H.T. Synergy, BIO-TEK) with excitation and emission wavelengths set at 485 ± 20 and 528 ± 20 nm, respectively, was used to monitor the oxidation of fluorescein and its prevention by tested antioxidants.
Hence, a reaction mixture (300 μL) containing 40 nM of fluorescein, 36 mM of AAPH, and variable amounts of each biomimetic structure were prepared. For all assays, radical initiator solution was freshly prepared by dissolution of AAPH in pre-heated buffer at 37 ºC before addition to microplate. Peroxyl radicals were generated at the beginning of the experiment by thermo-decomposition of AAPH at 37 ºC and at pH 7.4. For evaluation of antioxidant capacity, each antioxidant was added to the previously described reaction media, and the fluorescence intensity-time profile was followed up to 180 min.

Briefly, 50 μL of vesicles or micelles suspension were added to 100 μL of fluorescein solution. After that, 50 μL of test solution (Trolox or other antioxidants) were added and the mixture was shaken for 15 min at 37ºC before the addition of radical initiator. Finally, 100 μL of AAPH was added to each well using a multichannel pipette. The decay in fluorescence intensity of fluorescein was monitored every minute during 180, beginning after the first minute of reaction. Blank experiments were prepared in the same way, but without the antioxidants studied. For this, 50 μL of buffer was added instead of Trolox or antioxidant solutions. To evaluate the stability of the fluorescence reporter upon the reaction time (control experiments), 100 μL of buffer was added instead of AAPH solution. Moreover, the potential intrinsic fluorescence of the tested antioxidants was measured in the absence of fluorescence probes and radical initiator. For all compounds tested, different concentrations were evaluated and the results obtained correspond to the mean of three or more independent experiments, performed in triplicate (n = 6).

5.5 Calculation of antioxidant capacity as area under curve

The lipid peroxidation induced by $ROO^{\cdot}$ species was indirectly monitored by the fluorescence intensity decay of fluorescein. The data obtained for the fluorescence intensity decay were converted to relative fluorescence values, by dividing the fluorescence intensity at a given time by the fluorescence value attained after the first minute of reaction. The area under the curve (AUC) was calculated by integration of the curve obtained in the graphic representation of relative fluorescence values as a function of time. A linear relationship was established between AUC and antioxidant concentration (R^2 > 0.993; data not shown). Results obtained by the fluorimetric method correspond to the mean ± standard deviation of three experiments performed in triplicate (n = 9).

5.6 Results and discussion

5.6.1 Characterization of structures

All vesicles and micelles applied as biomimetic lipidic targets were evaluated concerning their effective diameter and zeta-potential. MLVs, LUVs and SUVs presented an effective

diameter of 997 ± 20, 112 ± 4, and 104 ± 2 nm, respectively. These values are within the expected values for these types of structures. For micelles, two populations were found, with effective diameter of ca. 6.8 nm and 181 ± 2 nm. This deviation disappeared by submitting the micelle suspension to two consecutive extrusion cycles.
Concerning the evaluation of zeta potential, the values obtained ranged from – 1.0 ± 0.9 to 5.3 ± 1.7, indicating that all structures can be regarded as globally neutral.

5.6.2 Oxidation profile of fluorescein probe

The ORAC method was adapted here to the microplate format in presence of biomimetic structures. As depicted in Fig. 2, the probe oxidation followed a similar kinetic profile in presence of micelles and MLVs. For LUVs and SUVs, the oxidation of fluorescein was delayed because, for these two structures, the amount of lipid prone (or accessible) to attack by peroxyl radicals is higher than that found in MLVs, where several layers of lipid are trapped and protected inside the vesicle. Hence, in terms of effective concentration, there is more lipid contacting the aqueous phase in the small and large unilamellar vesicles.

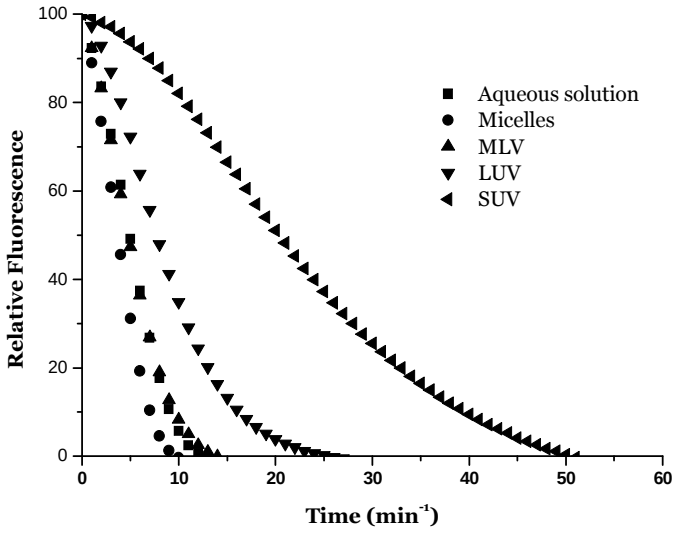

Figure 5.1 Fluorescein oxidation profile in presence of different biomimetic structures

5.6.3 Application to antioxidants

The addition of Trolox into the reaction media resulted in the profiles depicted in Fig. 3 where, for all conditions, a plateau corresponding to the first 20-40 minutes of reaction appeared when compared to the profile shown in Fig. 2. This delay on probe oxidation is due to peroxyl scavenging by Trolox. However, the profile is significantly different, depending upon the biomimetic lipidic structures present in the reaction media. Once again, the results for micelles and MLVs are quite similar, showing earlier probe oxidation when compared to the control performed in aqueous media. LUVs had a similar performance, with a slight delay on the last minutes of reaction. SUVs presented a remarkably different behavior, where the probe oxidation was significantly delayed. In opposition to what was first expected, probe oxidation in reaction media containing micelles, LUVs and MLVs took place before the control, probably because the lipidic structures, suffering from oxidation themselves, took an important role on peroxidation propagation.

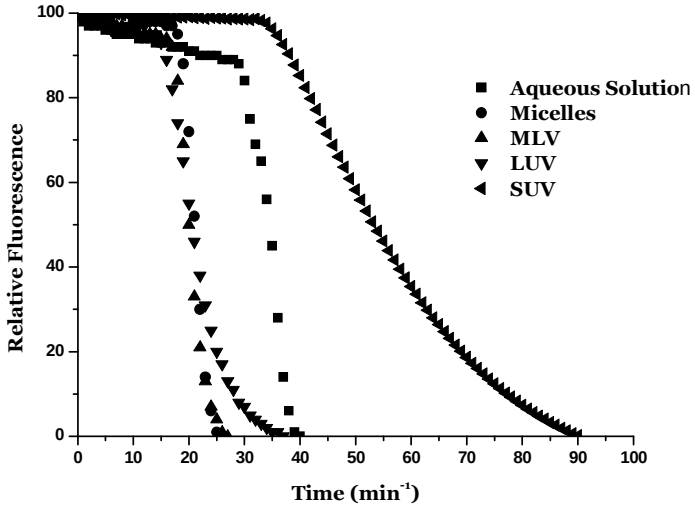

Figure 5.2 Fluorescein oxidation profile in presence of different biomimetic structures and antioxidant Trolox.

Biologically relevant antioxidants were also tested, presenting the sensitivities (slope of calibration curve AUC vs. concentration) given in Table 1. In general, the sensitivities are larger for reaction media containing SUVs, with increased protective features from antioxidants, comparable to those found in aqueous phase.

Table 5.1. Sensitivity[a] (relative fluorescence × min × μM^{-1}) for antioxidants in presence of different biomimetic structures

	No structure	Micelles	MLVs	LUVs	SUVs
Trolox	271 ± 45	97 ± 11	85 ± 11	74 ± 5	295 ± 52
Ascorbic acid	236 ± 67	75 ± 12	81 ± 11	66 ± 13	282
Glutathione	98 ± 21	29 ± 4	24 ± 2	17 ± 4	112
Uric acid	233 ± 4	101 ± 8	78 ± 2	108 ± 24	235

[a] mean value from 10 (Trolox) or 3 (other compounds) independent experiments.

In Table 6.2, the values for the ratio between the sensitivity attained by each antioxidant and the sensitivity presented by Trolox is given as a mean value of three independent experiment. For each experiment, Trolox was also processed, in order to eliminate biased results, sometimes attributed to the temperature dependent release of peroxyl radicals from AAPH. The relative reactivity is quite similar, except for glutathione in the presence of MLVs and LUVs that showed lower reactivity. An increased reactivity was presented by uric acid in reaction media containing LUVs.

Table 5.2. Ratio[a] between the sensitivities attained for a given antioxidant and that attained by Trolox in presence of different biomimetic structures

	No structure	Micelles	MLVs	LUVs	SUVs
Ascorbic acid	0.78 ± 0.09	0.74 ± 0.04	0.88 ± 0.09	0.92 ± 0.13	0.84
Glutathione	0.34 ± 0.02	0.28 ± 0.03	0.29 ± 0.02	0.24 ± 0.04	0.36
Uric acid	1.02 ± 0.04	1.06 ± 0.07	1.01 ± 0.06	1.35 ± 0.29	1.00

[a] mean value calculated from 3 independent experiments (except for SUVs), where the antioxidants and Trolox were analyzed simultaneously.

5.7 Conclusions

The methodology proposed here using a 96 well microplate format fostered the fast screening of scavenging capacity against peroxyl radicals in presence of biological targets. The miniaturization of the assay reduced its cost, leaving also a lower environmental footprint. Furthermore, a comparative evaluation of lipidic structures was performed, where vesicles prone to peroxidation and micelles structures were submitted to similar

reaction conditions in presence of a peroxidation inducer and antioxidants. The AUC, meaning the protection conferred by each antioxidant, was different for SUVs when compared to values obtained for other structures. Nevertheless, the relative antioxidant capacity of the tested compounds was quite similar, despite the lipidic structure tested. Future evaluation of this methodology using biological samples (serum, urina) will be undertaken.

5.8. References

Brand-Williams, W.; Cuvelier, M. E.; Berset, C. Use of a Free-Radical Method to Evaluate Antioxidant Activity. *Food Science and Technology-Lebensmittel-Wissenschaft & Technologie* **1995,** *28*, 25-30.

Cao, G. H.; Alessio, H. M.; Cutler, R. G. Oxygen-Radical Absorbency Capacity Assay for Antioxidants. *Free Radical Biology and Medicine* **1993,** *14*, 303-311.

Chaudhuri, S.; Pahari, B.; Sengupta, P. K. Ground and excited state proton transfer and antioxidant activity of 7-hydroxyflavone in model membranes: Absorption and fluorescence spectroscopic studies. *Biophysical Chemistry* **2009,** *139*, 29-36.

Dwiecki, K.; Neunert, G.; Polewski, P.; Polewski, K. Antioxidant activity of daidzein, a natural antioxidant, and its spectroscopic properties in organic solvents and phosphatidylcholine liposomes. *Journal of Photochemistry and Photobiology B-Biology* **2009,** *96*, 242-248.

Fernandes, E.; Costa, D.; Toste, S. A.; Lima, J.; Reis, S. In vitro scavenging activity for reactive oxygen and nitrogen species by nonsteroidal anti-inflammatory indole, pyrrole, and oxazole derivative drugs. *Free Radical Biology and Medicine* **2004,** *37*, 1895-1905.

Fukuzawa, K.; Saitoh, Y.; Akai, K.; Kogure, K.; Ueno, S.; Tokumura, A.; Otagiri, M.; Shibata, A. Antioxidant effect of bovine serum albumin on membrane lipid peroxidation induced by iron chelate and superoxide. *Biochimica Et Biophysica Acta-Biomembranes* **2005,** *1668*, 145-155.

Halliwell, B.; Gutteridge, J. M. C., *Free radicals in biology and medicine*. 4th ed.; Oxford University Press: Oxford, 2007.

Han, R. M.; Tian, Y. X.; Liu, Y.; Chen, C. H.; Ai, X. C.; Zhang, J. P.; Skibsted, L. H. Comparison of Flavonoids and Isoflavonoids as Antioxidants. *Journal of Agricultural and Food Chemistry* **2009,** *57*, 3780-3785.

Hassimotto, N. M. A.; Genovese, M. I.; Lajolo, F. M. Antioxidant activity of dietary fruits, vegetables, and commercial frozen fruit pulps. *Journal of Agricultural and Food Chemistry* **2005,** *53*, 2928-2935.

Magalhães, L. M.; Segundo, M. A.; Reis, S.; Lima, J. L. F. C.; Estela, J. M.; Cerda, V. Automatic in vitro determination of hypochlorous acid scavenging capacity exploiting multisyringe flow injection analysis and chemiluminescence. *Analytical Chemistry* **2007,** *79*, 3933-3939.

Magalhães, L. M.; Segundo, M. A.; Reis, S.; Lima, J. L. F. C. Methodological aspects about in vitro evaluation of antioxidant properties. *Analytica Chimica Acta* **2008,** *613*, 1-19.

Prior, R. L.; Wu, X. L.; Schaich, K. Standardized methods for the determination of antioxidant capacity and phenolics in foods and dietary supplements. *Journal of Agricultural and Food Chemistry* **2005,** *53*, 4290-4302.

Re, R.; Pellegrini, N.; Proteggente, A.; Pannala, A.; Yang, M.; Rice-Evans, C. Antioxidant activity applying an improved ABTS radical cation decolorization assay. *Free Radical Biology and Medicine* **1999,** *26*, 1231-1237.

Ribeiro, J. P. N.; Magalhaes, L. M.; Segundo, M. A.; Reis, S.; Lima, J. Hydrogen peroxide, antioxidant compounds and biological targets: An in vitro approach for determination of scavenging capacity using fluorimetric multisyringe flow injection analysis. *Talanta* **2010,** *81*, 1840-1846.

Schnitzer, E.; Pinchuk, I.; Lichtenberg, D. Peroxidation of liposomal lipids. *European Biophysics Journal with Biophysics Letters* **2007,** *36*, 499-515.

Tabart, J.; Kevers, C.; Pincemail, J.; Defraigne, J.-O.; Dommes, J. Comparative antioxidant capacities of phenolic compounds measured by various tests. *Food Chemistry* **2009,** *113*, 1226-1233.

Valko, M.; Leibfritz, D.; Moncol, J.; Cronin, M. T. D.; Mazur, M.; Telser, J. Free radicals and antioxidants in normal physiological functions and human disease. *International Journal of Biochemistry & Cell Biology* **2007,** *39*, 44-84.

Yin, M. C.; Chan, K. C. Nonenzymatic antioxidative and antiglycative effects of oleanolic acid and ursolic acid. *Journal of Agricultural and Food Chemistry* **2007,** *55*, 7177-7181.

CHAPTER 6

High-throughput fluorimetric methodologies for assessment of antioxidant capacity of drugs at different locations of phospholipid bilayers

High-throughput fluorimetric methodologies for assessment of antioxidant capacity of drugs at different locations of phospholipid bilayer

6.1. Introduction

The oxidative damage of polyunsaturated fatty acids of biomembranes is induced by an imbalance between the amount of reactive oxygen species (ROS) and/or reactive nitrogen species (RNS) produced and the antioxidant defenses. Among the reactive species formed, peroxyl radicals ($ROO^{\cdot}$) are the major oxidant species concerned in lipid peroxidation of biomembranes that disrupts their important structural, protective and functional role (Greig et al., 2012; Reis and Spickett, 2012). This pathologic process has been implicated in the etiology and/or in the development of several human diseases, such as chronic inflammation, cardiovascular and neurological disorders (Valko et al., 2007). Drugs used to correct and/or to treat these pathologies that present the additional property of prevent oxidative damage of biomolecules have been found to exhibit beneficial clinical effects (Tinkel et al., 2012). Actually, current therapeutic strategies are based on the design of multifunctional drug candidates that are able to interact with numerous disease related targets (Choudhary et al., 2012; Fernandez-Bachiller et al., 2012; Sawraj et al., 2012).

In this context, the assessment of capacity of drugs to prevent oxidative damage of biotargets has received much attention in the last decade, which is mirrored in the large diversity of analytical methodologies that have been developed (Beretta and Facino). Among them, those assays that use liposomes as membrane models for lipid peroxidation studies provide an additional information of antioxidant capacity since it takes into account not only the intrinsic scavenging characteristics of drugs but also their location and interactions with phospholipid bilayers (Lucio et al., 2007). These assays are more biologically relevant compared to those relied on scavenging of stable non-biological radicals ($DPPH^{\cdot}$ and $ABTS^{\cdot+}$) as well as those based on competitive assays performed in aqueous buffer media and using target molecules that do not represent any biomolecule found in living organisms (Beretta and Facino, 2010; Magalhaes et al., 2008). On the other hand, liposome based assays are cheaper and less affected by several uncontrolled factors compared to those performed with cells, animal models or human clinical trial studies. The analytical methodologies are based on the ability of test compounds to prevent and/or delay the oxidation of fluorescent probes used as reporters of lipid peroxidation induced by steady flux of $ROO^{\cdot}$ radicals generated by thermo-decomposition

of azocompounds (Reis et al., 2010). The kinetic of oxidation of fluorescence probes and its prevention by tested compounds is monitored by the increase or the decrease of fluorescence intensity over the time. Several fluorescence probes with distinct lipophilic properties and therefore with different locations within liposomes have been used namely, the hydrophilic probes as fluorescein (Lucio et al., 2008; Santos et al., 2008) and 2,7-dichlorodihydrofluoresecin (DCFH) (Li et al., 2009), the interface probe as hexadecanoyl aminofluorescein (HDAF) (Santos et al., 2008) and the lipophilic probes as diphenylhexatriene propionic acid (DPH-PA) (Lucio et al., 2008; Lucio et al., 2009), diphenyl-1-pyrenylphosphine (DPPP) (Tsuchiya et al., 2008; Tsuchiya et al., 2010) and 4,4-difluoro-5-(4-phenyl-1,3-butadienyl)-4-bora-3a,4a-diaza-s-indacene-3-propionic acid (C11-Bodipy$^{581/591}$) (Laszlo et al., 2012; Li et al., 2009; Takashima et al., 2012). Actually, previous works have explored the distinct lipophilic properties of fluorescence probes to correlate the antilipoperoxidant effect of drugs with their membrane location, membrane partition and the effect on membrane fluidity (Lucio et al., 2007; 2008; Lucio et al., 2009; Santos et al., 2008). Despite the feasibility of the mentioned lipid peroxidation assays, the long monitoring reaction times required for probe's oxidation (usually >120 min) and the fact that a single cuvette in a dedicated spectrofluorimeter is used makes these assays time-consuming, laborious and with determination rate not suitable for routine/screening assays. Moreover, the dissimilar reaction conditions between assays namely, probe, lipid and radical initiator concentrations limit the comparison of data. The down-scale to a microplate format and the standardization of reaction conditions, meets the requirements of high-throughput data improving also the precision and accuracy.

In the present work, we intend to develop simple, convenient and rapid 96-well microplate methodologies to assess the ability of drugs to counteract lipid peroxidation in different locations of phospholipid bilayer. For this, zwitterionic large unilamellar vesicles of egg L-α-phosphatidylcholine were used as membrane mimetic systems, while a steady flux of ROO· radicals generated from the thermal decomposition of 2,2´-azobis(2-methylpropionamidine) dihydrochloride (AAPH) was applied as the oxidant source. Different fluorescent probes with dissimilar locations in phospholipid bilayer were used, namely fluorescein and 5-dodecanoylaminofluorescein (DDAF) as fluorescent reporters in aqueous and in interface aqueous-lipid medium, respectively, while C11-BODIPY$^{581/591}$ was used as lipophilic probe. As the antilipoperoxidant effects of drugs cannot be assured without analysis of the results obtained and experimental conditions used, the effects of concentration of probe, egg L-α-phosphatidylcholine of liposomes and radical initiator were studied. The antioxidant capacity of drugs was indirectly determined by their ability to prevent/delay the fluorescence intensity decay of the fluorescent probes, fluorescein and DDAF, or the fluorescence intensity increase of labeled liposomes with C11-

BODIPY$^{581/591}$. Some nonsteroidal anti-inflammatory drugs (NSAIDs) with different locations within lipid bilayer were used and their antioxidant capacity was related to that attained for Trolox, used here as antioxidant standard.

6.2. Materials and methods

6.2.1 Chemicals

All chemicals used were of analytical reagent grade with no further purification. 2,2´-Azobis(2-methylpropionamidine) dihydrochloride (AAPH), egg L-α-phosphatidylcholine (EPC), as well as nonsteroidal anti-inflammatory drugs tested namely etodolac (E0516), indomethacin (I7378), meloxicam sodium salt hydrate (M3935) and tolmetin sodium salt dihydrate (T6779) were from Sigma-Aldrich (St. Louis, MO). Fluorescein sodium salt and Trolox (6-hydroxy-2,5,7,8-tetramethylchromane-2-carboxylic acid) were obtained from Fluka (Buchs, Switzerland). 5-Dodecanoylaminofluorescein (DDAF) and 4,4-difluoro-5-(4-phenyl-1,3-butadienyl)-4-bora-3a,4a-diaza-s-indacene-3-propionic acid (C11-Bodipy$^{581/591}$) were obtained from Molecular Probes (Invitrogen Corporation, Carlsbad, CA, USA). Water from Milli-Q system (resistivity > 18 MΩ cm) and absolute ethanol pro analysis (Panreac) was used for the preparation of all solutions. For preparation of large unilamellar vesicles (LUVs), methanol pro analysis from Merck (Darmstadt, Germany) and chloroform from Landilab (Porto, Portugal) were also used.

6.2.2 Preparation and fluorescence labeling of liposomes

To prepare and label liposomes with DDAF or with C11-BODIPY$^{581/591}$ fluorescence probes, the lipid solution in chloroform/methanol (3:1) and the fluorescence probe solution in methanol were dried together with nitrogen stream. After that, the lipid film was left under the same stream for at least 3 h to remove traces of the organic solvents. The resultant dried lipid film was dispersed into phosphate buffer (75 mM, pH 7.4) and the resultant mixture was vortexed to yield labeled multilamellar vesicles (MLVs). This suspension was then extruded through 100 nm pore size polycarbonate filters using an extruder apparatus (Lipex Biomembranes, Vancouver, BC, Canada) to convert MLVs to

large unilamellar vesicles (LUVs) labeled with probes, following a previously described procedure (Lucio et al., 2008; Lucio et al., 2009; Santos et al., 2008). Therefore, for experiments with DDAF and C11-BODIPY$^{581/591}$, the probes were incorporated during LUV preparation. The fluorescent labeled LUVs were freshly prepared each day and protected from light. For assays using fluorescein as fluorescent probe, the resultant dried lipid film was dispersed into potassium phosphate buffer (75 mM, pH 7.4) and prepared in the same way but in the absence of the fluorescent probe. In fact, fluorescein solution was only added to the LUV suspension immediately before the measurements were taken.
EPC concentration in vesicle suspensions was obtained by phosphate analysis using the phosphomolybdate method (McClare, 1971). Different ratios of lipid to fluorescence probe were tested, considering that for studies with lipophilic probes (DDAF and C11-BODIPY$^{581/591}$) the incorporation procedure was performed.

6.2.3Microplate fluorimetric protocols for assessment of the antilipoperoxidant effects of drugs

The capacity of NSAIDs to prevent lipid peroxidation of phospholipid bilayer (LUVs) was evaluated by high-throughput 96-well microplate fluorimetric procedures. Different fluorescent probes with dissimilar locations in lipid bilayer namely, fluorescein (aqueous medium), DDAF (interface) and C11-BODIPY$^{581/591}$ (lipophilic medium) were used (Li et al., 2009; Santos et al., 2008). In all cases, ROO$^{\cdot}$ radicals were generated by thermo-decomposition of AAPH at 37 ºC and at pH 7.4. A microplate reader (H.T. Synergy, BIO-TEK) with excitation and emission wavelengths set at 485 ± 20 and 528 ± 20 nm, respectively, was used to monitor the oxidation of probes and its prevention by drugs.
Hence, a reaction mixture (300 μL) containing the following final concentrations of LUV suspension (800 μM) and AAPH (50 mM) was applied for all fluorescence probes tested. The concentration of fluorescein was fixed at 6 nM, while for experiments with DDAF and C11-BODIPY$^{581/591}$, the concentration was fixed at 50 nM. For all assays, radical initiator solution was freshly prepared by dissolution of AAPH (50 mM) in pre-heated phosphate buffer at 37 ºC before addition to microplate. Briefly, 150 μL of fluorescence-labelled liposomes (DDAF and C11-BODIPY$^{581/591}$ experiments) or 50 μL of non-labeled liposomes in addition 100 μL of fluorescein solution were placed in each well. After that, 50 μL of test solution (phosphate buffer, Trolox or NSAIDs) were added and the mixture was shaken for 15 min at 37ºC before the addition of radical initiator. Finally, 100 μL of AAPH was added to each well using a multichannel pipette. The decay in fluorescence intensity of

fluorescein or DDAF was monitored every minute during 180 and 240 min, respectively, beginning after the first minute of reaction. The same approach was applied to lipophilic probe C11-BODIPY$^{581/591}$, but in this case the fluorescence increase due to oxidation of probe was monitored during 90 min. Blank experiments were prepared in the same way, but without the drugs studied. For this, 50 μL of buffer was added instead of Trolox or NSAIDs solutions. To evaluate the stability of the fluorescence reporter upon the reaction time (control experiments), 100 μL of buffer was added instead of AAPH solution. Moreover, the potential intrinsic fluorescence of drugs was measured in the absence of fluorescence probes and radical initiator. For all drugs tested, different concentrations were evaluated and the results obtained correspond to the mean of two independent experiments, performed in triplicate (n = 6).

6.2.4 Calculation of antioxidant capacity values expressed as IC_{50} or IC_{25}

The lipid peroxidation induced by ROO$^{\cdot}$ species was indirectly monitored by the fluorescence intensity decay of probes (experiments with fluorescein and DDAF) or by the fluorescence intensity increase due to oxidation of C11-BODIPY$^{581/591}$ (Li et al., 2009; Santos et al., 2008). The data obtained for the fluorescence intensity decay were converted to relative fluorescence values, by dividing the fluorescence intensity at given time ($FI_{x\ min}$) by the fluorescence value attained at first minute ($FI_{1\ min}$) (equation 1):

$$\mathbf{(FI_{x\ min} / FI_{1\ min}) \times 100}$$

Eq. 1

For the results obtained with lipophilic probe (C11-BODIPY$^{581/591}$), the fluorescence intensity at a given time was divided by the maximum of fluorescence intensity obtained by probe's oxidation in the absence of antioxidant species (blank experiments). Both values were subtracted by the intrinsic fluorescence intensity of C11-BODIPY$^{581/591}$ determined in the absence of radical species. The following equation (eq. 2) was used to express the kinetic profile of lipophilic probe oxidation upon reaction time:

$$\mathbf{[(FI_{x\ min} - FI_{bodipy}) / (FI_{max\ blank} - FI_{bodipy})] \times 100}$$

Eq. 2

The ability of Trolox and NSAIDs to prevent and/or delay the oxidation of probe was analysed considering the kinetic profile of probe's oxidation in the presence and in the absence of drug during the reaction time. For experiments performed with fluorescein and DDAF as fluorescent probes, the area under the curve (AUC) obtained for sample and blank were assessed, since these parameter combines both inhibition time (correspondent to the initial plateau phase) and inhibition degree (correspondent to the decay profile) (Cao et al., 1993). These data were determined for each drug concentration tested and the antioxidant capacity (AC) was determined using the following equation:

$$AC = \frac{AUC_{Trolox/NSAIDs} - AUC_{blank}}{AUC_{blank}} X\ 100$$

Eq. 3

A linear relationship was established between antioxidant capacity (%) and drug concentration ($R^2 > 0.995$; data not shown). The same approach was applied for experiments with C11-BODIPY$^{581/591}$ in the presence of Trolox but in this case the area above the curve (ABC) was determined since when antioxidant is present the fluorescent product formed by probe's oxidation is delayed. The linear fits allowed the determination of the IC_{50} and IC_{25} values for NSAIDs, which are defined as the concentration (in μM) of each compound required to obtain a ratio of prevention of lipid peroxidation equal to 50 or 25%, respectively (the latter was calculated when it became impossible to reach the IC_{50} within the drug concentration range studied). Results obtained by these microplate fluorimetric methods correspond to the mean ± standard deviation of two experiments performed in triplicate ($n = 6$).

6.3. Results and discussion

In general, the assays used to determine the ability of drugs to prevent lipid peroxidation of phospholipid bilayers have the following components: *i*) a lipid structure to mimic phospholipid bilayer, usually large unilamellar vesicles (LUVs); *ii*) a thermal radical initiator to provide a steady flux of $ROO^{\cdot}$ radicals in air-saturated solution; *iii*) an oxidation-sensitive fluorescent probe for reaction monitoring progress; *iv*) test compound that competes with probes for the radicals which prevents or retards the probe oxidation

and *v*) acquisition of reaction kinetics parameters, usually the area under curve, for assessment of antioxidant capacity (Reis et al., 2010). Therefore, the antilipoperoxidant effects determined depend on several factors, including the chemical composition and concentration of liposomes, the type and concentration of the inducer of peroxidation and the fluorescence reporter molecule selected (Schnitzer et al., 2007). In order to provide high-throughput and straightforward microplate assays for assessment the inhibition of lipid peroxidation in different locations of phospholipid bilayers a thorough analysis of these analytical parameters were studied.

6.3.1 Influence of probe concentration

The concentration of the probe determines the fluorescence intensity values of the methodology and the amount of radical species needed to oxidize almost all the sensitive fluorescent probe. Hence, higher probe concentrations provide higher analytical signals that present better reproducibility in inter and intraday assays, nevertheless higher amounts of radical species are required to guarantee that all fluorescent reporter molecules were oxidized. This matter implies higher amounts of antioxidants to protect fluorescence probes from oxidation, which could be difficult to perform due to limited solubility of drugs. Moreover, it is necessary to assure that the fluorescence probe is stable during the monitoring time. Taking into account theses issues, different concentrations of fluorescein (from 2.0 to 10.0 nM), DDAF (from 12.5 to 100 nM) and C11-BODIPY$^{581/591}$ (from 25 nM to 250 nM) were tested with fixed ratio of LUVs of EPC:probe (300:1). This ratio of lipid to probe was selected to prevent changes in the structure of the liposomes induced by the fluorescence probe (Lucio et al., 2007). Since the oxidized product of the lipophilic C11-BODIPY$^{581/591}$ probe is the fluorescent compound monitored at the emission wavelength (528 ± 20 nm), AAPH (10 mM) was added to the reaction media. The results obtained for different concentrations of lipophilic probe tested are described in Figure 1. After reaching the maximum of fluorescence intensity due to the formation of the green fluorescent product a continuously decrease in fluorescence intensity was observed due to further oxidation of fluorescent product to non-fluorescent derivative (Drummen et al., 2004). It is important to state here that neither C11-BODIPY$^{581/591}$ nor its oxidation products are able to spontaneously leave the lipid bilayer (Drummen et al., 2002). For all probes tested, a linear relationship was established between fluorescence intensity and probe concentration (nM), providing a slope value of 7438 nM^{-1} for fluorescein (R = 0.9985), 787 nM^{-1} for DDAF (R = 0.9991) and 232 nM^{-1} for C11-BODIPY$^{581/591}$ (R =

0.99990). For fluorescein and DDAF, the decrease of fluorescence intensity during analysis time (180 and 240 min, respectively) due to photobleaching effects was < 15% (data not shown). Considering the aforementioned aspects, the concentrations of fluorescein, DDAF and C11-BODIPY$^{581/591}$ selected for further studies were 6, 50 and 50 nM, respectively.

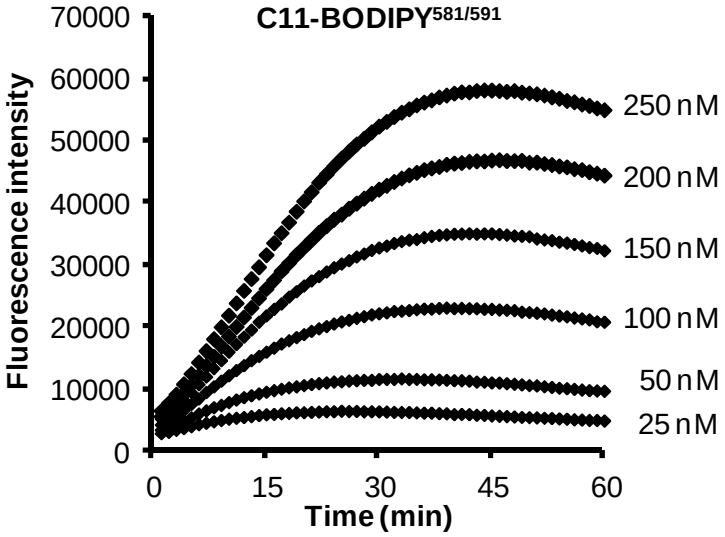

Figure 6.1. Fluorescence intensity upon reaction time for different concentrations of lipophilic probe C11-BODIPY$^{581/591}$ obtained in the presence of 10 mM of AAPH. The concentration ratio between large unilamellar vesicles of egg L-α-phosphatidylcholine (EPC) and fluorogenic probe was fixed at 300:1, respectively.

6.3.2 Influence of lipid and AAPH concentration

The amount of large unilamellar vesicles of egg L-α-phosphatidylcholine (EPC) influence the fluorescence intensity of the oxidized product of the lipophilic probe C11-BODIPY$^{581/591}$, while for hydrophilic and interface fluorescent probes the fluorescence intensity obtained was independent of the concentration of EPC tested. Figure 2 describes the fluorescence intensity obtained for the different probes in the presence of increasing EPC concentrations, ranging from 100 to 1000 μM. In fact, for fluorescein and DDAF probes, the fluorescence intensity was similar for all EPC concentrations tested (p>0.05), but for lipophilic probe a fluorescence intensity increase was obtained up to 800 μM of

EPC (corresponding to 16000:1 of lipid: probe ratio). This dependency of fluorescence intensity of oxidized product of C11-BODIPY$^{581/591}$ for lipid concentration is related to the necessity to have sufficient lipid to encompass the lipophilic fluorescent reporter and also to prevent the excimers formation (dimers oxidized C11-BODIPY$^{581/591}$) that could interfere with the determination by self-quenching or by resonance energy transfer (Drummen et al., 2002). Considering that the EPC concentration affect the rate of lipid peroxidation (Schnitzer et al., 2007) and consequently the probe's oxidation which could bias the antioxidant capacity data, the same EPC concentration (800 μM) was selected for all fluorescence probes.

The addition of the ROO· generator (AAPH) to LUV suspensions, in the absence of antioxidant species (blank assay), has triggered the peroxidation of the probes yielding a gradual decay in fluorescence intensity of fluorescein and DDAF-labeled liposomes and a gradual increase in fluorescence intensity of C11-BODIPY$^{581/591}$ labeled liposomes (Figure 3). The kinetic of probe oxidation was dose-dependent of the initial AAPH concentration because it determines the rate of ROO· radical produced in aqueous media (Niki, 1990). Hence, for higher concentrations of AAPH, that yields higher amounts of ROO· radicals per time, the rate of probe oxidation measured by the fluorescence intensity decrease or increase was faster. Comparing the results obtained for fluorescein (used as hydrophilic probe) with that obtained with DDAF, which has a hydrophobic chain inserted into apolar part and the analogue fluorescein near the polar head groups of LUVs, the kinetic oxidation of fluorescein was higher. In fact, for similar initial AAPH concentration (150 mM, Figure 6.3A (6), 6.3B (6)) about 60 min were necessary to oxidize fluorescein (6 nM) present in the aqueous phase, while for the interface fluorescent probe DDAF about 180 min were required. This takes place because the major amounts of ROO· radicals are generated in the aqueous phase and therefore the fluorescein suffers oxidation easily than its analogue positioned in the interface of phospholipid bilayer. The lipophilic probe showed higher oxidation rate than DDAF due to the higher sensibility of C11-BODIPY$^{581/591}$ for peroxyl radicals (Drummen et al., 2002; Yoshida et al., 2003). Figure 3C shows that the maximum of fluorescence intensity obtained due to the formation of oxidized product of lipophilic probe was independent of the initial AAPH concentration, but the time required to oxidize almost all probe decreased as the concentration of radical initiator increase. Moreover, the decline of fluorescence intensity due to further oxidation of fluorescent product of C11-BODIPY$^{581/591}$ increase as the AAPH concentration increase; in fact for 75 mM of AAPH after 90 min there is no fluorescence intensity. Therefore, the application of high initial AAPH concentrations may oxidize the fluorescence probes in short reaction times, nevertheless to verify the prevention of probe oxidation by tested

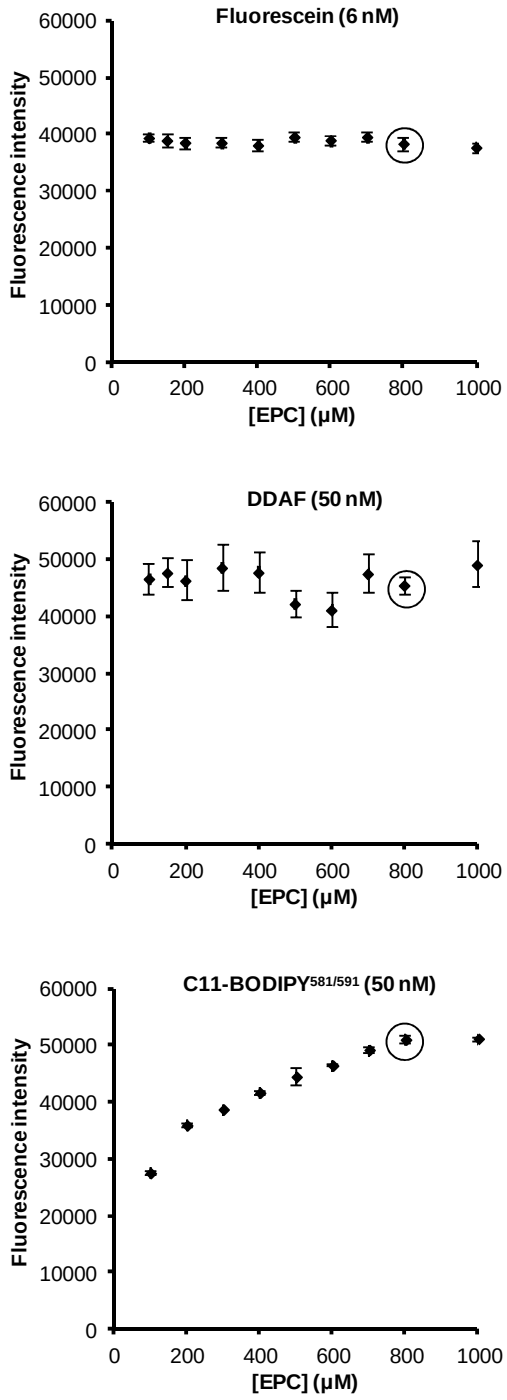

Figure 6.2. Fluorescence intensity obtained for fluorescent hydrophilic probe (fluorescein), fluorescent interface probe (5-dodecanoylaminofluorescein, DDAF) and for fluorogenic lipophilic probe C11-BODIPY$^{581/591}$ in the presence of different concentrations (μM) of large unilamellar vesicles of egg L-α-phosphatidylcholine (EPC). Fluorescein was added to LUV suspension immediately before the measurements, while the DDAF and C11-BODIPY$^{581/591}$ were incorporated during vesicles preparation. For experiments using C11-BODIPY$^{581/591}$, the concentration of peroxyl radical generator (AAPH) was fixed at 10 mM. The circles show the EPC concentration selected for further studies.

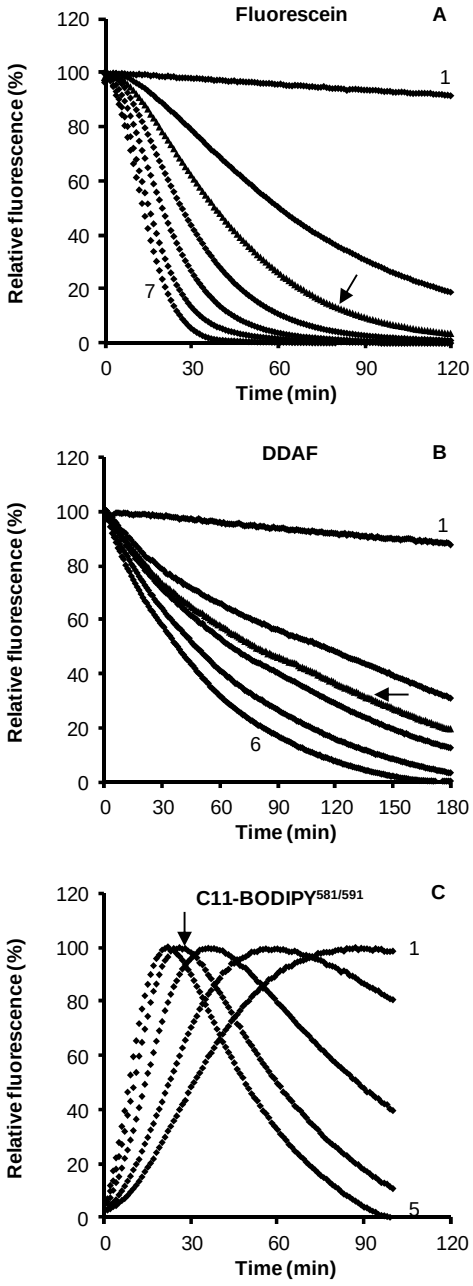

Figure 6.3. Relative fluorescence intensity (%) of fluorescein (6 nM), DDAF (50 nM) and C11-BODIPY$^{581/591}$ (50 nM) in the presence of large unilamellar vesicles of egg L-α-phosphatidylcholine (EPC) (800 μM) and different concentrations (μM) of peroxyl radical generator AAPH: **A)** (1) 0, (2) 25, (3) 50, (4) 75, (5) 100, (6) 150, (7) 200; **B)** (1) 0, (2) 25, (3) 50, (4) 75, (5) 100, (6) 150; **C)** (1) 5; (2) 10, (3) 25, (4) 50, (5) 75. The arrows indicate the concentration of AAPH (50 mM) that was selected.

compounds, higher antioxidant concentrations are required. Regarding to the results obtained for the different fluorescence probes (Figure 3) and aiming to implement straightforward microplate procedures, the initial concentration of AAPH selected was 50 mM, which at 37 °C corresponds to about 0.068 x 10^{-6} mol/L/s of ROO· radicals generated (Niki, 1990).

6.3.4 Ability of NSAIDs to counteract lipid peroxidation in different locations of phospholipid bilayers

To evaluate the applicability of the proposed fluorimetric methodologies for assessment of ability of drugs to prevent lipid peroxidation in different locations of phospholipid bilayers, some NSAIDs that have dissimilar partition coefficients in lipid-aqueous media were selected namely etodolac, indomethacin, meloxicam and tolmetin (see supplementary data, Figure S1). At pH 7.4, all drugs tested are predominantly negatively charged due to deprotonation of carboxyl groups (pKa < pH of the medium). Indomethacin is the most lipophilic drug due to its high partition coefficient determined in LUVs of EPC (K_p = 1442 ± 59) (de Castro et al., 2001) compared to that determined for meloxicam (K_p = 685 ± 70) (Lucio et al., 2007) and for tolmetin (K_p = 220 ± 70) (Lucio et al., 2004). Etodolac does not present partition into lipid bilayers of EPC in the concentration ranges used as it was previously described (Lucio et al., 2008). Therefore, in this case the drug concentrate preferentially in the aqueous phase and partly at the surface of LUVs with the negative charge of its molecule oriented toward the positive pole of the zwitterionic phosphatidylcholine head-group. For Trolox, used here as antioxidant standard compound, a 20% of partition in membrane/water system has been described in the literature (Barclay and Vinqvist, 1994).

Figure 4A and 4B depicts the ability of indomethacin and tolmetin, respectively, to prevent fluorescein oxidation in the presence of LUVs of EPC. It can be observed that both drugs retards the oxidation of the aqueous fluorescent probe induced by ROO· radicals in a concentration-dependent manner. Figure 4C and 4D, shows the relationship between the antioxidant capacity (AC) and the concentration of the drug (μM). The AC was calculated as the percentage of increase of the area under curve (AUC) relative to that obtained for fluorescein in the absence of the drug (blank), which allows the assessment of IC_{50} values (concentration of drug that provide an AUC 50% higher of that obtained in the absence of drug). As it can be observed in Figure 4B, for highest concentrations of tolmetin (30 and 40 μM) after 180 min of reaction monitoring, some fluorescein was not oxidized yet. This

issue can be easily observed by the deviation of the linearity in Figure 4D for the highest tolmetin concentrations. The same data treatment was performed for results obtained with DDAF-labeled liposomes. The results obtained for Trolox and tolmetin are described in Figure S2 (see supplementary data). Trolox avoided the immediate decay of fluorescence and lead to a plateau where the fluorescence is stable (similar results were obtained with fluorescein, data not shown). This fluorescence plateau corresponds to an inhibition time, after which the oxidation process starts over when there is no more antioxidant left to scavenge ROO· radicals. Taking into account that DDAF oxidation was slower than that attained for fluorescein (Figure 2) and that Trolox will retard probe's oxidation, even after 240 min of reaction monitoring part of fluorescent probe was not oxidized (Figure S2, supplementary data). Hence, a deviation of linearity is attained which is aggravated for shorter reaction times, unless the AUC after reaction monitoring is considered (time > 240 min). This approach can be performed for Trolox because the kinetic of oxidation of probe is similar to that obtained for blank, but for almost all NSAIDs it cannot be applied since the plateau phase is not present and the kinetic of probe oxidation is different from that determined in the absence of drug (blank experiments).

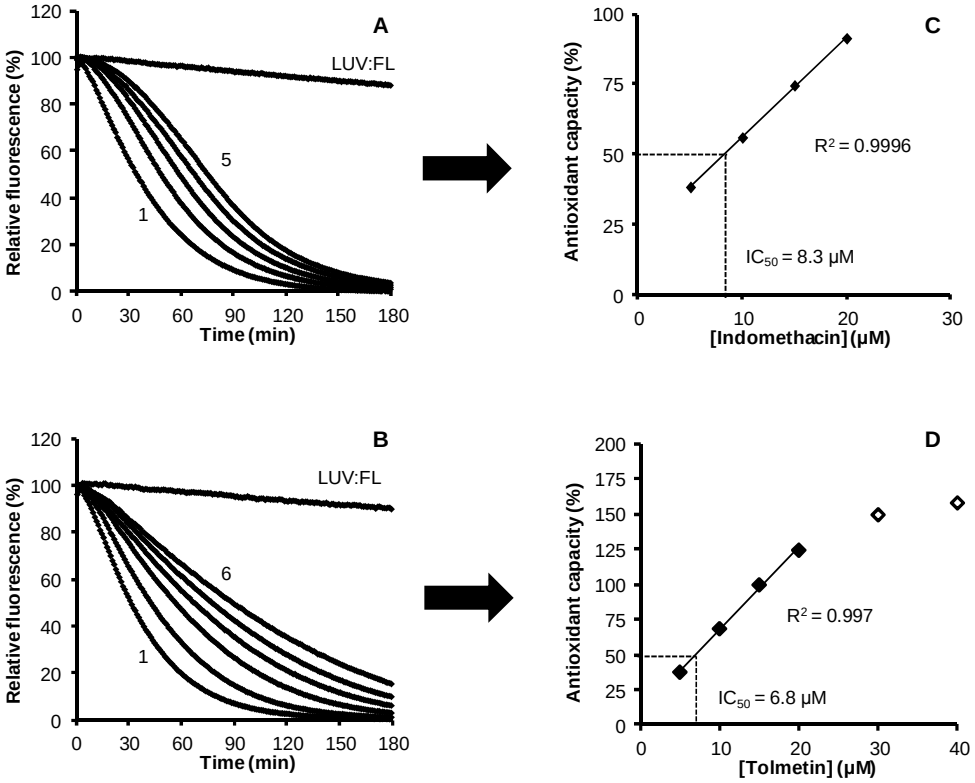

Figure 6.4. Relative fluorescence intensity (%) of fluorescein (A and B) and antioxidant capacity (C and D) obtained in the presence of different concentrations of indomethacin (0, 5, 10, 15, 20 µM) and tolmetin (0, 5, 10, 15, 20, 30, 40 µM) in large unilamellar vesicles

of EPC (800 μM) and with the AAPH concentration (50 mM). Antioxidant capacity was determined using the following equation, $[(AUC_{Trolox/NSAIDs} - AUC_{blank}) / (AUC_{blank})] \times 100$. For both drugs, AUC was calculated after 240 min. LUV:FL, correspond to the fluorescent intensity obtained by liposomes in the presence of aqueous fluorescent probe (fluorescein) in the absence of peroxyl radical species.

The antioxidant capacity of drugs expressed as IC_{50} and IC_{25} (μM) in the presence of fluorescein and DDAF, respectively, as fluorescent probes are described in Table 1. Among the drugs tested, etodolac was the most potent scavenger preventing fluorescein and DDAF oxidation and therefore lipid peroxidation indirectly, as it can be observed for the lower IC values obtained (1.5 ± 0.2 μM and 12.0 ± 0.1 μM). Moreover, the antioxidant capacity of drugs was higher than that attained for antioxidant standard compound, Trolox. For all NSAIDs tested and Trolox, higher amounts of tested compounds were required to prevent oxidation of LUVs labeled with DDAF than for the same LUVs but with fluorescein in the aqueous media (increase of IC values). This takes place because higher concentrations of drugs are required to concentrate the drug at the surface of lipid bilayer and consequently prevent the oxidizable portion of the DDAF probe located at the interface lipid-aqueous phase, while for fluorescein the probe is present in the aqueous phase easily accessible to $ROO^{\cdot}$ radicals and its prevention by drugs, especially those with lower partition coefficient as etodolac, meloxicam and tolmetin. These results are in accordance with those obtained for etodolac and Trolox using fluorescein and hexadecanoyl aminofluorescein (HDAF) as fluorescent probes (Lucio et al., 2008). For straightforward comparisons between assays, the IC of Trolox was divided by the IC values of NSAIDs (Table 1), considering that high values correspond to higher scavenger capacity of drug compared to Trolox. The ratio obtained for etodolac with fluorescein probe was 11, which means that IC_{50} of etodolac was about 11 times lower than that determined for Trolox, nevertheless with DDAF this ratio decreased to 2.9, which means that the efficacy of etodolac to prevent the oxidation of DDAF probe decreased relatively to Trolox. For meloxicam a decrease of this ratio was also observed, while for indomethacin it remains stable. These results are in accordance with the drug distribution in the lipid-aqueous phase compared to Trolox, hence for "hydrophilic" drugs this ratio decrease while for "lipophilic" drugs a stable value was obtained. Despite of tolmetin is also considered as a "hydrophilic" drug due to its lower partition coefficient compared to indomethacin, the ratio is similar for both fluorescent probes because this drug exists preferentially at the surface of lipid bilayer preventing DDAF oxidation (Nunes et al., 2011). Moreover, the lower pKa value (3.5) also justifies its predominance as negative molecule that binds to the positively charged groups of phospholipid bilayer.

Table 6.1. Peroxyl radical scavenging capacity of Trolox and nonsteroidal anti-inflammatory drugs (NSAIDs) expressed as IC_{50} and IC_{25} values obtained with fluorescein and with 5-dodecanoylaminofluorescein (DDAF) as fluorescent probes.[a]

Compounds	Fluorescein (IC_{50}, μM)[b]	$IC_{50,\,(Trolox)}$ / $IC_{50,\,(NSAIDs)}$	DDAF (IC_{25}, μM)[b]	$IC_{25,\,(Trolox)}$ / $IC_{25,\,(NSAIDs)}$
Trolox	16.1 ± 0.8	1.0	34.6 ± 0.4	1.0
NSAIDs				
Etodolac	1.5 ± 0.2	11	12.0 ± 0.1	2.9
Indomethacin	7.8 ± 0.8	2.1	16.0 ± 0.4	2.2
Meloxicam	4.3 ± 0.6	3.8	36.4 ± 0.9	1.0
Tolmetin	6.4 ± 0.6	2.5	13.5 ± 0.4	2.6

[a] Concentration of egg L-α-phosphatidylcholine liposomes (800 μM) and concentration of peroxyl radical generator AAPH (50 mM). [b] IC values (μM) were calculated from the linear fit of $(AUC_{NSAIDs} - AUC_{blankl})/AUC_{blank}$ versus concentration of drug (μM); each value corresponds to the mean ± S.D. of two independent experiments performed in triplicate (n = 6). IC_{Trolox}/IC_{NSAIDs}, describes the peroxyl radical scavenging capacity of drugs related to Trolox (higher values correspond to high capacity to scavenge peroxyl radicals compared to Trolox).

For lipophilic probe C11-BODIPY$^{581/591}$ buried in the hydrophobic region of LUVs of EPC, the formation of oxidized green fluorescent product was monitored as the increase of fluorescence intensity at 528 ± 20 nm (Drummen et al., 2002; Li et al., 2009). The antioxidant behavior of Trolox was similar to that observed for the other fluorescent probes. The antioxidant standard avoided the immediate increase of fluorescence intensity (plateau phase), which after antioxidant depletion the kinetic of formation of oxidized product of C11-BODIPY$^{581/591}$ was similar to that presented in the absence of antioxidant (Figure 5A). The subsequent formation of the non-fluorescent derivate compound formed by oxidation of green fluorescent product, which is observed by the decrease of fluorescence intensity after reach the maximum value, was not affected by the antioxidant compound. Hence, the antioxidant capacity of Trolox was determined as the area above curve (ABC) that reflects the ability of compound to protect C11-BODIPY$^{581/591}$ for peroxyl radical oxidation. The IC_{50} value determined for Trolox was 1.9 ± 0.2 μM, which shows the potency of the antioxidant standard to prevent oxidation of the lipophilic probe. Nevertheless, when NSAIDs were analysed an effect different from that observed for

Trolox was obtained, exemplified here for etodolac (Figure 5B) and for indomethacin (Figure 5C). In the case of etodolac (similar results were obtained for tolmetin and meloxicam), the kinetic of C11-BODIPY$^{581/591}$ oxidation was not affected, but the maximum of fluorescence intensity obtained was higher than that observed in the absence of drug (blank). This takes place because under these reaction conditions (AAPH concentration), the drugs were not able to prevent probe's oxidation due to its high sensitivity for ROO$^{\cdot}$ radicals, but the further oxidation of fluorescent oxidized product of C11-BODIPY$^{581/591}$ was delayed providing therefore an increase of maximum of fluorescence intensity. For indomethacin, the kinetic of C11-BODIPY$^{581/591}$ oxidation seems to be accelerated by increasing concentrations of drug, while the antioxidant effect toward fluorescent oxidized product was not observed. This result could be explained by the formation of fluorescent products resulting for indomethacin oxidation that interferes in the methodology or by the change of membrane fluidity mediated by the lipophilic drug that results in higher exposition of hydrophobic probe to ROO$^{\cdot}$ generated in the aqueous media.

Further investigation with this lipophilic probe is required to provide a suitable technique for measurement of ability of drugs to prevent lipid peroxidation in hydrophobic media of LUVs. Therefore, lower AAPH concentrations should be tested or the C11-BODIPY$^{581/591}$ oxidation should be monitored at its maximum emission at 595 nm (Drummen et al., 2004; Drummen et al., 2002), instead of green fluorescent oxidized product at 520 nm, which is less sensible to probe's oxidation and may circumvent the effects observed with oxidized fluorescent probe.

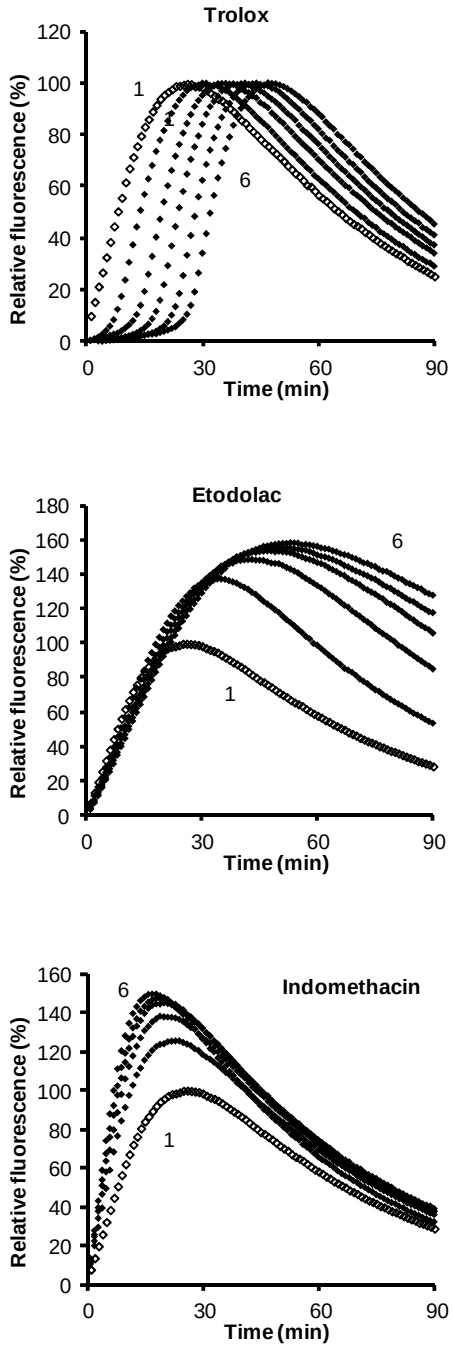

Figure 6.5. Relative fluorescence (%) intensity of lipophilic fluorogenic probe C11-BODIPY$^{581/591}$ in the presence of large unilamellar vesicles of EPC (800 μM), AAPH concentration (50 mM) and different concentrations of Trolox (0, 4, 8, 12, 16, 20 μM), etodolac (0, 5, 10, 15, 20, 30 μM) and indomethacin (0, 5, 10, 15, 20, 30 μM). The numbers (1 to 6) correspond to increasing concentrations of Trolox or NSAIDs. Relative fluorescence was determined by dividing the fluorescence intensity at a given time by the maximum of fluorescence intensity obtained for probe's oxidation in the absence of antioxidant species (see section 2.4).

6.4. Conclusions

Different microplate fluorimetric methodologies were implemented for high-throughput assessment of ability of drugs to prevent lipid peroxidation in different locations of phospholipid bilayer. The effect of some analytical parameters as fluorescence probe concentration, lipid concentration and initial concentration of radical initiator were evaluated aiming to attain uniformed microplate procedures to allow easy comparison of data. The ratio of IC values obtained for antioxidant standard (Trolox) and tested drugs permit this requirement. Among the drugs tested, etodolac was the most potent for prevention $ROO^{\cdot}$ oxidation in aqueous and interface media using fluorescein and DDAF as fluorescent reporters.

6.5 References

Barclay, L. R. C.; Vinqvist, M. R. MEMBRANE PEROXIDATION - INHIBITING EFFECTS OF WATER-SOLUBLE ANTIOXIDANTS ON PHOSPHOLIPIDS OF DIFFERENT CHARGE TYPES. *Free Radical Biology and Medicine* **1994,** *16*, 779-788.

Beretta, G.; Facino, R. M. Recent advances in the assessment of the antioxidant capacity of pharmaceutical drugs: from in vitro to in vivo evidence. *Analytical and Bioanalytical Chemistry* **2010,** *398*, 67-75.

Cao, G. H.; Alessio, H. M.; Cutler, R. G. OXYGEN-RADICAL ABSORBENCY CAPACITY ASSAY FOR ANTIOXIDANTS. *Free Radical Biology and Medicine* **1993,** *14*, 303-311.

Choudhary, A. N.; Kumar, A.; Juyal, V. Design, Synthesis and Evaluation of Chalcone Derivatives as Anti-Inflammatory, Antioxidant and Antiulcer Agents. *Letters in Drug Design & Discovery* **2012,** *9*, 479-488.

de Castro, B.; Gameiro, P.; Lima, J.; Matos, C.; Reis, S. Location and partition coefficients of anti-inflammatory drugs in EPC liposomes. A fluorescence quenching study using n-(9-anthroyloxy)-stearic probes. *Colloids and Surfaces a-Physicochemical and Engineering Aspects* **2001,** *190*, 205-212.

Drummen, G. P. C.; van Liebergen, L. C. M.; Op den Kamp, J. A. F.; Post, J. A. C11-BODIPY581/591, an oxidation-sensitive fluorescent lipid peroxidation probe:

(Micro)spectroscopic characterization and validation of methodology. *Free Radical Biology and Medicine* **2002,** *33*, 473-490.

Drummen, G. P. C.; Gadella, B. M.; Post, J. A.; Brouwers, J. F. Mass spectrometric characterization of the oxidation of the fluorescent lipid peroxidation reporter molecule C11-BODIPY581/591. *Free Radical Biology and Medicine* **2004,** *36*, 1635-1644.

Fernandez-Bachiller, M. I.; Perez, C.; Monjas, L.; Rademann, J.; Rodriguez-Franco, M. I. New Tacrine-4-Oxo-4H-chromene Hybrids as Multifunctional Agents for the Treatment of Alzheimer's Disease, with Cholinergic, Antioxidant, and beta-Amyloid-Reducing Properties. *Journal of Medicinal Chemistry* **2012,** *55*, 1303-1317.

Greig, F. H.; Kennedy, S.; Spickett, C. M. Physiological effects of oxidized phospholipids and their cellular signaling mechanisms in inflammation. *Free Radical Biology and Medicine* **2012,** *52*, 266-280.

Laszlo, J. A.; Evans, K. O.; Compton, D. L.; Appell, M. Dihydrolipoyl dioleoylglycerol antioxidant capacity in phospholipid vesicles. *Chemistry and Physics of Lipids* **2012,** *165*, 160-168.

Li, L.; Chen, C. Y. O.; Chun, H. K.; Cho, S. M.; Park, K. M.; Lee-Kim, Y. C.; Blumberg, J. B.; Russell, R. M.; Yeum, K. J. A fluorometric assay to determine antioxidant activity of both hydrophilic and lipophilic components in plant foods. *Journal of Nutritional Biochemistry* **2009,** *20*, 219-226.

Lucio, M.; Ferreira, H.; Lima, J.; Matos, C.; de Castro, B.; Reis, S. Influence of some anti-inflammatory drugs in membrane fluidity studied by fluorescence anisotropy measurements. *Physical Chemistry Chemical Physics* **2004,** *6*, 1493-1498.

Lucio, M.; Ferreira, H.; Lima, J.; Reis, S. Use of liposomes to evaluate the role of membrane interactions on antioxidant activity. *Analytica Chimica Acta* **2007,** *597*, 163-170.

Lucio, M.; Ferreira, H.; Lima, J.; Reis, S. Use of liposomes as membrane models to evaluate the contribution of drug-membrane interactions to antioxidant properties of etodolac. *Redox Report* **2008,** *13*, 225-236.

Lucio, M.; Nunes, C.; Gaspar, D.; Ferreira, H.; Lima, J.; Reis, S. Antioxidant Activity of Vitamin E and Trolox: Understanding of the Factors that Govern Lipid Peroxidation Studies In Vitro. *Food Biophysics* **2009,** *4*, 312-320.

Magalhaes, L. M.; Segundo, M. A.; Reis, S.; Lima, J. Methodological aspects about in vitro evaluation of antioxidant properties. *Analytica Chimica Acta* **2008,** *613*, 1-19.

McClare, C. W. F. Accurate and convenient organic phosphorus assay. *Analytical Biochemistry* **1971,** *39*, 527.

Niki, E. Free-radical initiators as source of water-soluble or lipid-soluble peroxyl radicals. *Methods in Enzymology* **1990,** *186*, 100-108.

Nunes, C.; Brezesinski, G.; Lopes, D.; Lima, J.; Reis, S.; Lucio, M. Lipid-Drug Interaction: Biophysical Effects of Tolmetin on Membrane Mimetic Systems of Different Dimensionality. *Journal of Physical Chemistry B* **2011,** *115*, 12615-12623.

Reis, A.; Spickett, C. M. Chemistry of phospholipid oxidation. *Biochimica Et Biophysica Acta-Biomembranes* **2012,** *1818*, 2374-2387.

Reis, S.; Lucio, M.; Segundo, M.; Lima, J., Use of Liposomes to Evaluate the Role of Membrane Interactions on Antioxidant Activity. In *Liposomes: Methods and Protocols, Vol 2: Biological Membrane Models*, Weissig, V., Ed. Humana Press Inc: Totowa, 2010; Vol. 606, pp 167-188.

Santos, F.; Teixeira, L.; Lucio, M.; Ferreira, H.; Gaspar, D.; Lima, J.; Reis, S. Interactions of sulindac and its metabolites with phospholipid membranes: An explanation for the peroxidation protective effect of the bioactive metabolite. *Free Radical Research* **2008,** *42*, 639-650.

Sawraj, S.; Bhardawaj, T. R.; Sharma, P. D. Design, synthesis, and evaluation of novel indomethacin-antioxidant codrugs as gastrosparing NSAIDs. *Medicinal Chemistry Research* **2012,** *21*, 834-843.

Schnitzer, E.; Pinchuk, I.; Lichtenberg, D. Peroxidation of liposomal lipids. *European Biophysics Journal with Biophysics Letters* **2007,** *36*, 499-515.

Takashima, M.; Horie, M.; Shichiri, M.; Hagihara, Y.; Yoshida, Y.; Niki, E. Assessment of antioxidant capacity for scavenging free radicals in vitro: A rational basis and practical application. *Free Radical Biology and Medicine* **2012,** *52*, 1242-1252.

Tinkel, J.; Hassanain, H.; Khouri, S. J. Cardiovascular Antioxidant Therapy: A Review of Supplements, Pharmacotherapies, and Mechanisms. *Cardiology in Review* **2012,** *20*, 77-83.

Tsuchiya, H.; Ueno, T.; Mizogami, M.; Takakura, K. Antioxidant Activity Analysis by Liposomal Membrane System and Application to Anesthetics. *Analytical Sciences* **2008,** *24*, 1557-1562.

Tsuchiya, H.; Ueno, T.; Tanaka, T.; Matsuura, N.; Mizogami, M. Comparative study on determination of antioxidant and membrane activities of propofol and its related compounds. *European Journal of Pharmaceutical Sciences* **2010,** *39*, 97-102.

Valko, M.; Leibfritz, D.; Moncol, J.; Cronin, M. T. D.; Mazur, M.; Telser, J. Free radicals and antioxidants in normal physiological functions and human disease. *International Journal of Biochemistry & Cell Biology* **2007,** *39*, 44-84.

Yoshida, Y.; Shimakawa, S.; Itoh, N.; Niki, E. Action of DCFH and BODIPY as a probe for radical oxidation in hydrophilic and lipophilic domain. *Free Radical Research* **2003,** *37*, 861-872.

CHAPTER 7

General conclusions

7. General conclusions

The potentialities of biophysical techniques, such as π-A isotherms and BAM imaging, were exploited in this work to try to shed some light on aspects related to peroxidation and antioxidant protection. For this, 2D (monolayers) and 3D (vesicles and micelles) biomimetic models of biological membranes were applied. In the first case, studies about the biophysical properties of phosphatidylcholine monolayers upon exposure to peroxidation conditions were performed. The interaction of several biologically relevant antioxidants (α-tocopherol, ascorbic acid, uric acid and glutathione) with membranes was clearly established by the observed changes in biophysical parameters and by formation of domains visualized by the BAM technique.

Another important result from this thesis is the clear interaction established between the 2D model applied here and the peroxidation products formed from derived species of AAPH, even in presence of antioxidants. This result is certainly relevant and should foster a deeper investigation about the nature of these products and the possibility of their selective extraction and concentration in the biological membrane.

From an analytical point of view, the presence of biomimetic structures within the reaction media should be mandatory when antioxidant assessment is aimed. From our results, it was possible to show how the interactions of antioxidants (both endogeneous and exogenous) with the biological targets of oxidation may reveal a different behavior when compared to ideal analytical situations, when a single species is challenged in a rather simple medium, against a colored radical, for instance.

For the future, it is clearly necessary to establish some order in this field because the literature is now filled with low quality data regarding antioxidant effects of nutrients, for instance, while the evaluation of redox status is disputable for many scientists. One of the main reasons for that is the inadequacy of methods applied for the target samples. Hence, standardization and clear discussion about the contextualization and implications of antioxidant assessment should be regarded as hot topics in a near future.